AD 205196

CWL Special Publication 2

Report of Symposium VIII. Volume I.

SPRAY DISSEMINATION OF AGENTS

Conducted by
U. S. Army Chemical Warfare Laboratories
4, 5 and 6 March
at
Army Chemical Center, Maryland.

July 1958

U. S. ARMY CHEMICAL WARFARE LABORATORIES
Army Chemical Center, Maryland

CWL Special Publication 2

REPORT OF SYMPOSIUM VIII
Volume I

SPRAY DISSEMINATION OF AGENTS (U)

Conducted by U. S. Army Chemical Warfare Laboratories
4, 5, 6 March 1958

Colonel Lloyd E. Fellenz, Commanding

Chairman: Mr. L. Benjamin, Headquarters, U. S. Army Chemical Corps Research and Development Command

Co-Chairmen:	Col M. T. Moree,	U. S. Army CmlC Board
	Dr. B. Berger	U. S. Army CW Laboratories
	Mr. B. M. Zeffert,	U. S. Army CW Laboratories
	Mr. A. Koblin,	U. S. Army CW Laboratories

Administrative
Chairman: Dr. R. Macy

DISPOSITION

When this document has served its purpose, DESTROY it. DO NOT return to U. S. Army Chemical Warfare Laboratories.

Chemical Warfare Laboratories Special Publication 2
REPORT OF SYMPOSIUM VIII
SPRAY DISSEMINATION OF AGENTS (U)

Volume I

APPROVED:

Date Submitted for Publication: 11 April 1958

S. D. SILVER
Deputy Commander for
Scientific Activities

CONTENTS

CONTENTS (Contd)

CONTENTS (Contd)

PRINCIPLE OF BALANCED STRESSES AND THE MECHANICAL FORMATION OF AEROSOLS

W. E. Ranz

The Pennsylvania State University
University Park, Pennsylvania

INTRODUCTION

Sometimes a simple concept (a way of looking at a problem) makes a difficult process understandable. Sometimes this concept provides a key to a complex analysis; sometimes it satisfies the research worker's physical intuition and common sense. I shall attempt here to suggest such a concept for that exceedingly complex and difficult process, the mechanical formation of aerosols.

A dynamical system, such as the mechanical formation of aerosols, can be analyzed in terms of characteristic stresses at work in the system. By comparing stresses one can eliminate unimportant variables and establish the limits of various stable dynamic states. A stress analysis is one step better than a dimensional analysis in that mechanisms are postulated and Newton's law is applied.

Examples of the principle of balanced stresses will be given for predicting drop survival diameter, wave lengths of surface disturbances, conditions for electrostatic atomization, and the effect of viscosity.

Characteristic Stresses

The best way to analyze a dynamical process is to consider characteristic stresses in the system. Balanced stresses mark the limits of various stable dynamic states. Unbalanced stresses define regions of acceleration and deceleration. Table I is a list of some of the characteristic stresses which are involved in the mechanical formation of aerosols.

Table I - Characteristic Stresses Involved in the Mechanical Formation of Aerosols

Type of Stress	Force Per Unit Area of Interface
Phase Being Dispersed:	
Impact or Inertial Stress	$\rho_l V^2/2g_c$
Shear Stress	$\mu_l V/L$
Normal Stress of Electrical Charge	$q_{ac}{}^2/8K_o$
Ambient Phase:	
Impact or Inertial Stress	$\rho g V^2/2g_c$
Shear Stress	$\mu g V/L$
Surface Normal Stress	$2\sigma/L$

In this table, V is the characteristic velocity and L the characteristic length, the velocity gradient V/L is assumed to be the characteristic velocity gradient for viscous shear, and L is assumed to be the characteristic radius for the interfacial normal stress. In a specific system, such as the spray for an orifice nozzle, L might become the radius or diameter of the orifice, and V might become volumetric average flow velocity, both measurable quantities. It must be remembered, however, that the trick in analysis is obtaining the proper relationship between actual lengths and velocities and their characteristic values.

Mechanical Formation of Aerosols

To create mechanically a spray of large surface area one must force a liquid mass to assume an unstable free liquid configuration of even larger surface area. This is usually accomplished by imparting to the liquid or gas sufficient kinetic energy to cause the liquid, on flowing through some spraying device, to assume the form of filaments or sheets or to create such inertial and frictional forces with the gas phase as to tear off filaments or sheets originating at ripples on its surface. Because of

surface tension the configuration of large surface areas is unstable, and, on undergoing random disturbances, some of which are more probable and speedier than others, it breaks up into a drop system of smaller surface area.

The formation of the unstable intermediate state and the breakup usually happen in times of the order of one millionth of a second. Because such times for microscopic occurrences are too short for known photographic and recording techniques, the mechanism is not fully understood. Some kinetic energy imparted to the liquid mass appears as surface energy in the spray, but the larger portion of the kinetic energy is retained by the spray drops, causing them to penetrate into and mix with the gas. Because of the wide ranges of relative velocities and because of the innumerable types of disturbances which cause breakup, the drop sizes in a spray are widely distributed.

Minimum Drop Sizes Obtained by Mechanical Methods

As an example of balanced stresses, let us consider the maximum possible relative air velocity which a liquid drop can withstand before it breaks up or, conversely the survival diameter of drops at a given relative velocity. Air strikes the drop surface with an impact stress of the order of $\rho g V^2/2g_c$. The stress which the drop surface can support by virtue of its surface tension is $4\sigma/D$. Equating the two stresses gives a drop "survival" diameter for a relative velocity of V; or, similarly, their ratio, a Weber number, can be set equal to unity. Thus

$$\frac{\rho g V^2 D}{8\sigma g_c} \approx 1 \qquad \ldots(1)$$

for the survival diameter. One can say that the liquid mass breaks up because the impact of the air equals or exceeds the ability of the drop surface to withstand the force. One can also say that Eq. 1 specifies the minimum "average" drop sizes which can be produced by spraying devices which develop relative velocities V.

By experiment Lane (2) and Hinze (1) have demonstrated that Eq. 1 holds for liquids with low viscosities. However, the disruptive impact stress was found to be about half again as much as the surface normal stress. For a more accurate Eq. 1 the critical Weber number should be given the value of 1.5 instead of unity.

What are the consequences of such a simple concept? Since almost all "practical" spraying devices are limited to sonic velocities and to atmospheric air densities, the minimum average size which one can expect from improvements in design is about five microns.

In the same terms the inherent difference between liquid-pressurized and gas-pressurized nozzles is apparent. An applied gauge pressure, which is a stress, results in either a relative velocity of liquid inertia, $\rho_l V^2/2g_c$, or gas inertia, $pgV^2/2g_c$. Because of a relatively small gas density, a gauge pressure of only one atmosphere is needed to produce a compressible flow of sonic velocity in a gas, whereas a gauge pressure of around 3000 pounds per square inch is required to cause a velocity of half the speed of sound in a liquid. The criterion for drop survival suggests that, at half the relative velocity, the drop size is four times larger. There are the approximate comparative results which one obtains from these two types of atomization.

Relative Importance of Stresses; Elimination of Variables

Having focused attention on the various stresses which cause, promote, and retard breakup, one has insight into the mechanism of aerosol formation. For a given physical situation one can decide, by comparing stresses, whether a stress is important or unimportant. Quantitatively these comparisons are ratios which are the pertinent dimensionless numbers for any experimental analysis of the system.

In high speed atomization a stress comparison usually leads to the conclusion that the important stresses are the impact stress of the ambient phase, the interfacial normal stress, and, to a smaller extent, the shear stresses in the liquid.

A comparison of stresses, therefore, leads to a logical elimination of unnecessary variables. Such comparisons can also give semi-quantitative evaluation of novel forces and stresses which might be introduced into new types of spraying devices. If the novel stress built into the device does not measure up to existing stresses, it will not be effective in producing a smaller drop size. As in every branch of engineering there are few "miracles", and those which do occur can usually be explained in terms of Newton's law.

Generation of Waves; Initiation of Breakup Process

In spraying devices relative velocities between liquid and air occur between volumes of each phase which are very large in comparison to the final drop size. Relative flow is side-by-side, not head on. Close observation has shown that wavelike disturbances are generated on the surface between the phases and that these waves grow into extended filaments and films which are subsequently blasted apart by high relative velocities or, being extended to a dynamic stress balance at maximum surface area, break up of their own accord.

A surface instability analysis of the Rayleigh type consists of imposing known, but infinitely small disturbances on a fluid surface. Each of the infinite number of possible disturbances has a wave length and an amplitude with a time factor for growth, e^{at}. If all the disturbances are excited simultaneously, that wave length with the largest positive time constant, a, on its amplitude will ultimately predominate. If the time constant is positive, the disturbance will grow. If the time constant is negative, the disturbance dies out and the system is stable to this particular perturbation. A Rayleigh jet is stable to varicose swellings with wave lengths less than the circumference of the liquid column. Swellings with wave lengths equal to about 4.5 times the diameter of the liquid column have the largest time constant, grow the fastest, and represent the most probable breakup length. In this case, instability is dependent only on the existence of surface tension.

Let us now apply the principle of balanced stresses to the problem of the wave length of waves generated by a wind blowing over a liquid surface. Imagine for a moment a finite sine wave which has grown to such a size that the impact stress of the air $\rho g V^2/2g_c$, on the side of the wave equals the interfacial stress maintaining the surface contour of the wave. For the wave one can substitute two half circles of radius $\lambda/4$ and arrive at a critical Weber number.

$$\rho g V^2 \lambda / 8 \sigma g_c \approx 1 \qquad \ldots(2)$$

for the minimum possible wave length (in this case the surface is cylindrical in shape).

Elegant theoretical calculations by Taylor (4) show that the simple minded approach is not far wrong. Instead of unity the right side of Eq. 2 should read $2\pi/8$ for the minimum possible wave length. Shorter

waves damp out and do not grow with time. For the "most probable wave length" the right side of Eq. 2 should read $3\pi/8$. Wave lengths longer than the most probable one also grow with time but at increasingly smaller rates of growth.

The flaglike flapping of a liquid sheet was investigated by Squire (3). In this case the right side of Eq. 2 should read $4\pi/8$ for the most probable wave length.

Atomization by Electrostatic Forces

A liquid mass will break up under the action of electrostatic forces when the electrostatic stress exceeds the interfacial stress. The critical condition is given by the ratio.

$$q_{ac}^2 R/2\sigma K_o \approx 1 \qquad \ldots(3)$$

where R is the diameter of a spherical surface with a surface charged density qac.

If one were to increase the potential applied to a water drop until the surface charged density was about the maximum possible in air (2.65×10^{-5} columb/cm^2), any liquid radius larger than about 1.5 mm would begin to disintegrate. The potential for these conditions is around 5000 volts.

At an applied potential of around 5000 volts any disturbance will create a protuberance of small radius on the surface. The surface charged density at the point momentarily will be inversely proportional to this radius. The disruptive stress is inversely proportional to the square of this radius. Since the opposing stress of surface tension is only inversely proportional to the radius of such a disturbance, all disturbances are unstable and grow under a net stress which is inversely proportional to the radius of the disturbed surface. It is not surprising that electrostatic spraying results under these conditions.

Effect of Viscosity

Experience teaches us that very viscous liquids are difficult to atomize. The principle of balanced stresses should be able to tell us how viscous the liquid must be before a particular nozzle fails to produce a spray.

So far we have assumed that viscous shear stresses* are negligible. When either the velocity becomes very large or the length scale becomes very small, for example, a small filament or drop size, causing the viscous stress to become of the same order of magnitude as the impact or interfacial stress, then corrections must be made for the effect of liquid viscosity.

A comparison of liquid inertial stress and liquid viscous stress produces a Reynolds number, the best known of the dimensionless groups. We are always tempted to use such a familiar variable. However, what we really want to compare here is the gas inertial stress or the interfacial stress, which we know to be important, and the liquid viscosity stress, whose importance we question. The problem is further complicated by the fact that internal movements of liquids involve also the inertial stress of the liquid phase.

It has become the custom, more or less by accident, to compare the liquid shear stress with the square root of the liquid inertial stress multiplied by the interfacial stress. Figure 1 shows the correction to be applied to several of the dynamic systems described previously (1, 4, 5). Similar corrections of the same order of magnitude can be expected for all systems.

It is not surprising that corrections are negligible for values of the viscosity parameter of the order of 10^{-2} and less. It is also not surprising that corrections become significant, even dominant, when the viscosity parameter reaches the order of unity. Thus, with respect to absolute values of dimensionless ratios, one notes that they should be defined so that they have values near unity when they are the most important independent variable.

Figure 1 is not intuitively obvious on the basis of the principle of balanced stress. Because four independent stresses are involved, three independent dimensionless groups would be required to make a formally complete mathematical picture. Only two groups are given here showning the value of the theory. In effect, one independent combination of variables was eliminated.

---

* Viscous stretching and contracting normal stresses are also involved. The characteristic stress is written in the same way, but the velocity gradient is now taken in the direction of flow instead of right angles to it.

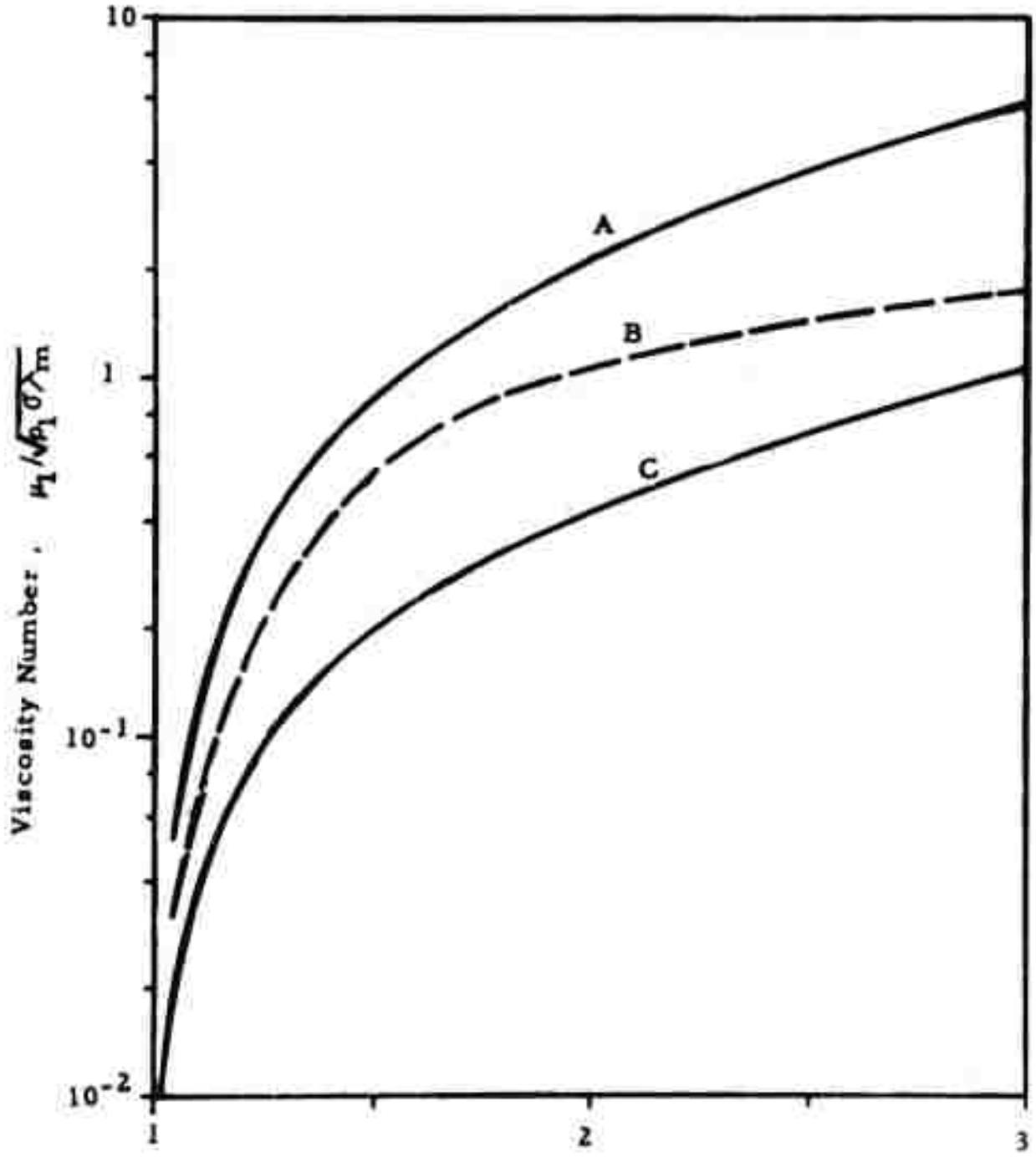

Fig. 1 - Effect of Liquid Viscosity on Stability

A - Sinuous waves on a viscous liquid jet, $\lambda_m/D_o = \sqrt{2}\pi f$

B - Survival diameter of drop subjected to air blast ($_m$ survival diameter), $\rho_g V^2 \lambda_m / 8\sigma g_c \approx 1.5\ f$

C - Wind blown waves on viscous liquid, $\rho_g V^2 \lambda_m / 8\sigma g_c = (3\pi/8) f$

(A - Ref. 5; B - Ref. 1; C - Ref. 4)

Because liquid properties are usually based on shear stress as a function of velocity gradient, non-Newtonian liquids can also be treated in terms of a spray stress analysis. For example, breakup of ideal and psuedo plastics probably would not occur unless

$$\frac{\rho g V^2}{2 g_o \tau_o} \gtrsim 1$$

and viscous effects would not be dominant until

$$\frac{\mu_s + \tau_o L/V}{\sqrt{\rho_l \sigma L}} \gtrsim$$

Stress Analysis Compared with Dimensional Analysis

Stress comparisons, without careful analysis, often lead to what appear to be contradictory results. For example, the liquid inertial stress is always of the order of one thousand times the gas inertial stress. Superficially, it is the dominant stress at all times. However, it is only the dominant stress with regard to penetration into the surrounding gas and formation of a spray zone. With regard to the breakup process, the liquid inertial stress, based on the characteristic velocity, is important only so far as the characteristic velocity represents "relative" internal motions of the liquid itself.

The principle of balanced stresses is not a substitute for analytical thought. It is only a method of thought which seems to produce useful results and evaluations without a complete theoretical or experimental solution.

A stress analysis is one step better than a dimensional analysis in that mechanisms are postulated and Newton's law is applied. As with dimensional analysis one gets no more out of a stress analysis than he puts into it and the amount he puts into it is usually directly proportional to his previous experience with similar types of problems.

References

1) Hinze, J. O., A.I.Ch.E Journal 1, 289 (1955).

2) Lane, W. R., Ind. Eng. Chem. 43, 1312 (1957).

3) Squire, H. B., British Journal of Applied Physics 4, 167 (1953).

4) Taylor, G. I., "Generation of Ripples by Wind Blowing over a Viscous Fluid", unpublished research item.

5) Weber, C., Zeits. f. Angewandte Math. u. Mech 11, 136 (1931).

Table of Symbols

D	Drop diameter.
g_c	Dimensional conversion constant for use of engineering units. g_c = 32.2 (lb. mass/lb. force) (ft/sec^2) = 1 (gm. mass/dyne) (cm/sec^2)
L	Characteristic length.
q_{ac}	Electrostatic charge per unit of surface area.
R	Radius of surface curvature
V	Characteristic velocity.
K_o	Permittivity of free space. $K_o = 8.85 \times 10^{-12}$ (coulombs^2/joule meter).
λ	Wave length.
μ_g	Gas viscosity.
μ_l	Liquid viscosity.
μ_s	Pseudo viscosity of plastic liquid.
ρg	Gas density.
ρ_l	Liquid density.
σ	Interfacial tension.
τ_o	Yield stress of plastic liquid

BREAKUP OF LIQUID DROPLETS, THICKENED AND UNTHICKENED

James D. Wilcox
Research Directorate
U. S. Army CW Laboratories
Army Chemical Center, Maryland

When considering spray of chemical warfare agents from high speed aircraft, the particle size and the time of fall to the target are necessarily important factors, for these factors directly affect the spread pattern of the spray. If the particle size is very small the agent particle concentration will be of such value that it has very little effectiveness. Comparing the settling rate and cloud travel of small aerosols and that of drops, one finds that in order to place the agent on a target area one must use the larger particle sizes such as drops of 500μ to 3 or 5 mm. in diameter.

If we wish to produce drops of liquid agents from a spray tank of a high velocity aircraft flying in the vicinity of Mach 1, we are faced with a problem entirely different from any other in aerosol formation. That problem is the over abundance of energy to break up the agent. The one main factor that controls the size of the breakup products of the liquid agent is the relative air velocity, and in the case of aircraft sprays this velocity is quite high. Surely, a pilot isn't going to reduce the speed of his plane to several hundred miles per hour in order to control the spray size. So we must find another way of controlling the breakup of the agent.

To start with first things first, one wants to know about the way liquids break up at these high velocities. Then after understanding something of this breakup process, we may attempt to control the breakup to give the desired particle size. In order to simplify and understand this breakup process our investigations were started with drops of 4mm. diameter. It was felt that understanding and controlling of the breakup of drops of this size would eventually lead to control of smaller particles; the smaller the particle the greater the energy required to break it up.

Numerous investigators such as Richardson (1), Lane (2), Miesse (3), a group from the University of Minnesota (4), and workers at the NACA (5), had observed drop breakup at velocities that were relatively low in comparison to velocities in the vicinity of Mach 1. Some of these investigators were merely concerned with determining the velocity at which the drop broke up and referred to this velocity as the critical breakup velocity, or the velocity at which the drop became unstable. Other investigators were concerned with effects produced by these breakup products, such as in the atomization of liquid fuels.

When we consider a liquid drop in an airstream there are mainly two groups of forces acting on the drop. These are the forces tending to tear the drop apart, and the forces tending to hold it together; or, we might say the external and internal forces. When the relative velocity is high enough to overcome the internal forces the drop becomes unstable and undergoes breakup.

The mechanisms of breakup will depend on how great the velocity exceeds the minimum velocity required to produce instability.

In our investigations air blasts and airstreams having a velocity in the vicinity of Mach 1 were needed. Our initial attempts at high velocity breakup observation was by and large an extension of the later work of W. R. Lane of Porton (6), in which he used a blast gun for producing subsonic air blasts. However, we felt that we could improve on his techniques by not only operating at much higher velocities, but by suspending the drop on a column of air as demonstrated by Blanchard (7) rather than using crosshairs or like methods, which in themselves could start the breakup process as a result of the drops tearing away from these supports.

Figure 1 shows graphically the blast gun equipment which was made as an extension of Lane's work. The drop is supported in front of the blast-gun barrel by a column of air. The contoured screen and the funnel act to reverse the regular velocity profile of the air coming from the drop-support air column. The blast gun is divided into two chambers which are separated by a frangible diaphragm. The closed chamber is a compression chamber and is pressured with nitrogen to the pressure required to give the desired velocity. The open ended chamber is the expansion chamber. Breaking of the frangible diaphragm, by dagger attached to the solenoid, causes the shock front and high velocity airstream to proceed up the expansion chamber. The shock front and high velocity airstream emerge from the end of the blast gun and strike the drop of suspended liquid. The action of this high velocity airstream upon the drop is recorded photographically. The passage of the shock front is sensed by a crystal pickup on the blast gun barrel. This signal is electronically delayed and fed into the trigger circuit which in turn causes the high intensity spark gap to fire. The light emission from this spark gap causes exposure of photographic film and the event is recorded as a spark shadowgraph. The delay circuit enables recording of the event at any desired time interval after the drop is initially struck by the shock front.

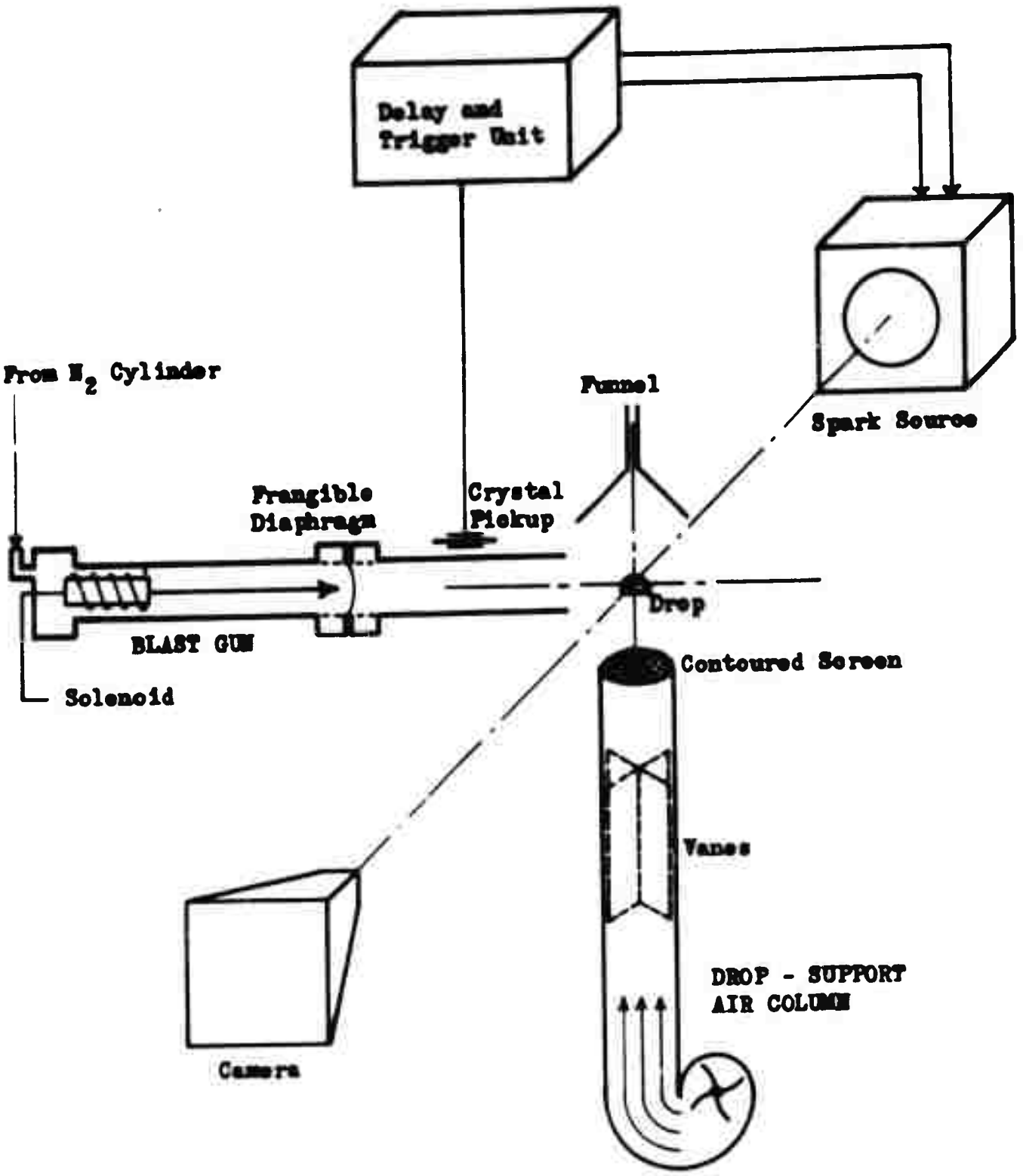

Fig. 1: DIAGRAM OF BLAST GUN

Figure 2 is an enlarged double spark shadowgraph of liquid drop breakup from the blast gun. The picture contains two exposures of the event. The end of the blast gun barrel is seen on the left with the high velocity airstream emerging and traveling from left to right. The first exposure shows the drop, the spherical expanding shock wave, and the high velocity airstream which is emerging and in the process of expanding from the end of the blast gun barrel. One can see the beginning of a vortex ring in the airstream at this point. The second exposure shows that the airstream has struck the drop, and has caused disruption of the drop which is seen by the shaded areas around the original drop. The turbulent wake downstream from the drop can be noted and a standing wave, "bow wave," or reflected wave can be seen formed around the drop.

One is able to observe just what is taking place by these clear shadowgraphs. However, it was apparent after several observations that there were a number of undesirable features to this setup which were built into this method. The vortex ring on passing around the test drop caused radial disruption of the drop. This disruption may be noted in Figure 2. The formation of various turbulences and extraneous reflected shock waves were undesirable. The pressure around the drop was not atmospheric and was difficult to estimate because of the rapidly expanding airstream. The velocity of the airstream striking the drop was difficult to measure and hard to keep constant from test to test.

As a result of the difficulties with the blast gun tests, the possibility of doing controlled laboratory experiments with a small shock tube were studied. This study resulted in the construction of a 2 in. ID shock tube for the production of controlled airstreams of high velocity.

Figure 3 is a block diagram of the shock tube and its associated equipment. The shock tube is divided into two chambers, the compression chamber which is pressured by nitrogen, and the expansion chamber which is partially evacuated. The two chambers are separated by a frangible diaphragm. The pressures in the chambers govern the airstream velocity, and the value of the pressure ratio controls the pressure in the test region at the time of testing. By varying the pressure a wide range of test conditions are available. The test liquid is introduced into the top of the vertical shock tube through a hypodermic needle. The drop falling from the hypodermic needle breaks a light beam, which triggers the series of events needed to photographically record the drop breakup. The light beam signal is delayed, amplified, and sent to the shock tube solenoid, which cause rupture of the diaphragm. Rupturing of the diaphragm in turn causes

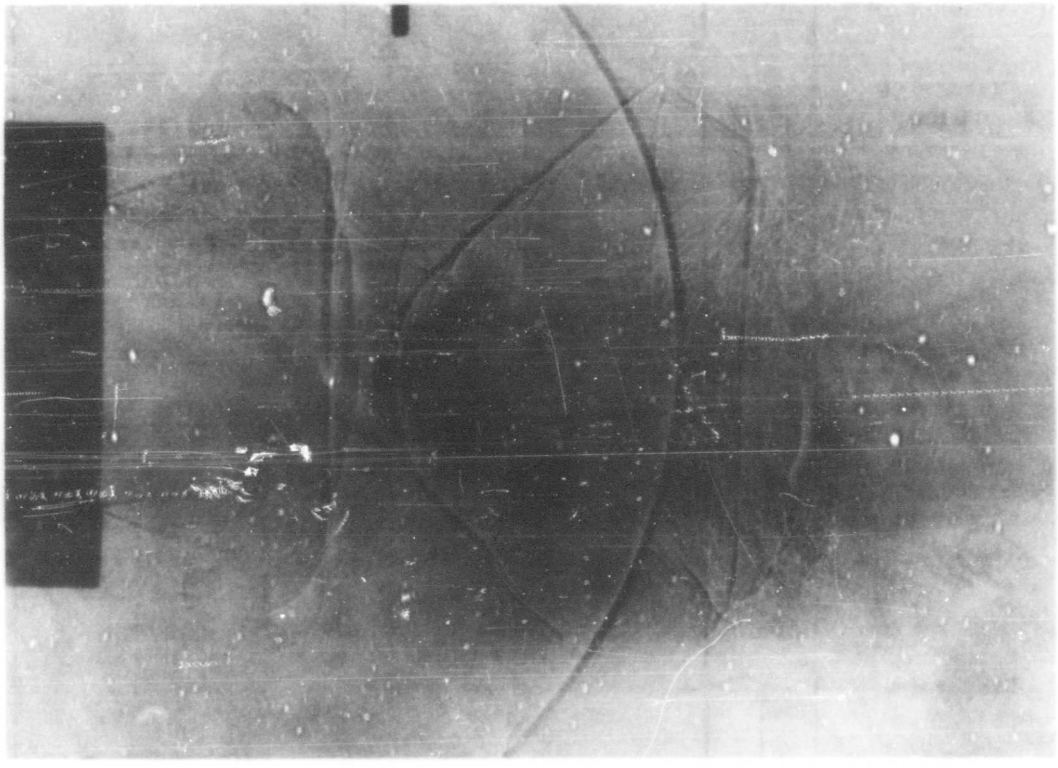

FIGURE 2

ENLARGED DOUBLE SPARK SHADOWGRAPH OF LIQUID DROP BREAKUP FROM BLAST GUN.

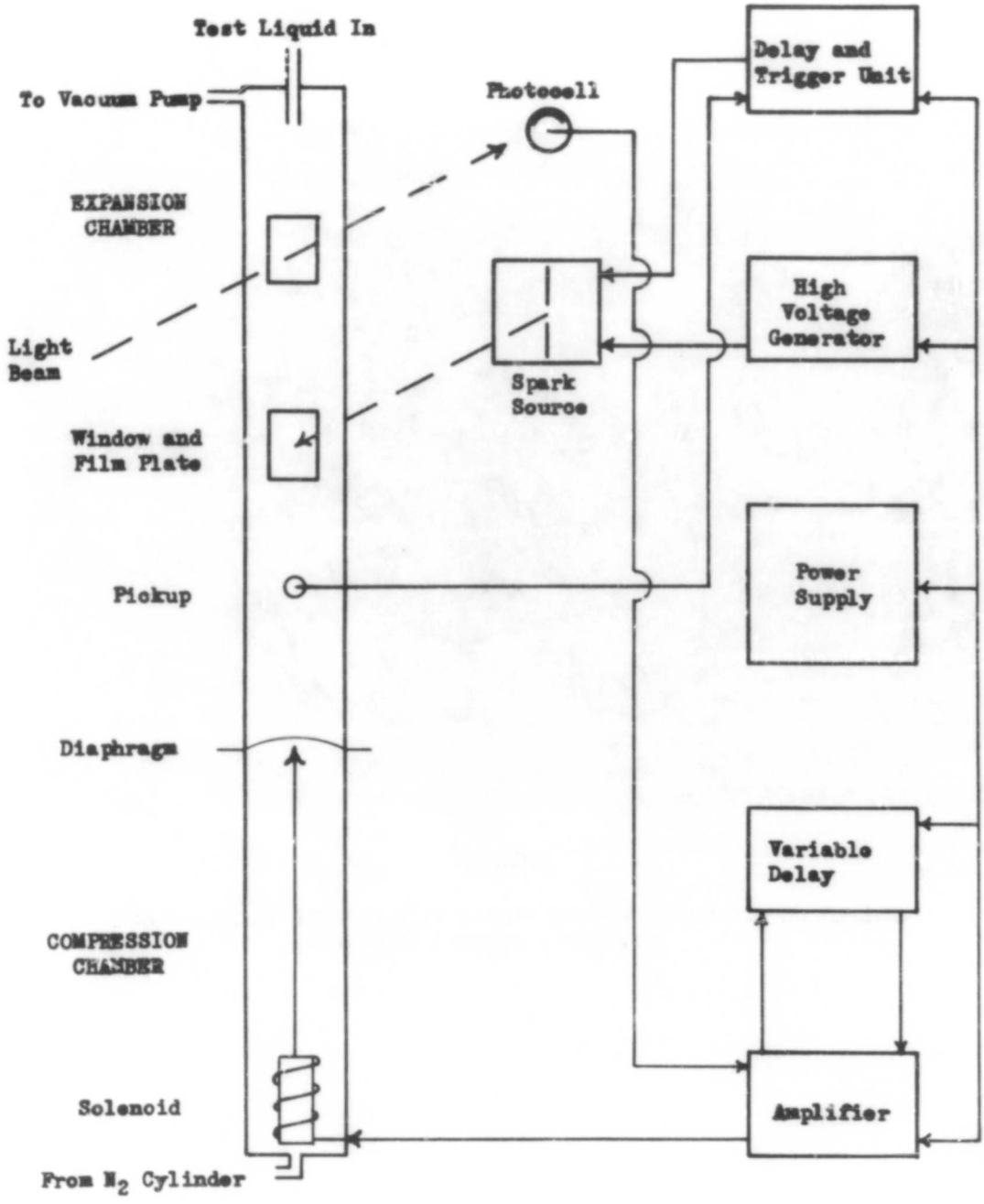

Figure 3

BLOCK DIAGRAM OF SHOCK TUBE

the formation of the shock front and high velocity airstream which progress up the shock tube. Passage of the shock front is sensed by a barium titanate crystal pickup located below the photographic observation window in the shock tube. This signal is delayed and used to fire the spark source. The two delay circuits enable synchronization of the event, so that the portion of the drop breakup process that is desired to be recorded takes place in front of the photographic window. The firing of the spark source causes exposure of a photographic plate at the observation and results in the photographic recording of the event as a single spark shadowgraph.

Figure 4 is a series of spark shadowgraphs of drop breakup by the shock tube technique. The drops are 3 mm. in diameter and are the liquid agent simulant, bis 2-(ethylhexyl) hydrogen phosphite, known as Bis. The velocity of the airstream acting upon the drop is 1200 ft./sec., or just slightly greater than Mach 1. The pressure at the time of the air action was 1 atmosphere. The time referred to below each picture is the time of the air action upon drop, or the time after the passage of the shock front. At 0μ sec. is shown the spherical drop with the shock wave approaching the drop, 70μ secs. shows the development of surface ripples on the drop and some initial downstream turbulence. At 150μ secs. flattening of the drop occurs and the initial surface stripping of the drop commences. In the 250 and 490μ secs. pictures continuation of breakup and surface stripping is shown. At 850μ secs. the drop has almost undergone complete disintegration with the pieces broken off from the drop undergoing surface stripping themselves.

Altering the physical properties of the liquid is a most versatile method of controlling the breakup process. The particle size range may be adjusted, by altering the physical properties of the liquid, to fit the particular needs.

It was known that retarding of drop breakup can be accomplished by agent thickening. In this work the agent thickeners were evaluated by subjecting test drops of thickened liquid to high velocity airstreams. The actual effect of thickener materials is to act as a damper to retard breakup. A drop subjected to a high velocity airstream has the maximum velocity forces acting on it during its first moment of exposure to the airstream. From the first moment the drop is accelerated, the relative velocity is decreased continuously until both airstream and drop are traveling at approximately the same velocity. This is what would happen to a solid particle. However, in the case of the liquid drop, if the damping effect of the thickener is great enough then the drop could decelerate to a velocity below the critical breakup velocity and remain as a single particle.

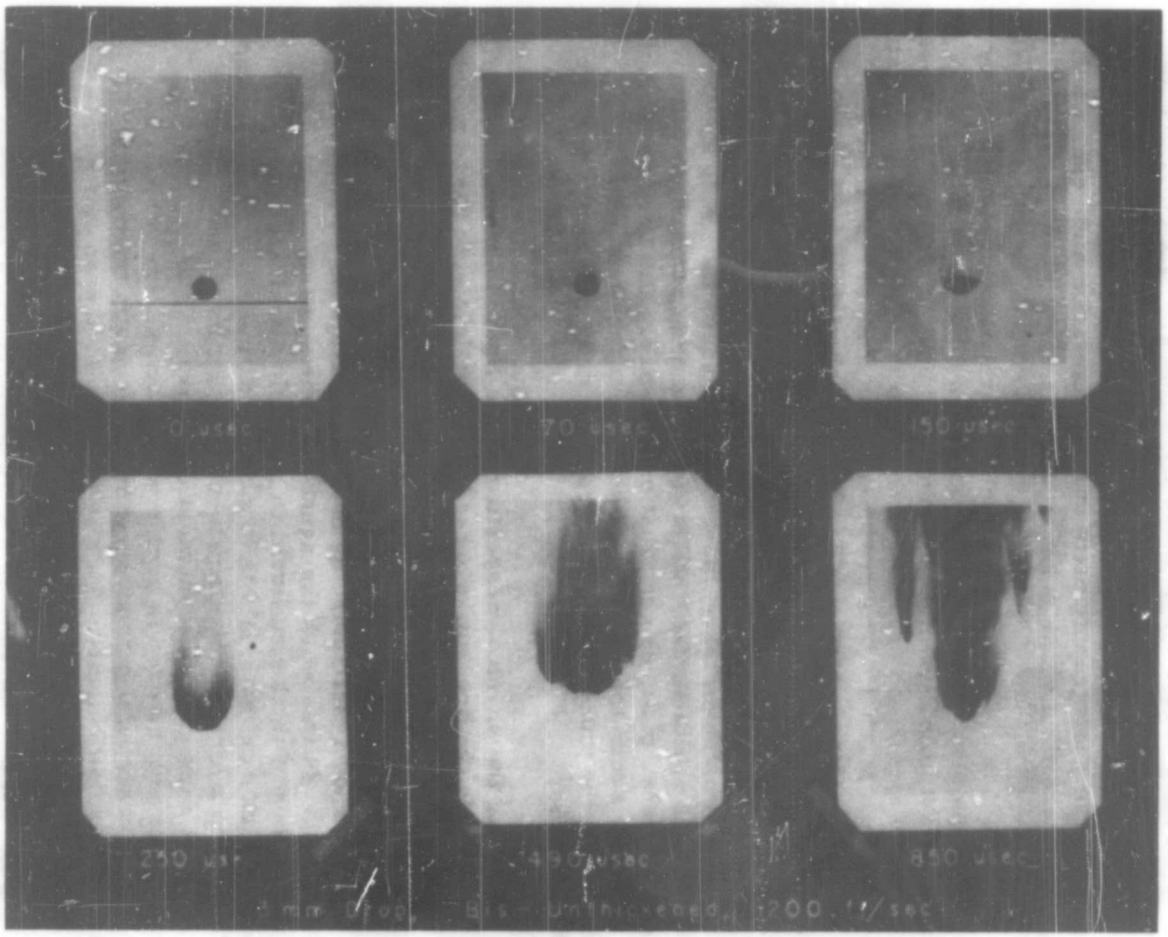

Figure 4

DROP BREAKUP BY THE SHOCK TUBE TECHNIQUE

Some effort has been made with thickening materials and a certain measure of success has been obtained. The thickening material should exibit the required damping or retarding effect on drop breakup and also be free-flowing at relatively low flow rates.

Figure 5 is a series of spark shadowgraphs of thickened drop breakup by the shock tube technique. The conditions of this experiment were the same as they were in the experiment shown in Figure 4,with the exception of the thickener added to the agent simulant "bis". The "bis" contains 2% poly(isobutylmethacrylate). It should be noted that the drop is not suspended by a string. The string attached to the drop was formed when the drop broke loose from the hypodermic needle, and the distance of fall of the drop was not great enough to collapse the string. Surface ripples are again shown in this experiment at 70μ secs. The rest of the series of the pictures show that instead of the drop being surface stripped into fine particles, the drop holds together for a longer period of time and is finally broken into large chunks. The process is somewhat similar to breakup by ligamentation which is indicative of low velocity breakup.

Figure 6 shows the effect of thickener concentration variation. In this figure it can be seen that quantities of thickeners as low as 0. 1% have a retarding effect on drop breakup.

Figure 7 shows several of the unsuccessful methacrylates that were tested. Of the two n-butyl methacrylates shown, one was a sample of 100,000-300,000 molecular weight obtained from Rohm & Haas, and the other was a sample of 1,000,000 molecular weight which was obtained from Picatinny Arsenal, Dover, N. J. There was no effective damping or retarding of drop breakup by these materials.

In order to get a picture of the effect of viscosity change on drop breakup, paraffin oil was added to the "bis" simulant, with a resulting increase in viscosity. Figure 8 is a series of shadowgraphs showing pure "bis", a paraffin oil in "bis" sample, and paraffin oil alone, in a drop breakup experiment. There was no significant breakup difference shown by this test, although the viscosity was increased by a factor of approximately 25.

The shadowgraphs presented here are intended to give a picture of what takes place during high velocity breakup, and they show that surface stripping appears to be the predominant mode of breakup at these velocities. It is shown that quantities of thickener as small as 0. 1% greatly retards breakup of the liquid drop. Also poly(isobutyl methacrylate) (IBM) is rather effective as a thickener.

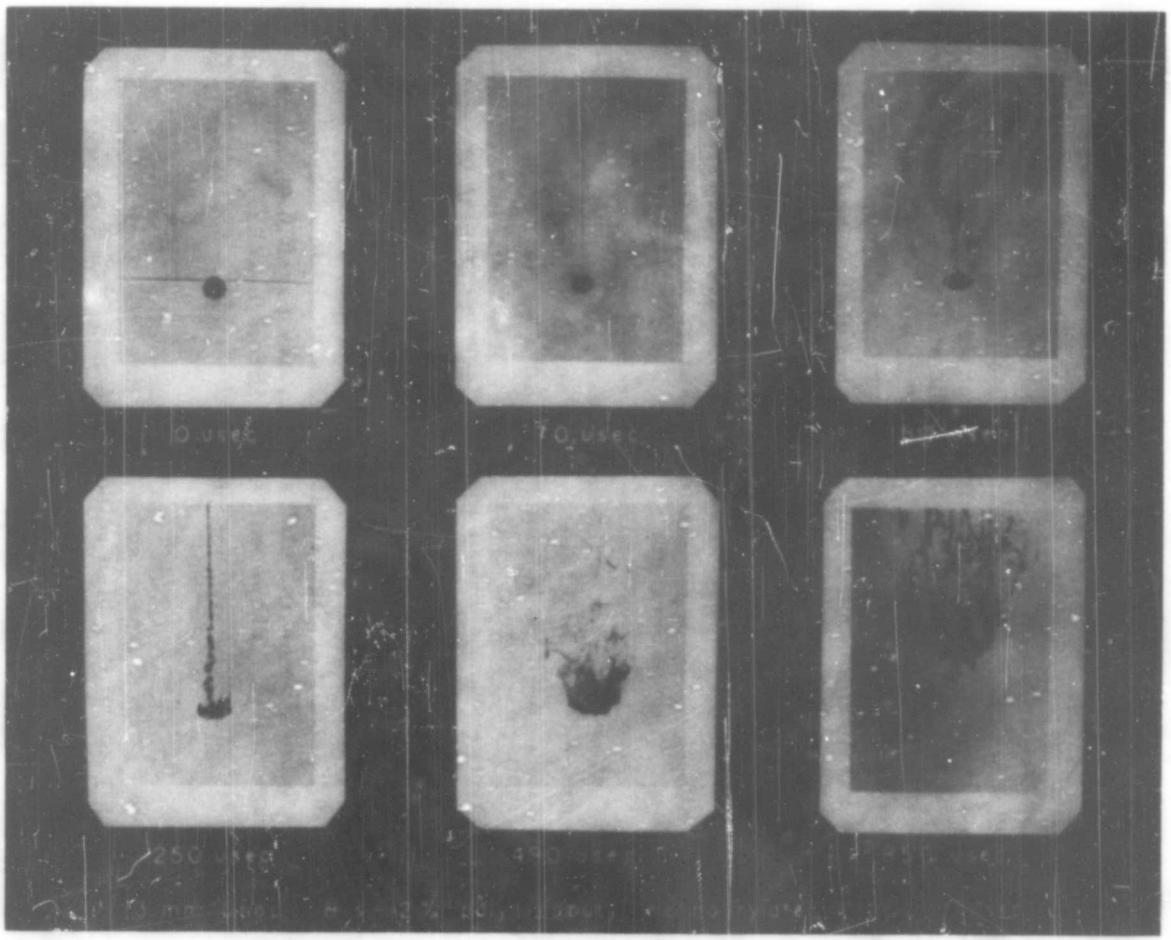

Figure 5

THICKENED DROP BREAKUP BY THE SHOCK TUBE TECHNIQUE

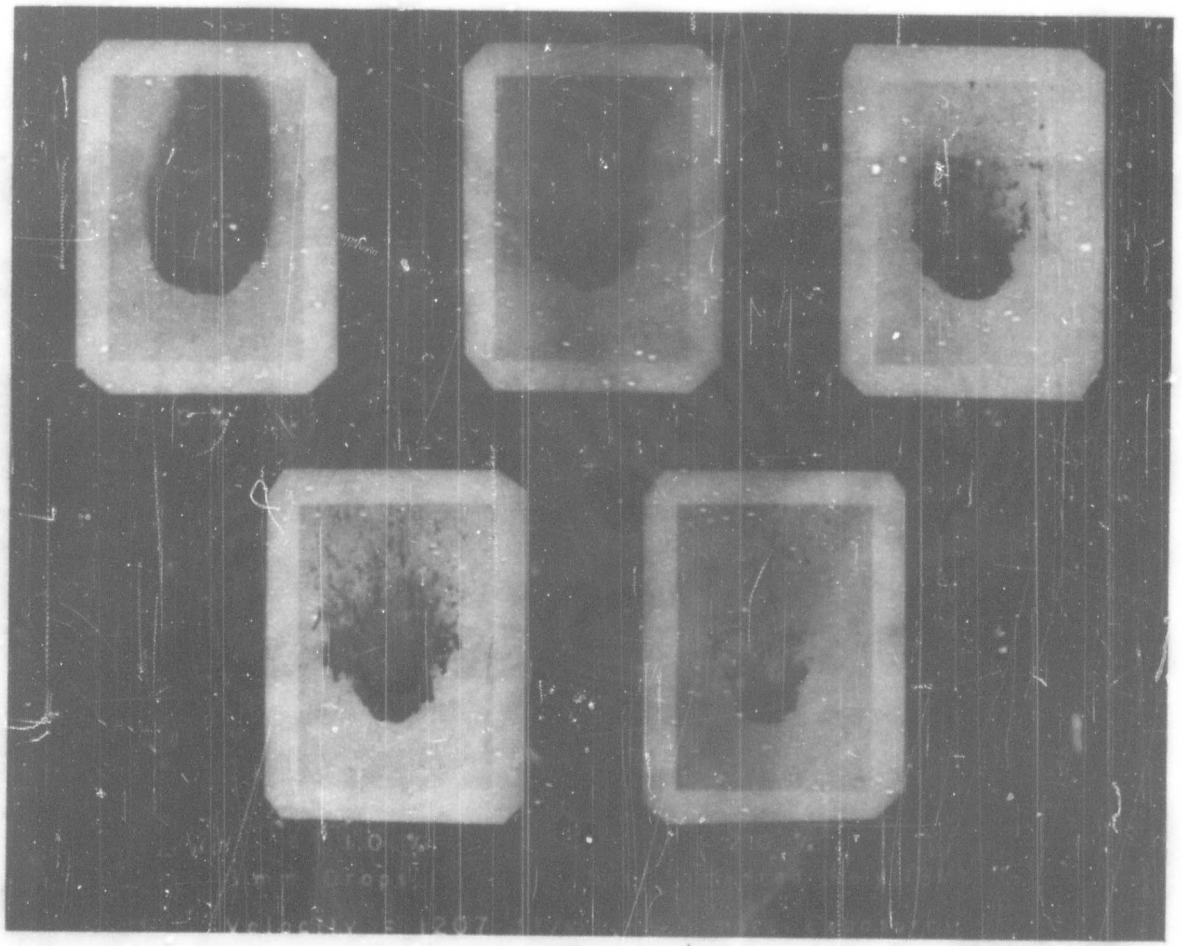

Figure 6

EFFECT OF THICKENER CONCENTRATION VARIATION

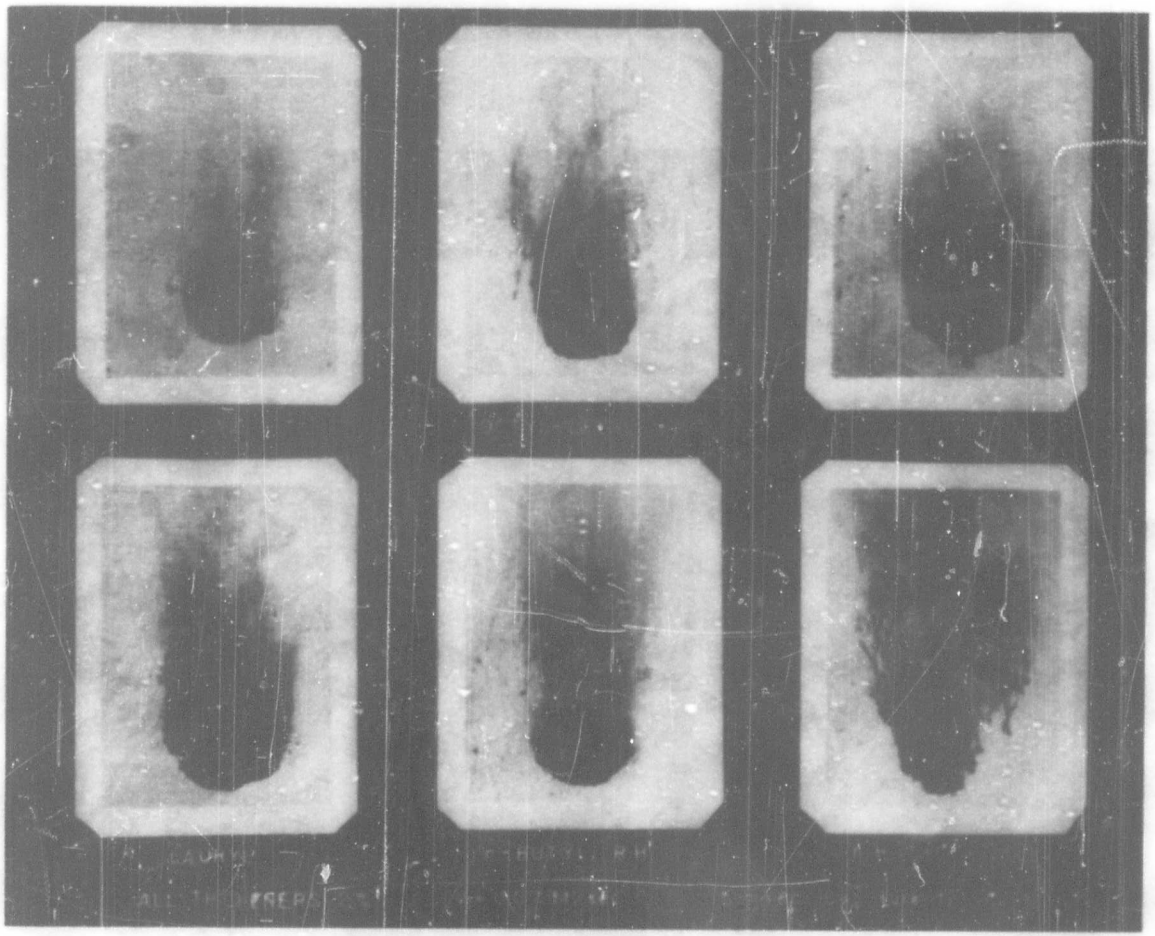

Figure 7

SEVERAL UNSUCCESSFUL METHACRYLATE THICKENERS

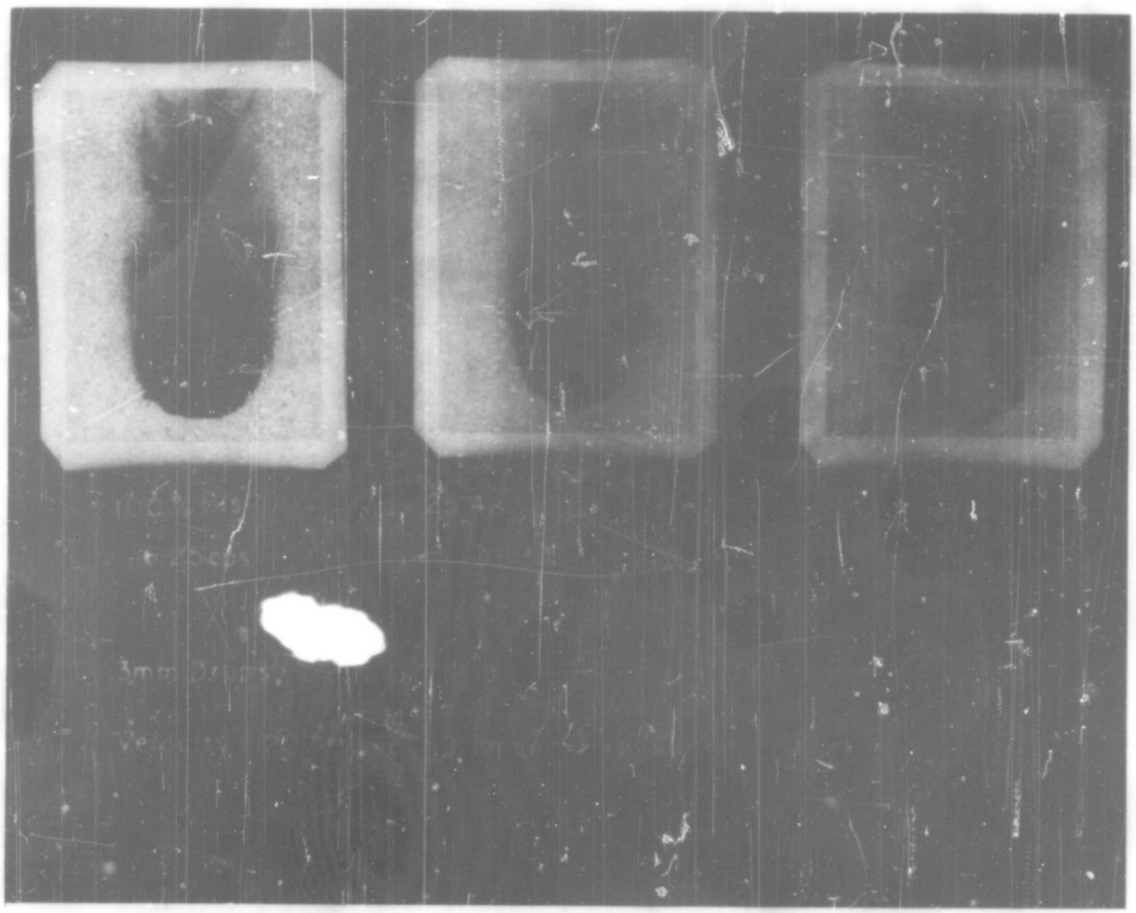

Figure 8

EFFECT OF VISCOSITY ON DROP BREAKUP

References Cited

1. (a) Richardson, E. G., "Mechanism of the Disruption of Liquid Jets," Appl. Sci. Res., A-4, 374 (1954)

1. (b) Richardson, E. G., and Merrington, A. C., "The Break-up of Liquid Jets," Proc. Phy. Soc., 59 (I), 1 (1947)

2. Lane, W. R., "Shatter of Drops in Streams of Air," Ind. Eng. Chem., 43, 1311 (1951)

3. (a) Miesse, C. C., "Correlation of Experimental Data on the Disintegration of Liquid Jets," Ind. Eng. Chem., 47, 1690 (1955).

3. (b) Miesse, C. C., "Recent Advances in Spray Technology,", Appl. Mech. Rev., 9, 321 (1956)

4. Hansen, A. R., and Domich, E. G., "An Experimental Investigation of Impact and Shock Wave Break-up of Liquid Drops," Univ. of Minn. Research Repts. 125 and 130 (1956)

5. (a) Foster, H. H., and Ingebo, R. D., "Evaporation of JP-5 Fuel Sprays in Air Streams," NACA RME55K02 (1956)

5. (b) Castlemen, R. A., Jr., "The Mechanism of Atomization Accompanying Solid Injection," NACA Report No. 440 (1932)

5. (c) Lee, D. W., and Spencer, P. C., "Photomicrographic Studies of Fuel Sprays," NACA Report No. 454 (1933)

6. Lane, W. R., and Dorman, R. G., "Further Experiments on the Shatter of Drops by a Supersonic Air Blast," Porton Technical Paper No. 279. (1952)

7. Blanchard, D. C., Project Cirrus, Occasional Report No. 7, G. E. C. Lab., New York (1948).

THE AERODYNAMIC BREAKUP OF DROPLETS

John W. Corcoran

The George Washington University Research Laboratory

and

U. S. Army Biological Warfare Laboratories
Fort Detrick, Maryland

Since the subject of my talk is an analog experiment for studying the formation of aerosols, I think it is pertinent to sketch a little background information to show how a laboratory interested in explosives became involved in "bath tub" engineering.

The scope of our contract includes the investigation of the factors affecting the explosive dissemination of aerosols. Mathematically this may be written:

$$B(t) = R_p(t)\, R_{CT}\, \epsilon^{-at}$$

where B(t) represents the fraction surviving of a disseminated bacteriological agent at any time, t; $R_p(t)$ represents the physical recovery and depends chiefly on aerosol size; R_{CT} is the fraction surviving the thermal and cavitation effects of the explosion; and the exponential represents the normal bacteriological death rate of the organism. The last term is completely determined by the organism. R_{CT} depends on the type of organism and its location with respect to the explosive. $R_p(t)$ depends on the physical properties of the liquid, the geometry of the charge and the strength of the shock. It is in connection with this term that we are interested in droplet breakup.

In this regard our laboratory has primarily based its work on that of Dr. Boyd, formerly chief of Applied Research Branch of M Division, and his paper, "Theory of the Sedimentation and Decay of Aerosols" (BLIR-7). He shows that for a continuously stirred aerosol, as in a closed chamber where most biological testing is carried on, the fallout due to Stokes' Law settling from an aerosol of uniform particle size leaves a remainder given by

$$R_r(t) = \exp\left[-\frac{4}{V}(\rho_1 - \rho_2)\frac{2g}{9\eta}\, r^2 t\right]$$

The term Φ is the ratio of the chamber area to its volume, ρ_1 and ρ_2 are the densities of the droplet and the medium, η the viscosity of the medium, g the acceleration of gravity, r the radius of the droplet and t is again time.

For an aerosol with a range of particle sizes, Boyd points out that it is necessary to sum the recoveries from the various size classes. Thus, the total recovery from all size classes is given by

$$R_p(t) = C_1 \epsilon^{-kr_1^2 t} + C_2 \epsilon^{-kr_2^2 t}$$

$$+ C_3 \epsilon^{-kr_3^2 t} + \ldots \text{ etc.},$$

where C_1, C_2 and C_3, etc. represent the fraction of the total mass of each radius. This series may be represented more concisely by the integral

$$R_p(t) = \int_0^\infty f(r)\, \epsilon^{-kr^2 t}\, dr$$

where f(r) is a distribution function representing the fraction of the total mass in the size interval dr, of size r, and the integration is carried out over all size classes.

While this is a complete mathematical expression it is not very useful until the function f(r) is defined. In order to use this equation, two things are necessary. First a form of distribution must be found which fits the aerosol, and second it must be of such a type as to permit the integration to be carried out.

Boyd himself suggests the Rossin-Rammler type of distribution primarily because it can be integrated. This is

$$f(r) = A(\nu)\, r^\nu\, \epsilon^{-br^2}.$$

Figure 1 shows a normalized form of these distributions. All curves contain a unit area. A generalized abscissa $\frac{r}{\bar{r}}$ is used, where $\bar{r}$

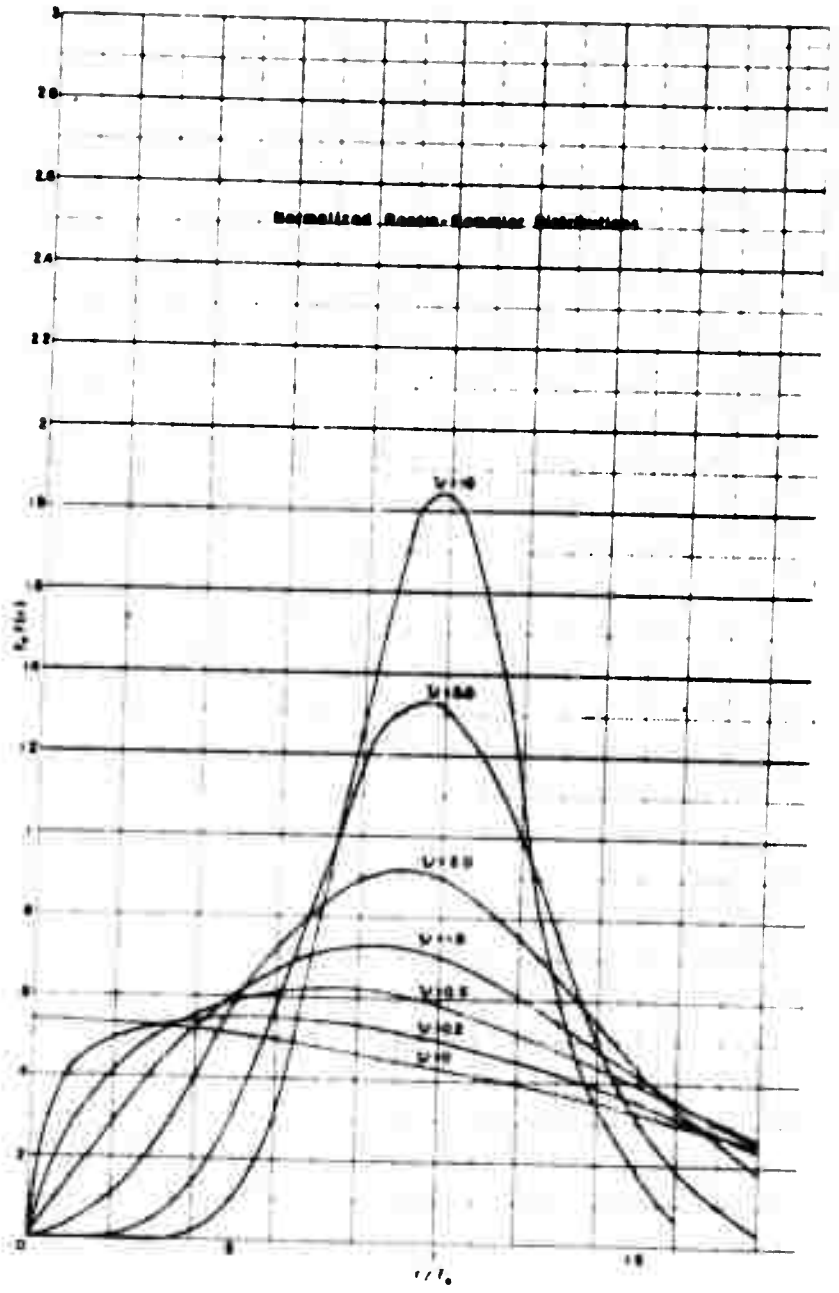
Normalized Range-Doppler Distribution
2.8
2.6
2.4
2.2
2
1.8
1.6
1.4
1.2
1
.8
.6
.4
.2
0
1
10
V=10
V=5.0
V=3.0
V=2.5
V=2.2
V=2.0
V=1.8

FIGURE 1

is the mass median. Thus, ν is the only parameter. It may be seen that low values of ν imply broad, flat distributions, whereas for high values of ν the aerosol particles approach uniform size. Integrating the Rossin-Rammler type of distribution gives a recovery function of the form:

$$R(t) = \left[1 + \frac{2r_o^2 t}{(2a + \nu)T}\right]^{-\frac{\nu+1}{2}} .$$

Figure 2 shows the form of these recoveries, again with ν as a parameter. It may be seen that for equivalent mass median radii low ν distributions decay less rapidly than high ν distributions. (Considerations of surface energy indicate a ν of zero can only be approached since this would require an infinite surface energy.)

I have gone through this to give you an idea of why we are interested in knowing what the droplet distribution f(r) is; how it dictates the physical recovery; and the necessity for knowing a scaling factor, the mass median radius, $\bar{r}$, and ν, the spread parameter. The principal object of the test to be described is to justify the assumption of a Rossin-Rammler distribution or to find a better one.

Our studies indicate that there are two types of aerodynamic breakup; one involves an increasing velocity, and the other a decreasing velocity. To give you some idea of how these arise, let me show you this chart of pictures taken of our conical devices. (Note by Editor: Unfortunately, it was not feasible to reproduce these pictures in this report. However, the explanation which follows is rather complete.) We have the complete expansion process for several mass ratios, that is, the ratio of the mass of fill to the mass of explosive was varied. Successive pictures in each row were taken at different times during the expansion. In all of these pictures the charge is silhouetted against a bright field of light to permit simultaneous observation of the profile of the fill and the position of the shock wave as a schlieren. In the larger mass ratios the shock wave is always observed in front of the fill. The air behind the shock has a mass velocity, u, and the aerodynamic forces acting on the fill may be considered to be proportional to the difference between the fill and mass velocities (v - u). This difference, initially zero, increases throughout the expansion. As an approximation it can be assumed to be due to the uniform acceleration of the fill:

$$(v - u) \simeq \dot{V}t.$$

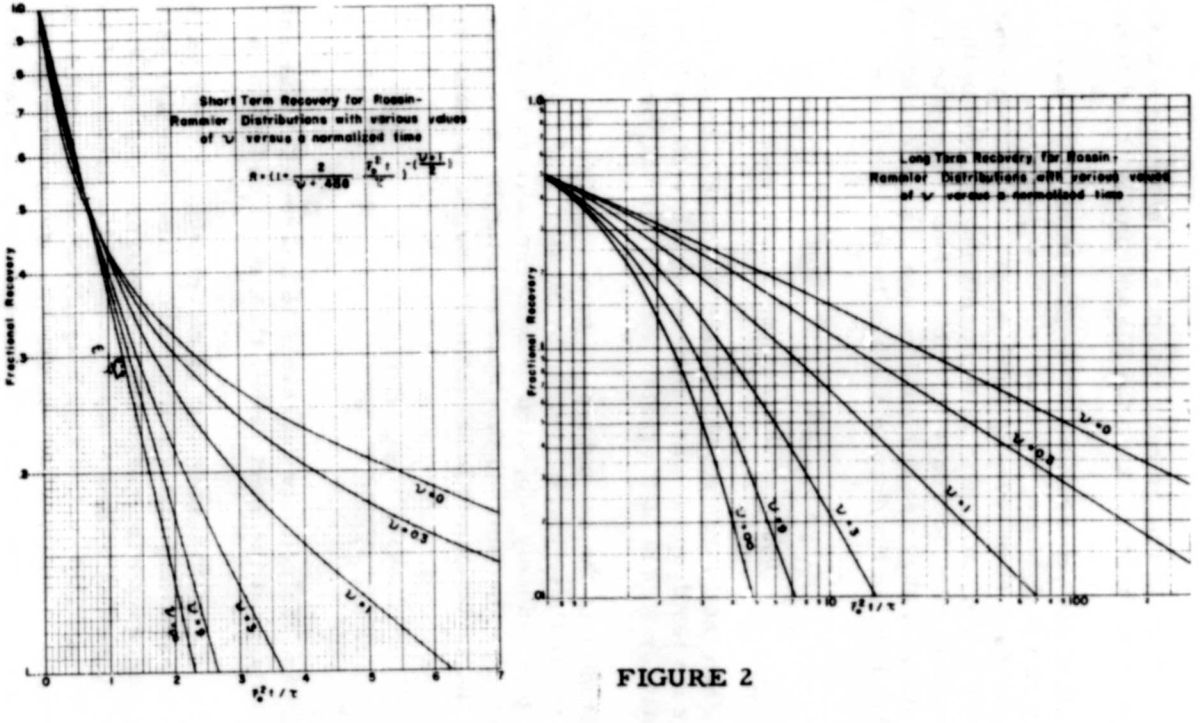
Short Term Recovery for Rosin-Rammler Distributions with various values of ν versus a normalized time
Fractional Recovery
ν=0
ν=0.3
ν=1
ν=2
ν=3
ν=10
Long Term Recovery for Rosin-Rammler Distributions with various values of ν versus a normalized time
Fractional Recovery
ν=0
ν=0.3
ν=1
ν=2
ν=3
ν=10
100

FIGURE 2

Now, on the other hand, in the low mass ratios, the shock wave does not appear until late in the expansion. The fill has initially penetrated the shock and is moving with a high velocity in still air.

Intermediate mass ratios display an alternation of these effects with first the shock in front, then the fill and finally the shock.

All of the experiments in the literature that I have encountered imply a study of either one or the other of these two types of breakup. Thus, Bond and Richardson have investigated the stability of drops under the acceleration of gravity and their experiments correspond to the first case, where there is a gradual increase in velocity and breakup with time. As a criterion of stability they use the Bond number, a dimensionless ratio of the hydrostatic head within the drop to surface tension pressure

$$B = \frac{\rho_D \, gd}{\sigma/d} = \frac{\rho g d^2}{\sigma} \quad .$$

When the hydrostatic head becomes much larger than the surface tension pressure the drop becomes unstable and breakup will ensue. They have found that for values of B greater than 15 this will probably occur.

Studies of the second type of breakup were made in an experiment by Volynski and in those just described by Messrs. Wilcox and Cohen. In these the drop is suddenly subjected to an abrupt change in its relative velocity with respect to the medium. In this case the stability criterion may be given as a ratio of the aerodynamic pressure to the surface tension pressure

$$W = \frac{\rho_M \, V^2}{\sigma/d} = \frac{\rho_M \, V^2 d}{\sigma} \quad .$$

In the second case the velocity decreases to a terminal value and the breakup occurs most rapidly at the start rather than at the end as in the first case.

The direct measurement of an aerosol distribution is a difficult process. Even assuming that a sufficiently refined sampler exists, one is plagued by the necessity for correcting for evaporation, coalescing and perhaps drop spreading. Direct observation of the breakup of a droplet in an explosion is also difficult. The high magnification required to see the droplet necessarily results in motion blur on the film of the order of the drop size. To avoid the difficulties which are inherent in the measurement of aerosols, it was decided to study an analogous physical problem subject to the same

stability limitations and the same dynamic laws but with magnified sizes and time scales.

To study the first type of breakup an experiment similar to that of Bond and Richardson using gravitational forces was chosen. However, it was found that considerably shorter falling distances would produce the same breakup if a dense liquid such as mercury was dropped through water. Thus, two feet of drop with mercury and water would be equivalent to a drop of more than 100 feet for water falling through air. This also had the advantage of eliminating the problem of evaporation.

A method was also sought for solidifying the droplets to permit size determination from droplet mass. The complete setup for such a test is shown on Figure 3. A drop of molten Wood's metal of known weight was held at the top of the tank in water heated to 65°C. It was released and allowed to break up in hot water and then was chilled while still falling to the bottom of the tank. Around the bottom you will see an ice brine bath which cooled the water to 4°C. Fragments were collected in the bottom to be assayed by weight. Figure 4 shows the fixture for releasing the drops. The experimental technique here is one of the more difficult problems involved in the test. Since the drops used are inherently unstable the release device must operate quickly enough to avoid any premature breakup. The actual release process is shown in Figure 5. The drop here is 40 grams of mercury, which was used in preliminary tests. Figure 6 shows the breakup process more completely using a drop of 38.6 grams of Wood's metal.

The breakup of large and small (the terms are used relative to the critical Bond number) drops appear to actually differ in mode. With the large drop you can see the process occur on the periphery, where the velocity is high, and the pressure vector is outward from the drop. Figure 7 shows that the shape of a drop near critical size (4 grams) changes several times before breaking up. (It is well known that small stable drops oscillate between oblate spheroidal and ellipsoidal shapes.)

Figure 8 shows some samples of recovered fragments. The larger pieces are concave convex discs whereas the small fragments are spherical. After enough tests were made with one drop size to give 300 or more fragments, they were assayed by weight and fractional mass distributions were determined. Figures 9 to 12 show the distributions obtained for four different drop sizes. It will be seen that with smaller initial drops the spread of the distribution narrows. Carrying this process to the limit, one would expect drops much smaller than critical to give infinitely narrow distributions.

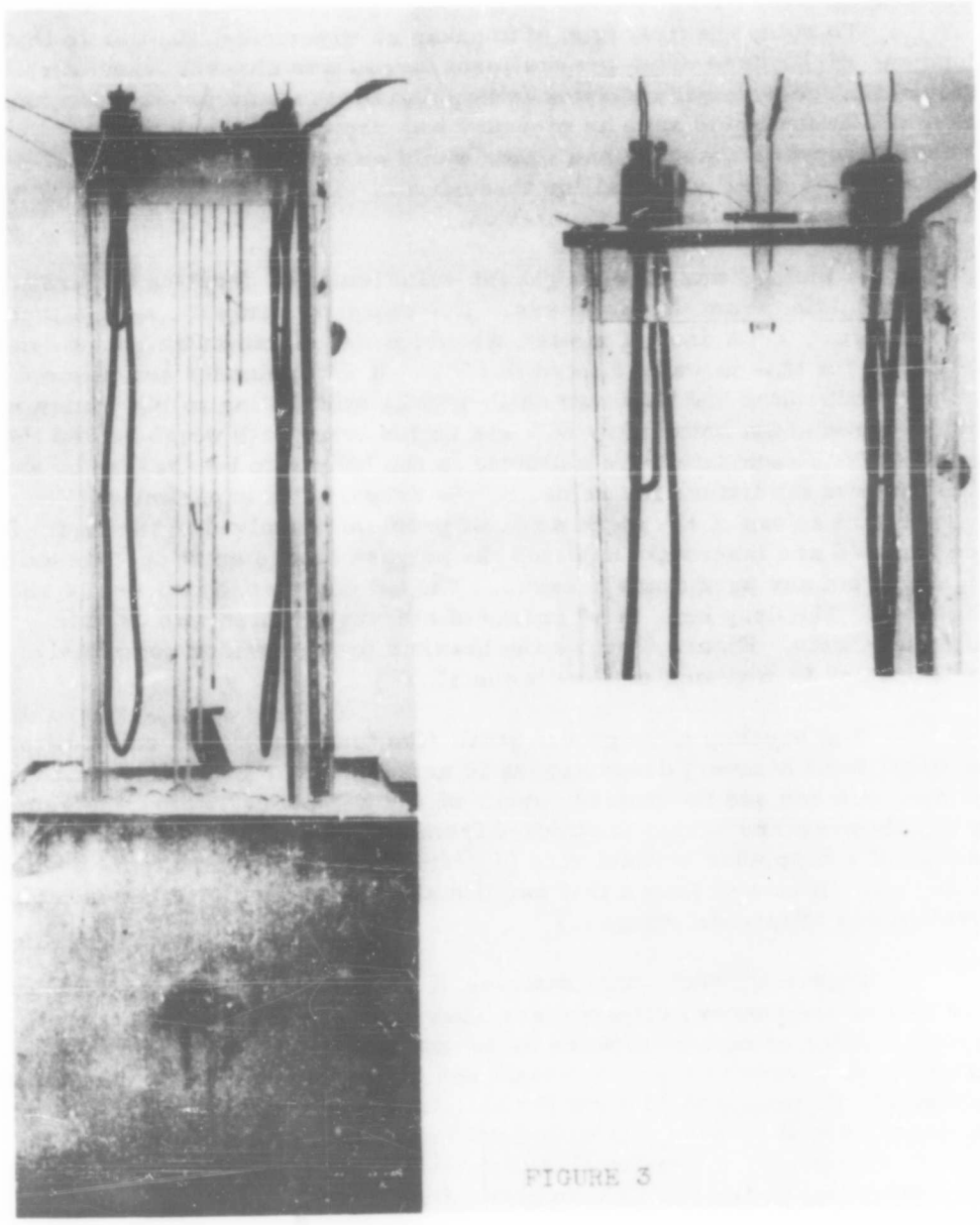

FIGURE 3

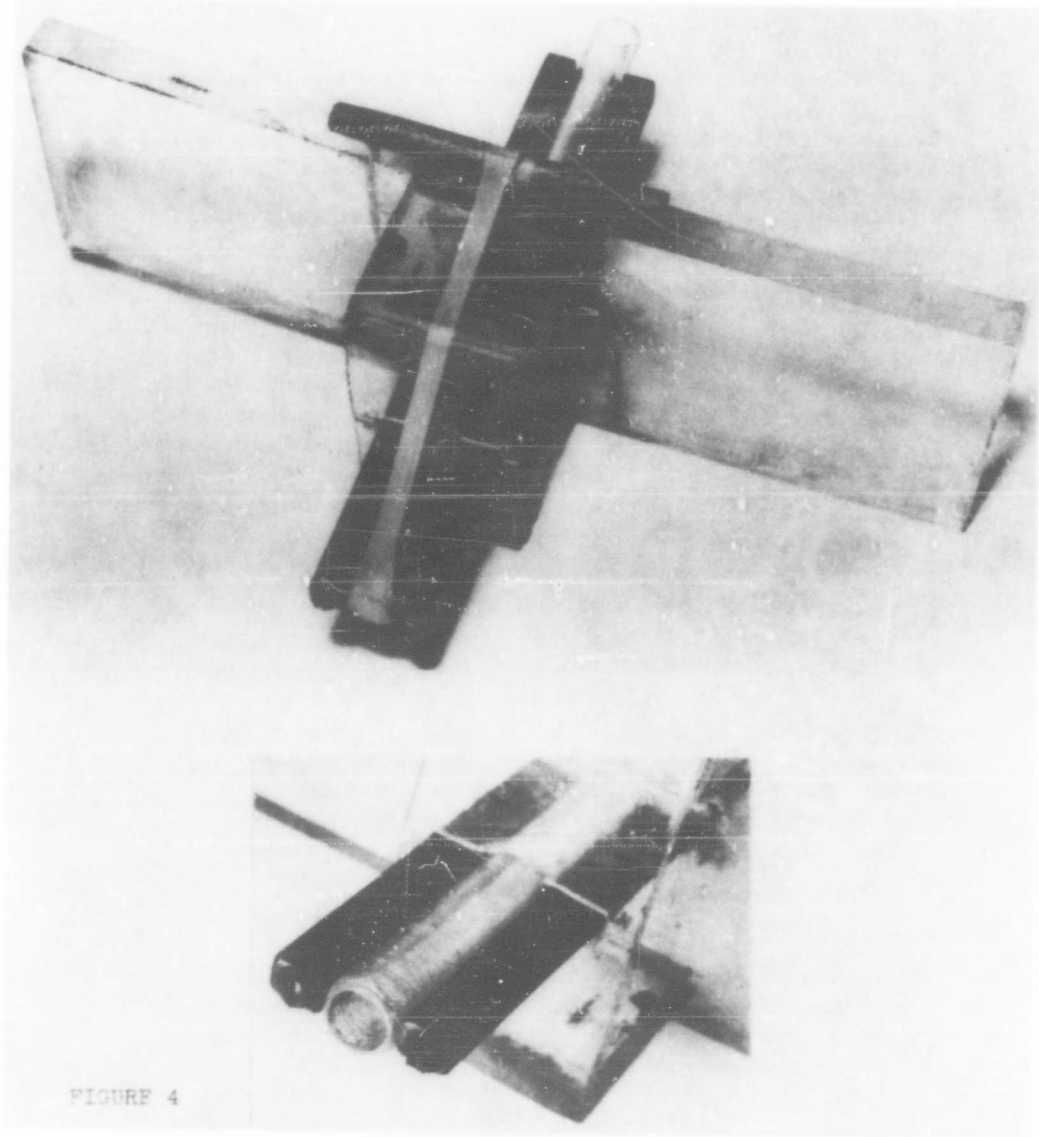

FIGURE 4

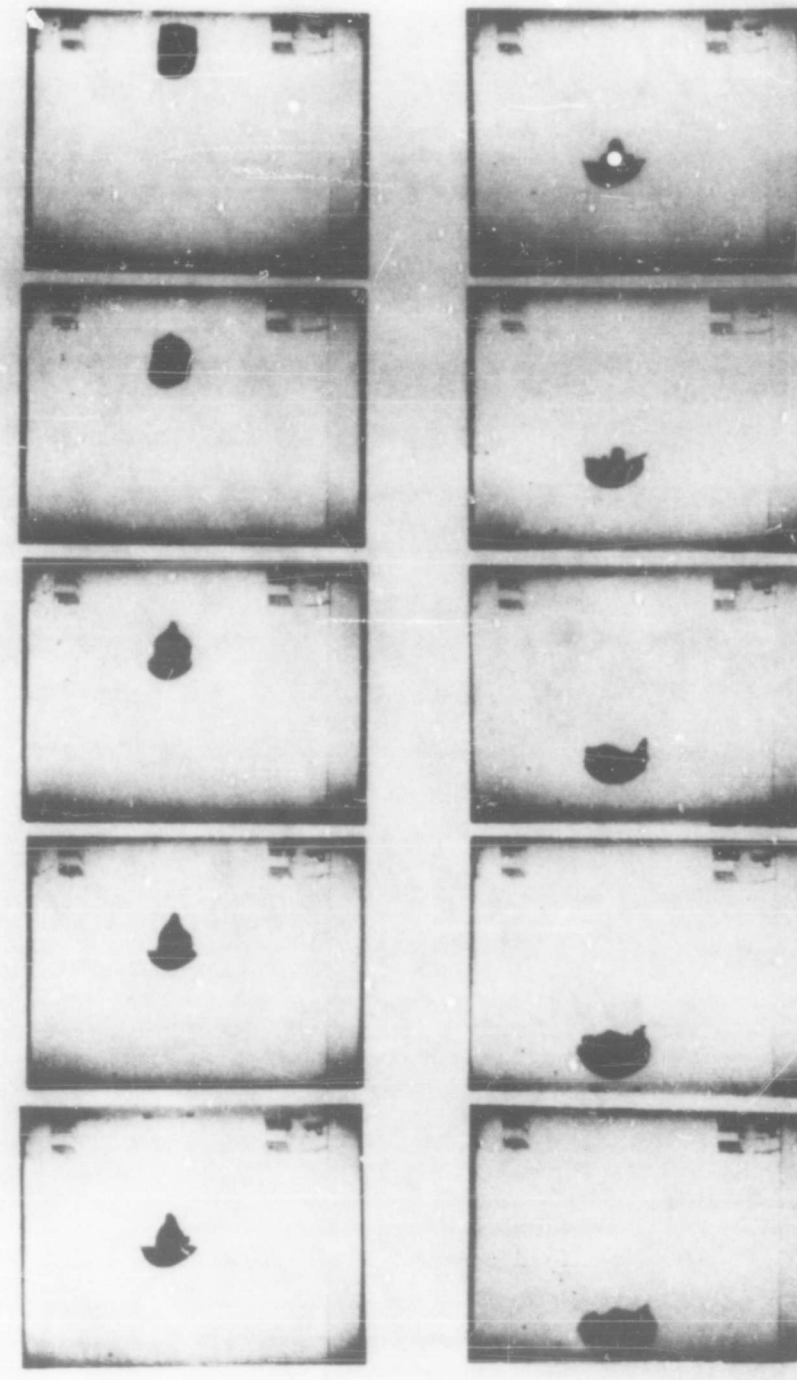

FIGURE 5

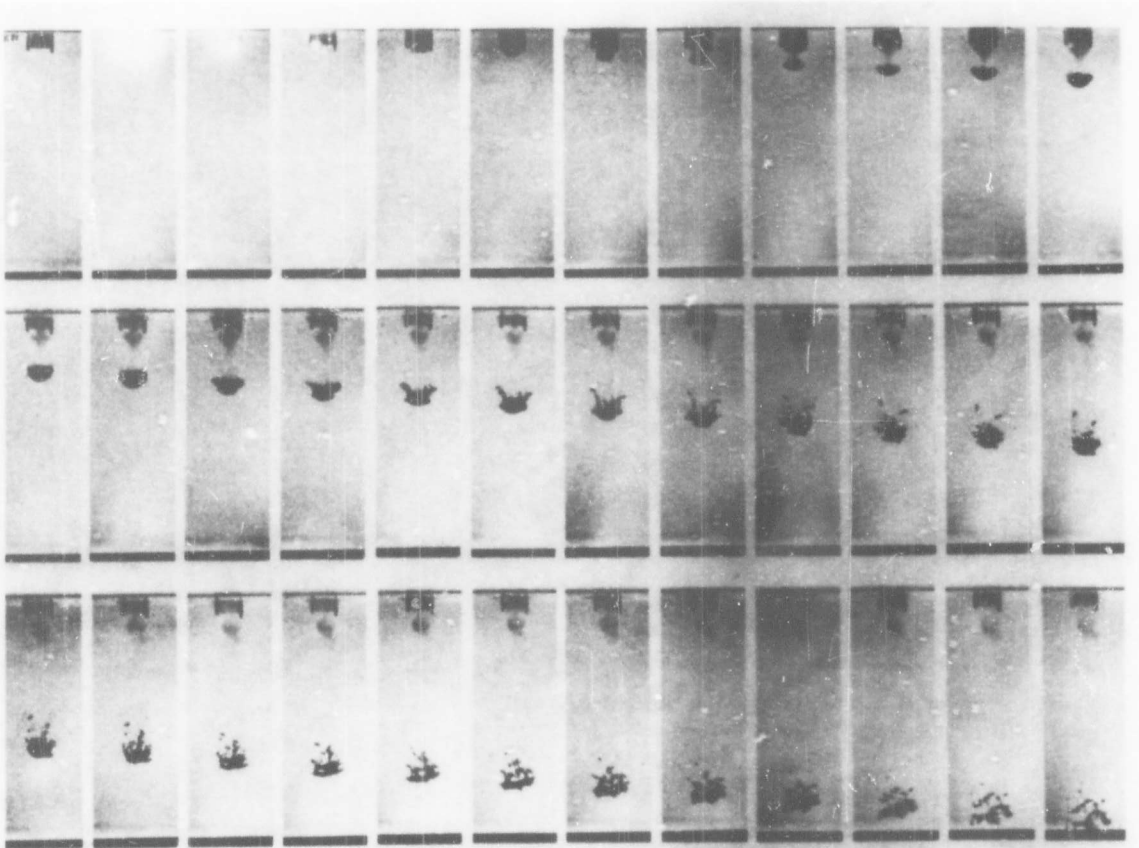

FIGURE 6 Breakup of a 38.6 grams drop of Wood's metal Taken at 80 frames / sec

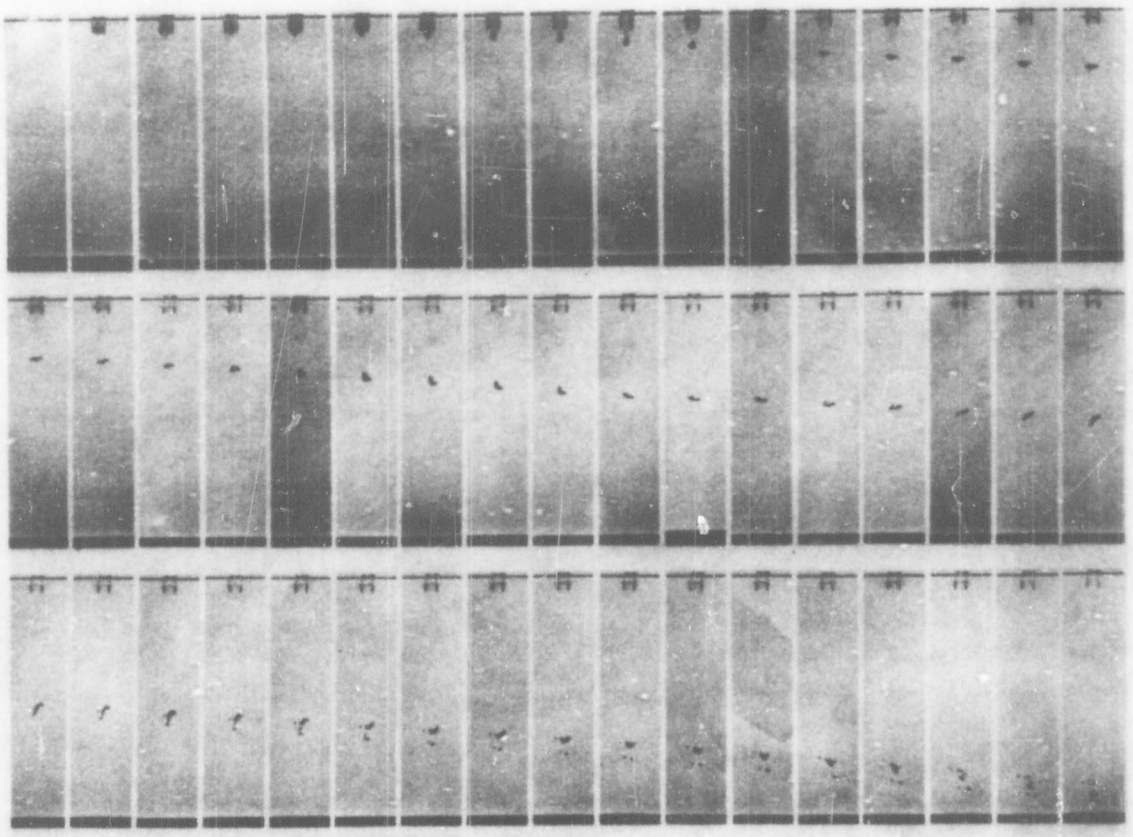

FIGURE 7 Breakup of a 4 gram drop
of Wood's metal
Taken at 128 frames / sec

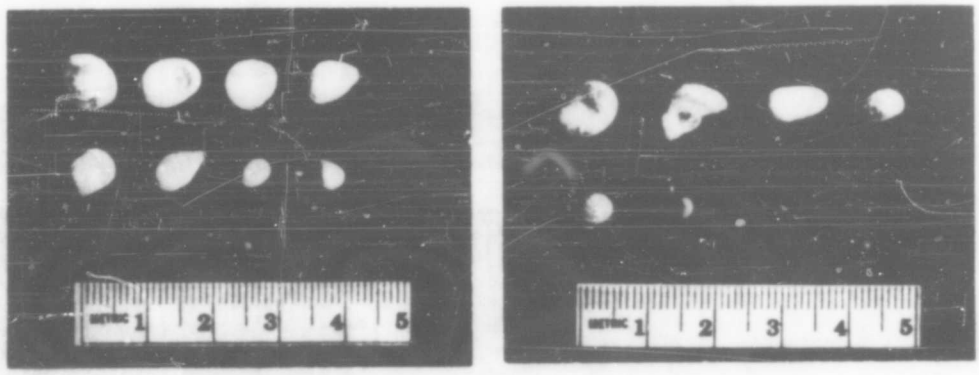

FIGURE 8

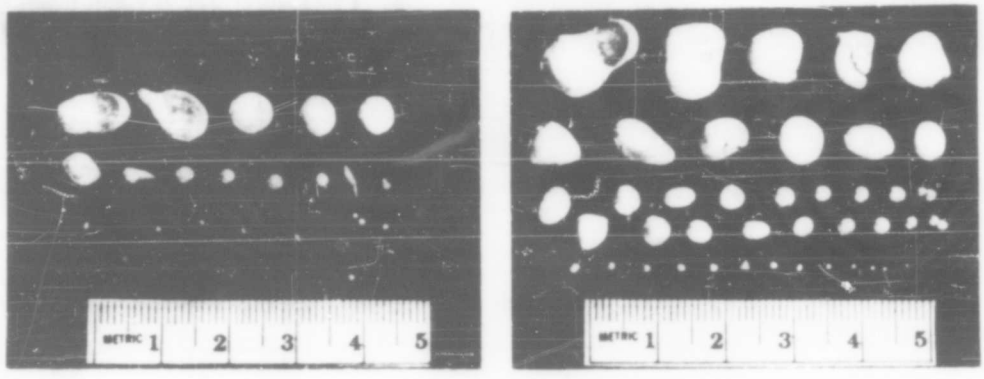

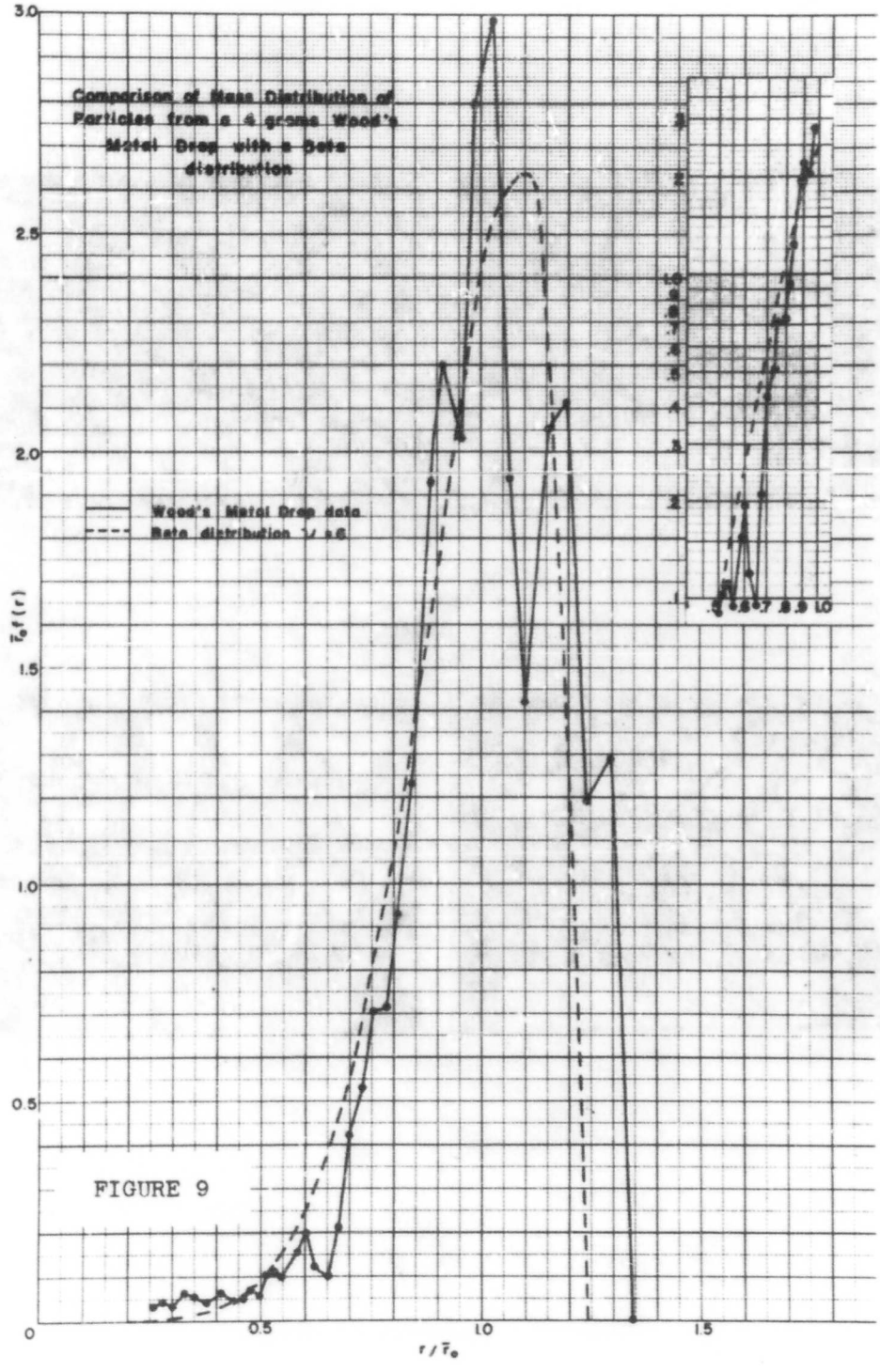
Comparison of Mass Distribution of Particles from a 4 grams Wood's Metal Drop with a Beta distribution
Wood's Metal Drop data
Beta distribution γ = 2.6
$\bar{r}_o f(r)$
$r/\bar{r}_o$
0
0.5
1.0
1.5
2.0
2.5
3.0

FIGURE 9

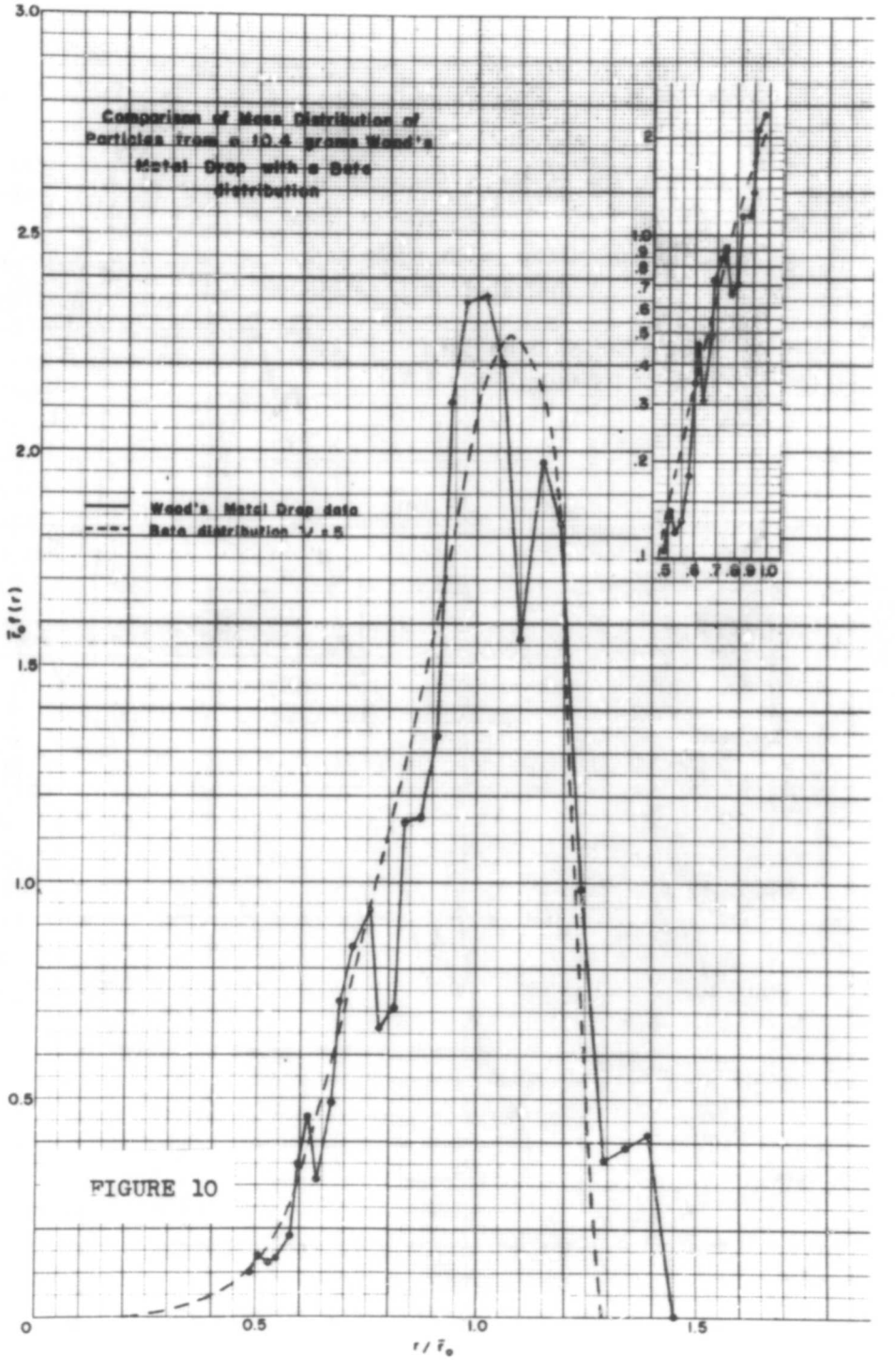
Comparison of Mass Distribution of Particles from a 10.4 grams Wood's Metal Drop with a Beta distribution
Wood's Metal Drop data
Beta distribution
3.0
2.5
2.0
1.5
1.0
0.5
0
0.5
1.0
1.5
r / r̄₀
f₀(r)

FIGURE 10

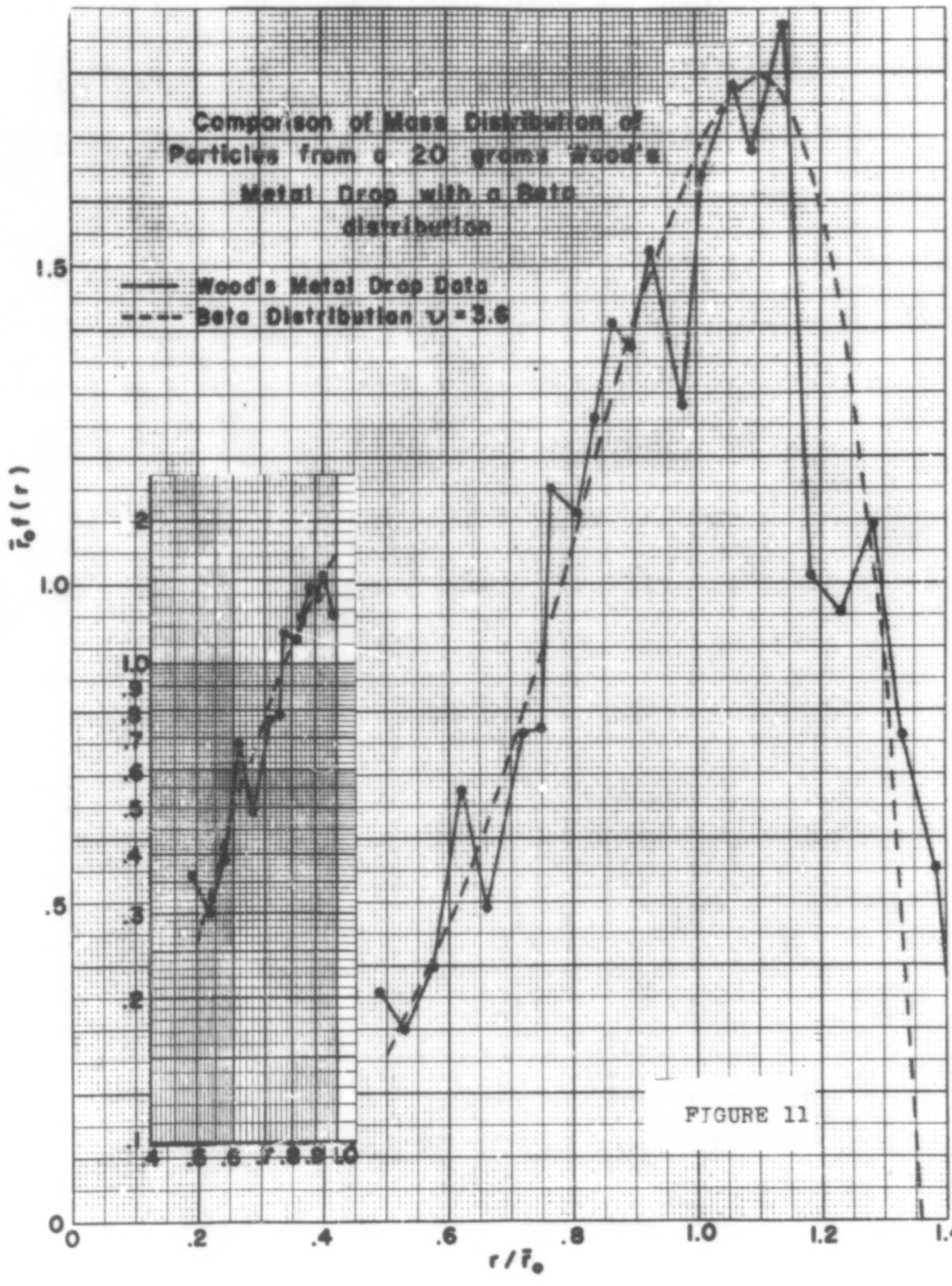
Comparison of Mass Distribution of Particles from a 20 grams Wood's Metal Drop with a Beta distribution
—— Wood's Metal Drop Data
---- Beta Distribution ν=3.6
$\bar{r}_o f(r)$
$r/\bar{r}_o$
0
.5
1.0
1.5
.2
.4
.6
.8
1.0
1.2
1.4

FIGURE 11

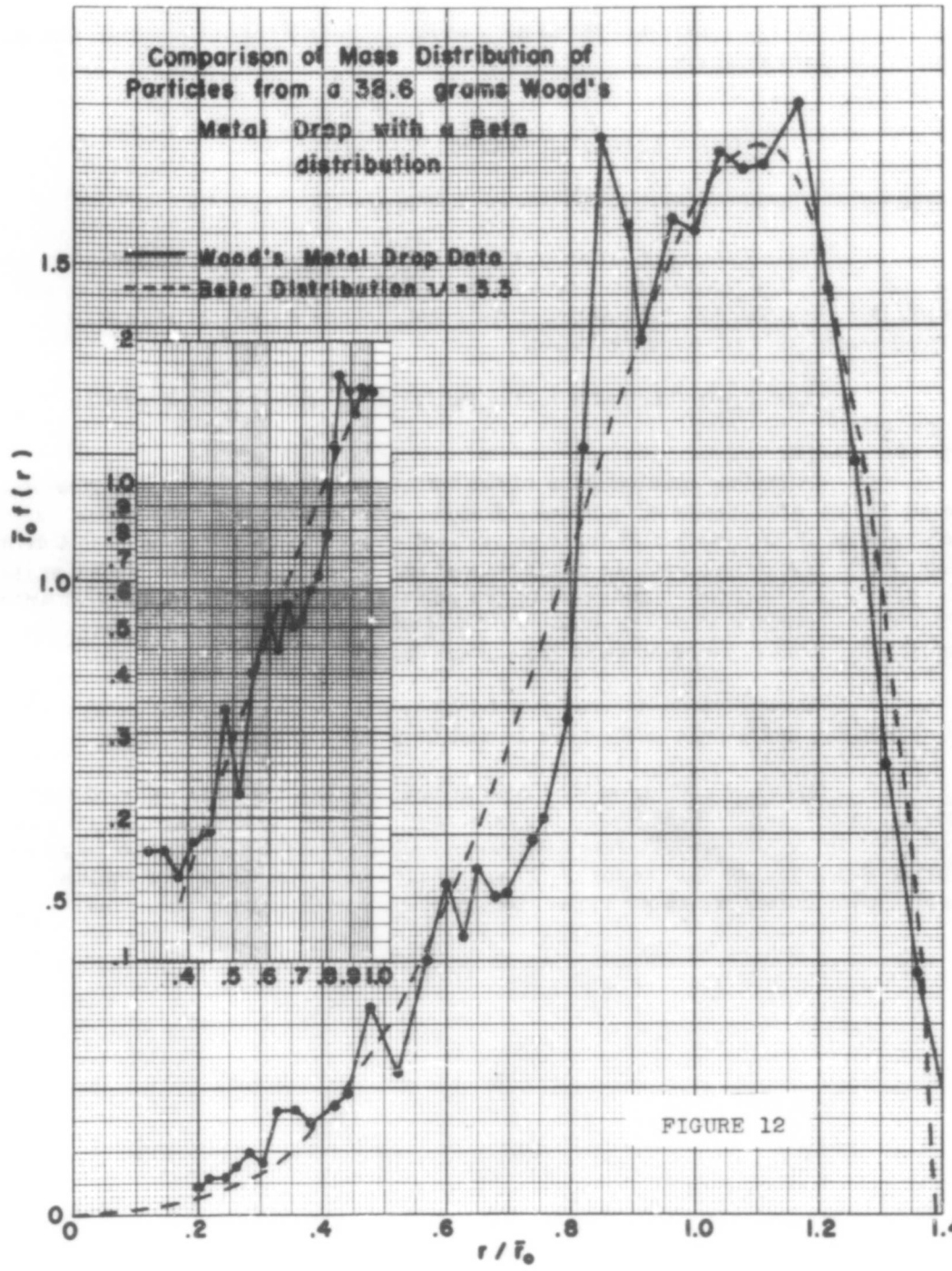
Comparison of Mass Distribution of Particles from a 38.6 grams Wood's Metal Drop with a Beta distribution
Wood's Metal Drop Data
Beta Distribution γ = 5.5
r̄₀ f(r)
r / r̄₀
0
.5
1.0
1.5
.2
.4
.6
.8
1.0
1.2
1.4

FIGURE 12

It was found that these data were generally fitted by a distribution called the Beta function

$$f(r) = A_1(\nu)\, r^{\nu} (1 - \beta r^2)$$

the general classes of which are shown on Figure 13.

This is very similar to the Rossin-Rammler, particularly for low values of ν. The major distinction is that this function implies an upper size cutoff whereas the Rossin-Rammler does not. Since a critical size is hypothesized this is more realistic.

The dependence of ν on the initial drop diameter is shown on Figure 14.

A simple modification of the water tank technique made it possible to study the other class of breakup. Instead of releasing the drop in the water the release fixture was held three to six feet above the surface. A small drop, 0.5 gram, known to be stable in air was used. Upon reaching the water surface the drop had a velocity considerably greater than its terminal velocity in water. The Weber number was thus suddenly changed from below to above that critical for this drop because of the change in ρ_M.

Figure 15 illustrates this breakup process and the resulting distributions are shown in Figures 16 and 17 for two initial velocities.

While the study of this type of breakup has not been carried far enough to thoroughly understand the effects of various parameters, it may be seen that the mass median size decreases and the distribution broadens as the initial Weber number increases. There is also evidence here of a multi-modal distribution which we expect to smooth out with higher velocities.

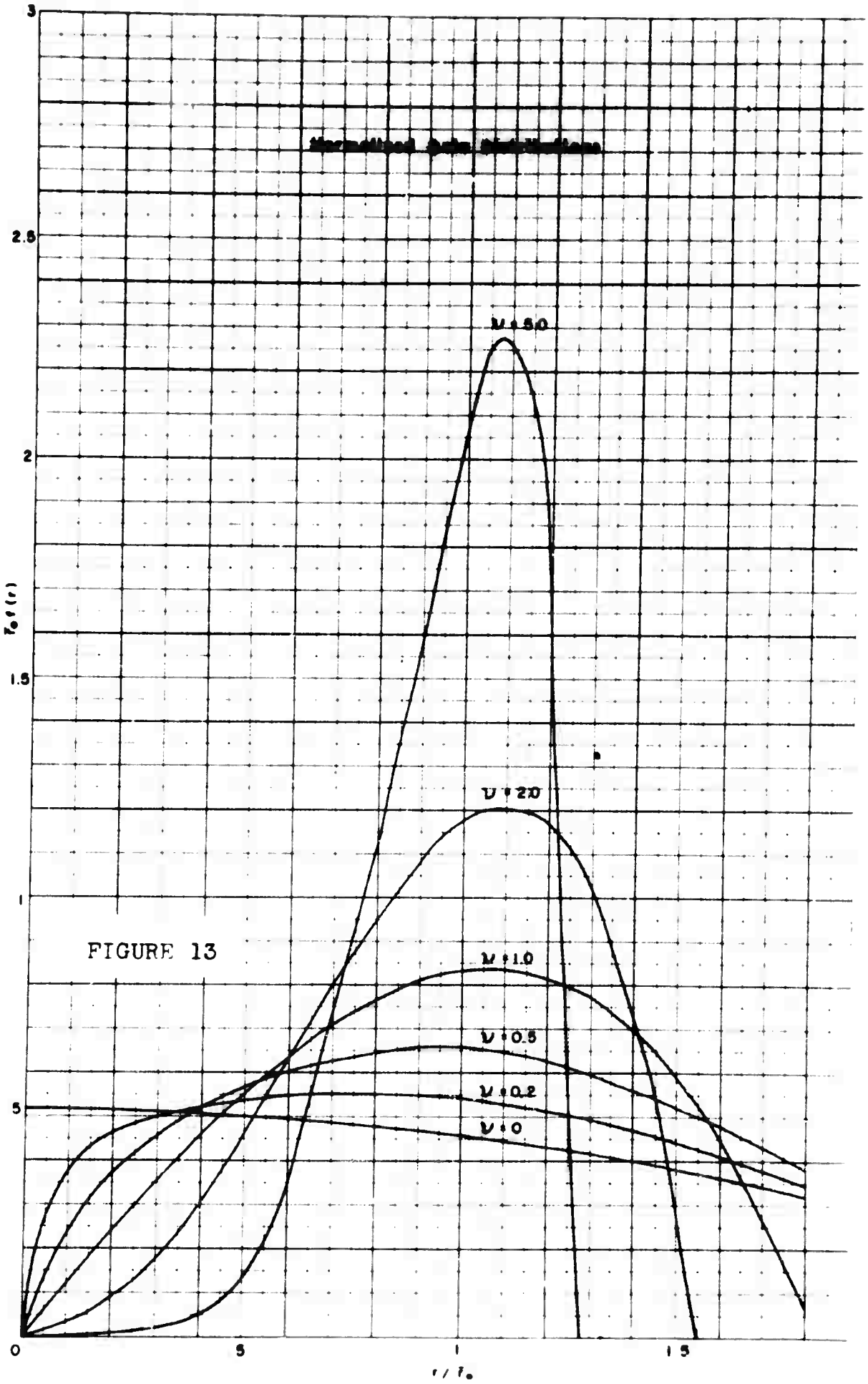

FIGURE 13

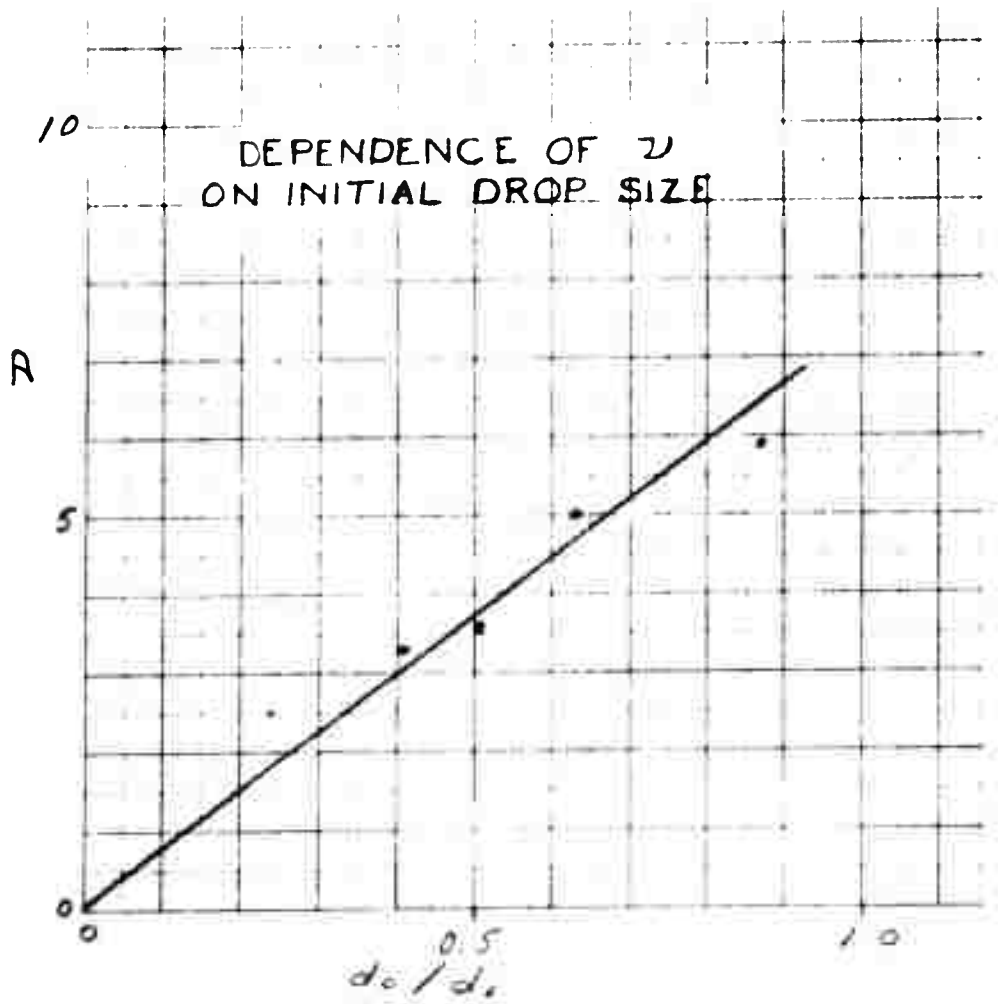

FIGURE 14

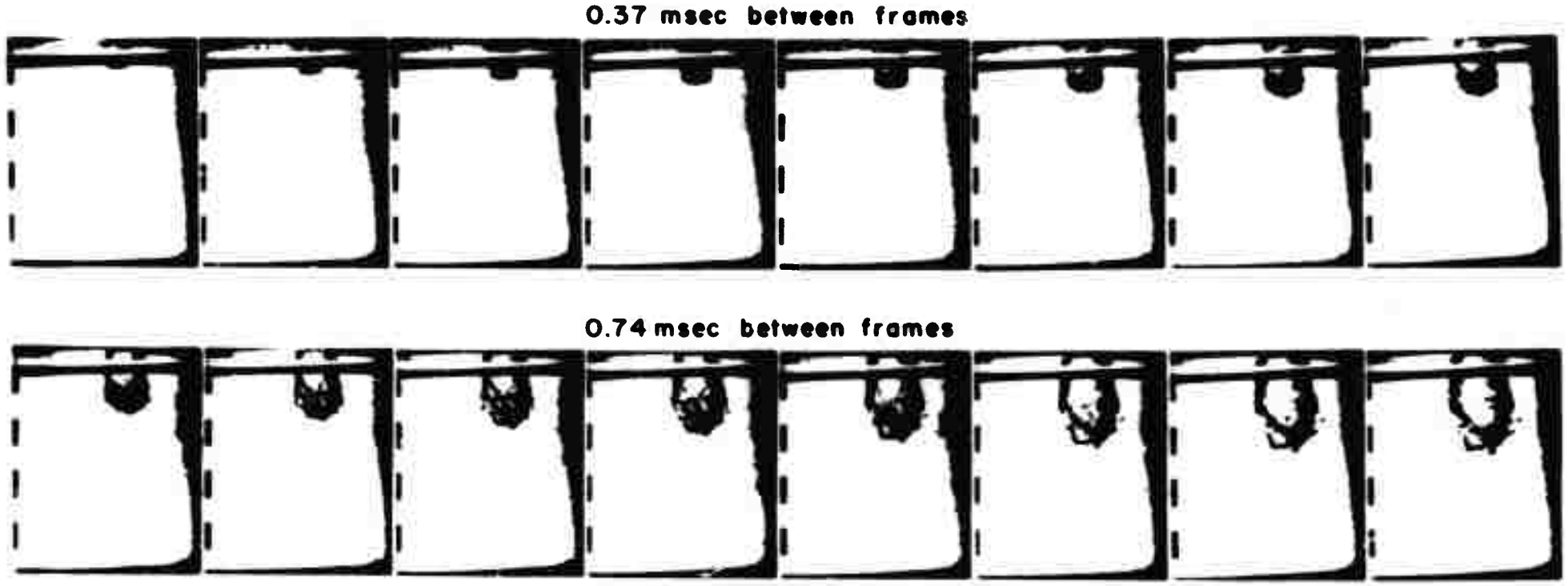

FIGURE 15 Breakup of a 0.5 gm drop of Wood's metal impacting a water surface at 580 cm/sec Fiducial marks are 1 cm long

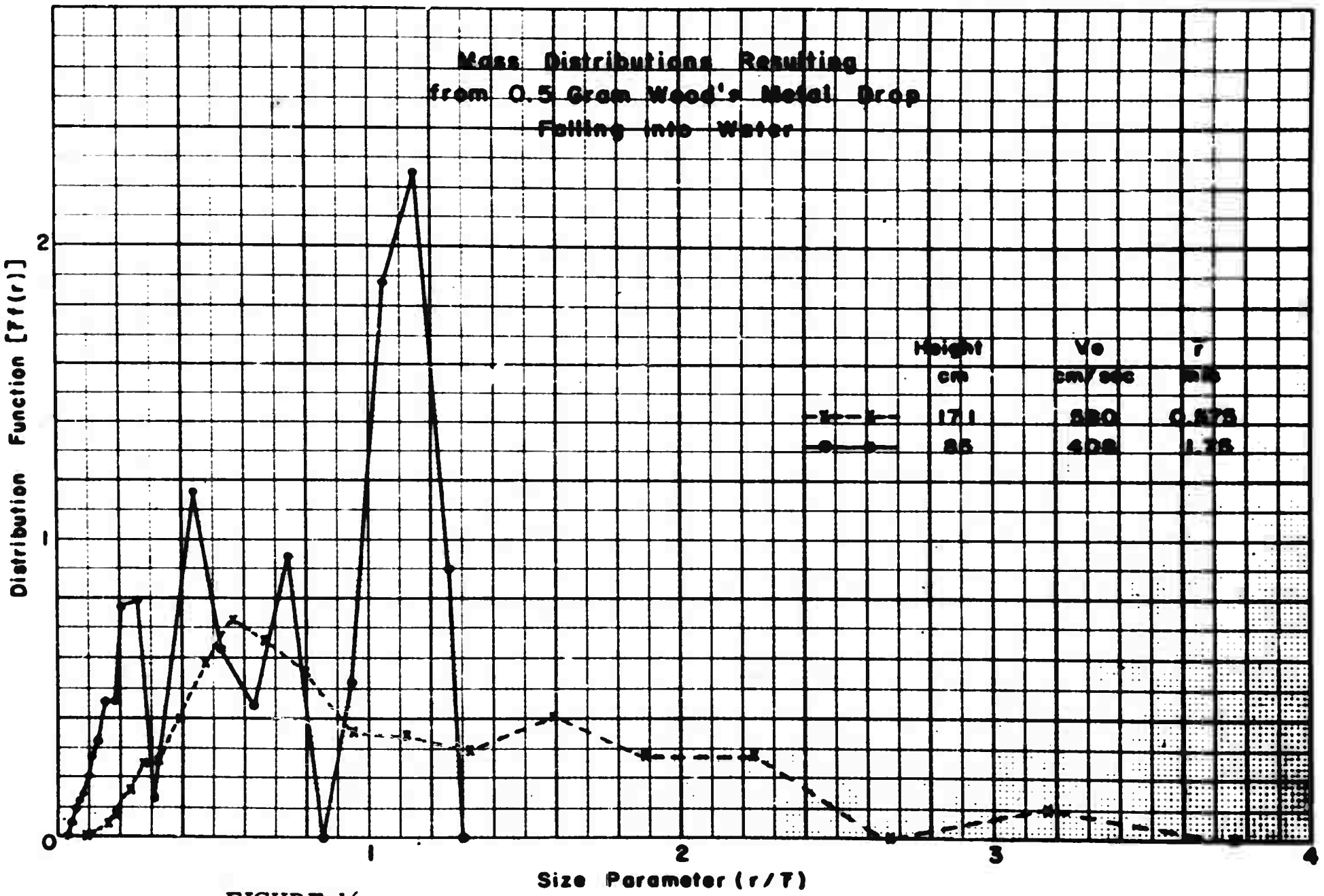
Mass Distributions Resulting
from 0.5 Gram Wood's Metal Drop
Falling into Water
Height
cm
Ve
cm/sec
r
mm
17.1
580
0.575
85
408
1.35
Distribution Function [Tf(r)]
2
1
0
1
2
3
4
Size Parameter (r/T)

FIGURE 16

Comparison of Aerodynamic Calculations With Aerosol Data and Explosive Expansion Results

(All data from conical devices with 6 gm PETN $\rho = 1.2$)

Smooth Charges

Mass Ratio	Initial Mass Median Diam. (μ)		Maximum Diameter (μ)		Acceleration cm/sec^2 x 10^7		Acc. Ratio
	From Recovery Data	Before Evap.	Calc. For $\nu = 0.3$	Meas. By Imping.	Calc. From Bond No.	Meas. In Expl.	
3	14.6	44	103	90	0.85	19.2	23
6	24	72	170	184	0.256	10	38
10	36.8	110	252	320	0.142	6.6	46

FIGURE 17

CWL TECHNICAL MEMORANDUM 5-1

CARAMU NOTE # 1

IMPACTION EFFICIENCY OF AEROSOL PARTICLES

15 January 1958

S. J. Magram

CARAMU Office
U. S. Army Chemical Warfare Laboratories
Army Chemical Center, Maryland

Armed Services Technical Information Agency

ARLINGTON HALL STATION
ARLINGTON 12 VIRGINIA

Abstract

Previously published data on impaction of particulate matter on cylindrical targets have been transformed into a form more useful for field evaluation for the range of parameters of interest for CW effects. These parameters are particle sizes 5-500 microns, wind speeds 2-20 miles per hour, and targets of 2, 10, 20, 35 and 50 cm. diameter (approximating the finger, arm, leg, torso and entire body of an average man). Curves of impaction efficiency for these values are given as Figures 2-7, for use in evaluating sampler and man data from field and wind tunnel experiments.

Table of Symbols

A area of target - projected area to the wind direction

C concentration of agent in cloud passing target

D_c characteristic linear dimension of impaction systems

D_p particle size

$N_D \equiv (\rho_p V/18\mu\, D_c)^{1/2} D_p$ - size parameter representing dimensionless particle size

N_I - fraction of total number of particles of size D_p which impact on the collecting surface

$N_{Re} \equiv D_p \rho_g U/\mu$ - Reynolds number of particle

$N_{\rho_g} \equiv 9\rho_g{}^2 V D_c/\rho_p \mu$ - parameter accounting for gas inertia effects during those times and under those conditions when Stokes' resistance law does not apply to the particle's motion

t - time

V - characteristic gas velocity in impaction process

μ - gas viscosity

ρ_g - gas density

ρ_p - particle density

I. Introduction

The purpose of this study is to employ the principles of inertial impaction to calculate the impaction efficiencies that could be expected on man in various situations for use in evaluation of wind tunnel and field data.

It is quite apparent that it would be impractical to obtain direct experimental data on the impaction efficiencies of human targets over all particle size distributions of droplets, all wind velocities, and all effective sizes of targets of chemical warfare interest. It is therefore desirable to determine to what extent theoretical calculations can be relied upon and whether it is possible to characterize the arms, legs, body, fingers, and head of man as being equivalent to cylindrical objects of certain diameters.

II. Theoretical

In a cloud of any given concentration the amount of liquid particles that will impact on a given surface depends on a variety of parameters. Before listing the possible factors the following problem is presented. Assume a cloud with a distribution of particle sizes moving at a given wind speed. If the projected area of the target is A, the wind speed V, the concentration of the liquid particulates C (including all particle diameters), then in time t there will be M grams passing through the area A so that

$$M = AVCt$$

However, the mass of liquid actually impacted on a target is m, and the impaction efficiency $\frac{m}{M}$ may vary from zero to one. Actually the impaction efficiency is greatly dependent on particle diameter and this value of $\frac{m}{M}$ is the integrated value over all particle diameters in the cloud for any specific target. A more detailed discussion is given in the Appendix.

It is the common practice to characterize an aerosol by determining the mass median diameter (MMD). However, in many cases as will be pointed out in this report, the impaction efficiency is markedly dependent upon diameter. There are many cases in the literature, especially in the region of particle diameters 5-20 microns, where a very small impaction efficiency is reported, and the particle size distribution of the aerosol is such that a significant fraction of the particles is very much larger in diameter than the MMD. In such cases it is highly likely that the

entire impaction is due to these larger particles and not to those at the reported MMD. It is therefore a mistake to report an aerosol cloud in terms of a single constant such as the MMD. Rather the entire distribution should be determined in order more fully to elucidate the relative behavior of the various fractions thereof.

Assume that by some independent measurement the particle size distribution has been determined:

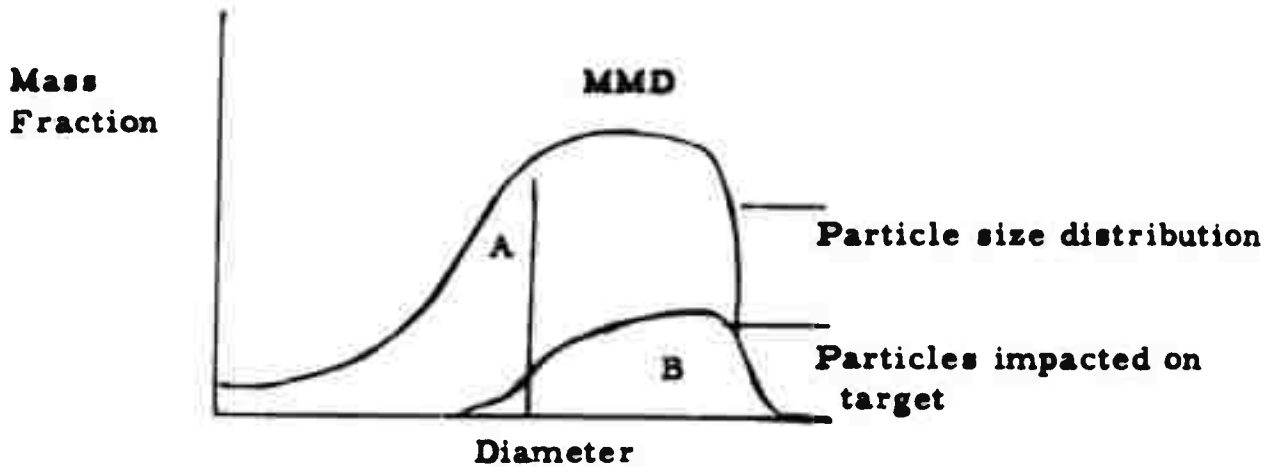

Usually the distribution gives an asymmetrical curve such as area A in the above sketch. A given sampling device or impaction target will trap a distribution as characterized by curve B. Since the impaction efficiency increases with the particle diameter, the over-all impaction efficiency, which is the ratio of area B to area A, will receive the greatest contribution from the larger diameter side of the MMD. One can see from this sketch that the contribution by particles equal to the MMD may be very small under such circumstances. However, the ratio of the ordinate B to the ordinate A for any given particle size should be equal to the impaction efficiency for the given target size and wind velocity.

The main purpose of this report is to produce graphs that will give the theoretical impaction efficiencies on cylinders as a function of particle diameter and other pertinent parameters, so that we will be able to calculate curve B if we know the initial distribution in the aerosol cloud as indicated by curve A. Curve A will vary with any given means of dissemination of agent and with time and meteorological conditions but this can be calculated or estimated. The problem then resolves itself into listing the factors that affect curve B, and calculating impaction efficiencies based on certain assumptions discussed below.

The following considerations may affect the amount of agent that will impact on man. The relative importance of these factors are discussed in Section IV.

1. Particle size distribution in a given concentration.

2. Wind velocity.

3. Over-all size of target.

4. Shape of target and roughness of surface.

5. Activity and position of personnel.

6. Nature of the agent (such as viscosity and surface tension) in relation to the surface of target.

The first three factors appear to be the most important for large particles but the last three factors may become increasingly more important for smaller particles (5 to 20 microns).

III. Results

A. Theoretical Impaction Curves

Calculations of impaction efficiencies of liquid particulates on body collectors, recessed collectors, ribbons, rectangular half-bodies cylinders, spheres and ellipsoids of various fineness ratios are available in a pamphlet entitled "Principles of Inertial Impaction" (1). Here the fraction impacted on an object for a given particle mass is given as a function of a dimensionless size parameter (a function where the particle diameter wind velocity and target diameter are the main variables), and a function of a dimensionless turbulence parameter (a function where the wind velocity and the target diameter are the main variables). From ref. 1 Figure 14 is reproduced as Figure 1 of this report. Detailed calculations are given in the Appendix. However, the curves presented in Figure 1 are not conveniently interpreted for use in chemical warfare,. For this purpose, Reynolds numbers, size parameters, and turbulence factors were calculated so that the impaction efficiencies on cylinders could be given as a function of particle diameter, wind velocity and size of target of interest. Other factors such as air viscosity and density of particles may be considered approximately constant in comparison to the

wider variations encountered in the other variables (see Appendix). The recalculated values for impaction are given in Figs. 2 through 7 and the numerical values are given in Table 1 in the Appendix. As shown in the Appendix, the size parameter for a particle may be expressed as follows:

$$N_D = .0118 \left(\frac{V}{D_c}\right)^{1/2} D_p$$

where V is the wind velocity in miles per hour, D_c is the target diameter in centimeters, and D_p the particle diameter in microns. The parameters are expressed in these units instead of the c.g.s. units because data on velocity and particle diameter are usually expressed in the above units.

The value for the turbulence factor or gas inertia effect is $N_{p_g} = 3.22\ VD_c$ where V is in miles per hour and D_c is in centimeters.

As a first approximation, it was assumed that the target diameters might be 2 cm. (fingers), 10 cm. (arms), 20 cm. (legs), 35 cm. (body), and 55 cm. (width of body and both arms at side of body so that no air moves between the arms and the body). This assumes that the cylinders have a large length-to-diameter ratio and that the edge effects do not markedly alter the over-all impaction efficiencies.

Wind velocities between 2 m.p.h. and 20 m.p.h. were chosen. However the narrower range between 4 m.p.h. and 10 m.p.h. covers most of the situations.

The particle diameter for liquid droplets is assumed to vary from 5 to 500 microns. This covers the range from almost zero impaction efficiency on the smallest target (2 cm. diameter) and highest wind speed (20 m.p.h.) up through over fifty per cent impaction efficiency on the largest target (55 cm. diameter) and lowest wind speed (2 m.p.h.)

In Fig. 8 a recalculation is made of Fig. 4. Here the impaction efficiency for a given particle diameter is multiplied by the diameter of the cylinder to give comparative values of the total quantity of liquid droplets impacted as a function of diameter of the cylinder (if we assume that the lengths of the cylinders are the same).

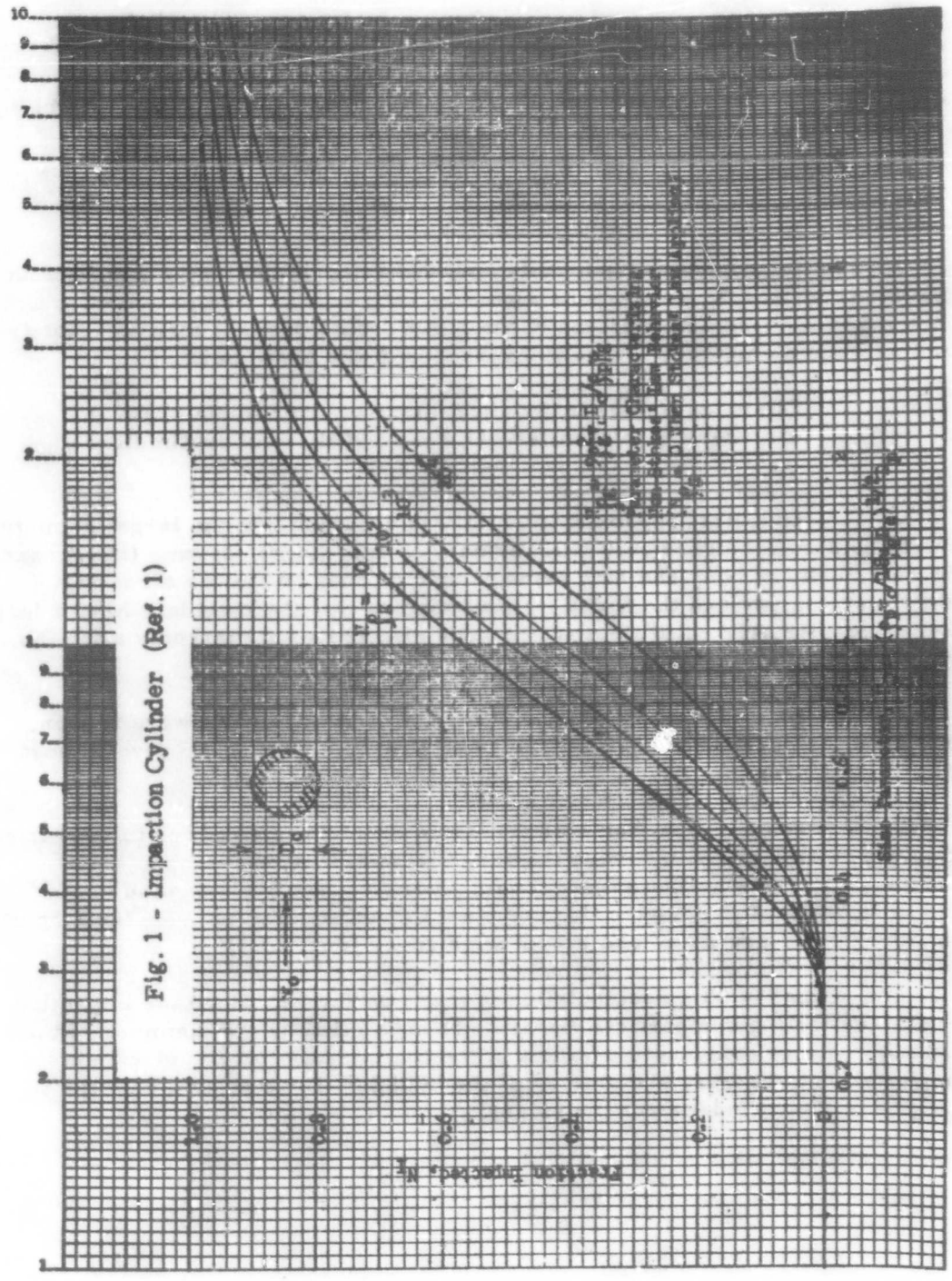

Fig. 1 - Impaction Cylinder (Ref. 1)

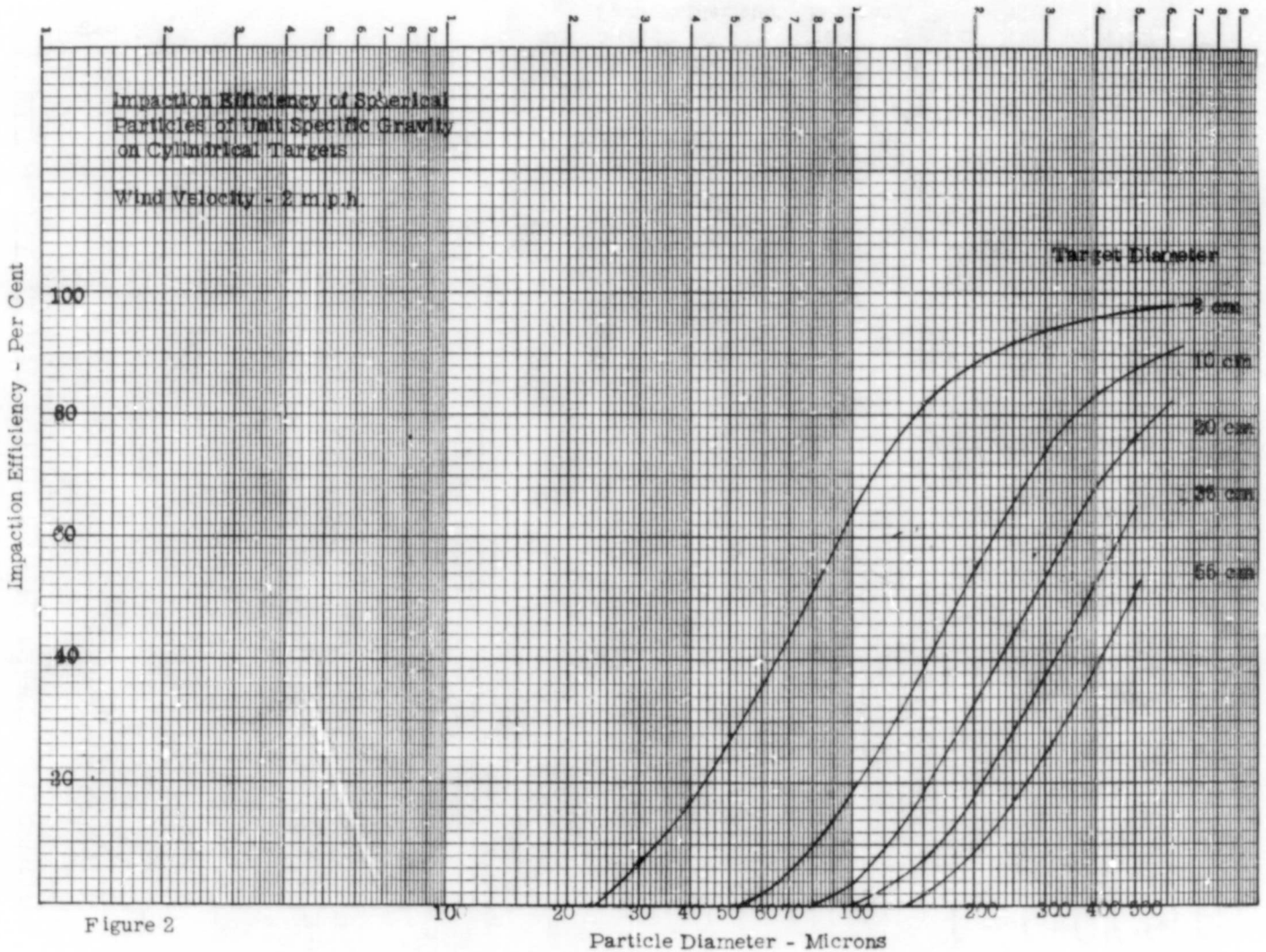
Impaction Efficiency of Spherical Particles of Unit Specific Gravity on Cylindrical Targets
Wind Velocity - 2 m.p.h.
Target Diameter
3 cm.
10 cm.
20 cm.
35 cm.
55 cm.
Impaction Efficiency - Per Cent
100
80
60
40
20
10
20
30
40
50
60
70
100
200
300
400
500
Particle Diameter - Microns

Figure 2

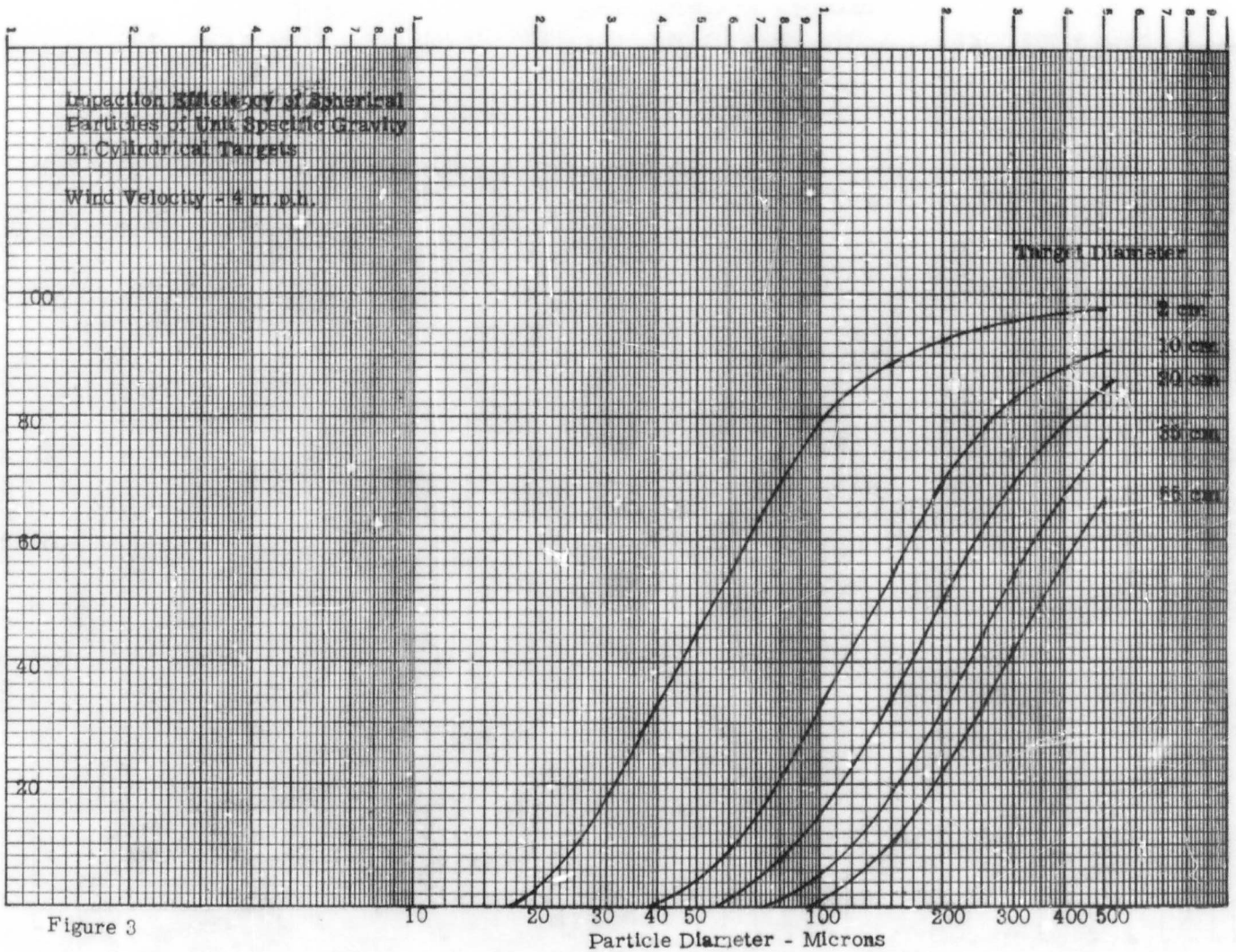
Impaction Efficiency of Spherical Particles of Unit Specific Gravity on Cylindrical Targets
Wind Velocity - 4 m.p.h.
Target Diameter
2 cm.
10 cm.
20 cm.
35 cm.
65 cm.
Impaction Efficiency - Per Cent
100
80
60
40
20
10
20
30
40
50
100
200
300
400
500
Particle Diameter - Microns

Figure 3

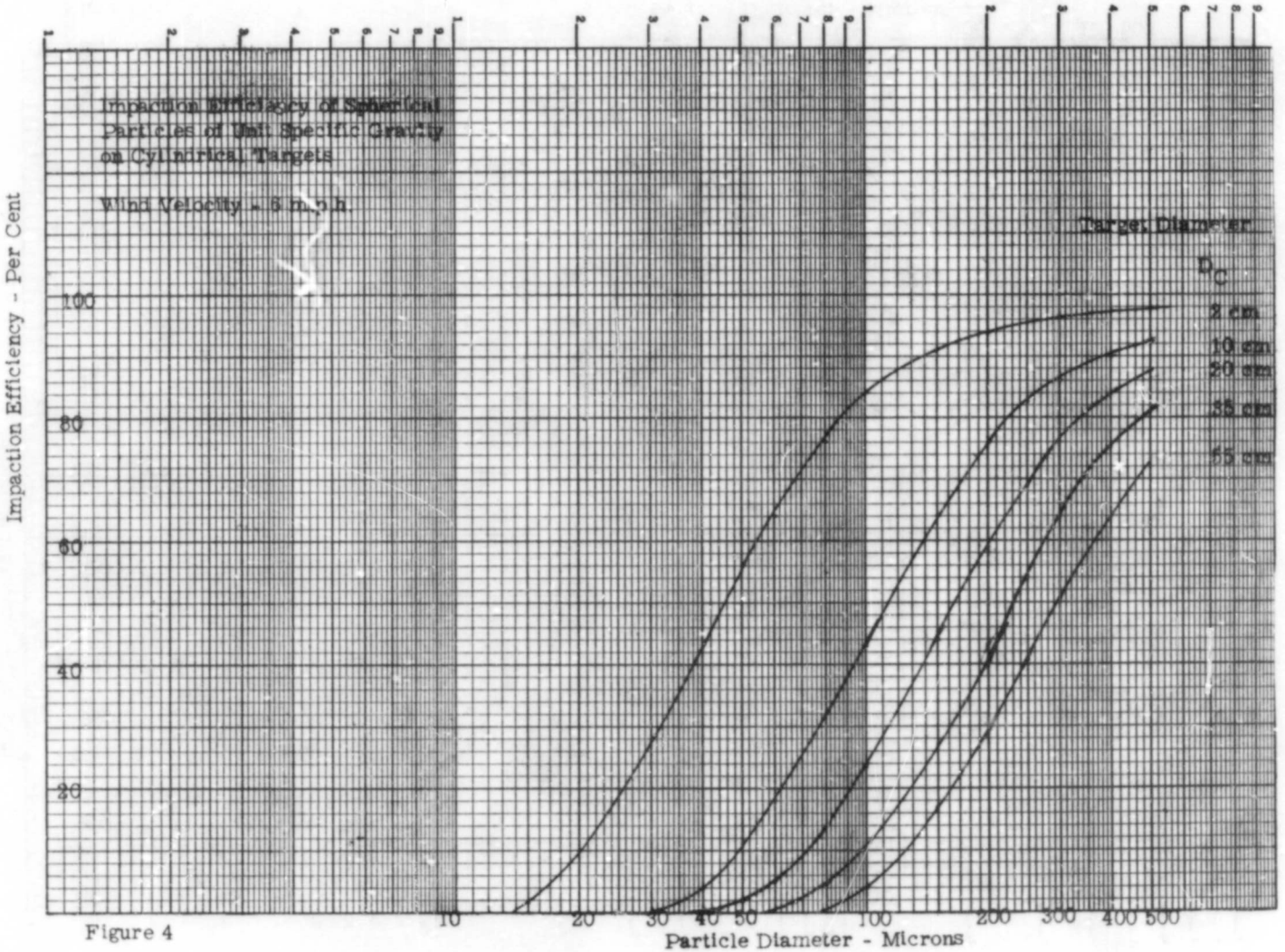
Impaction Efficiency of Spherical Particles of Unit Specific Gravity on Cylindrical Targets
Wind Velocity = 5 m.p.h.
Target Diameter, D_C
2 cm.
10 cm.
20 cm.
35 cm.
65 cm.
Impaction Efficiency - Per Cent
100
80
60
40
20
10
20
30
40
50
100
200
300
400
500
Particle Diameter - Microns

Figure 4

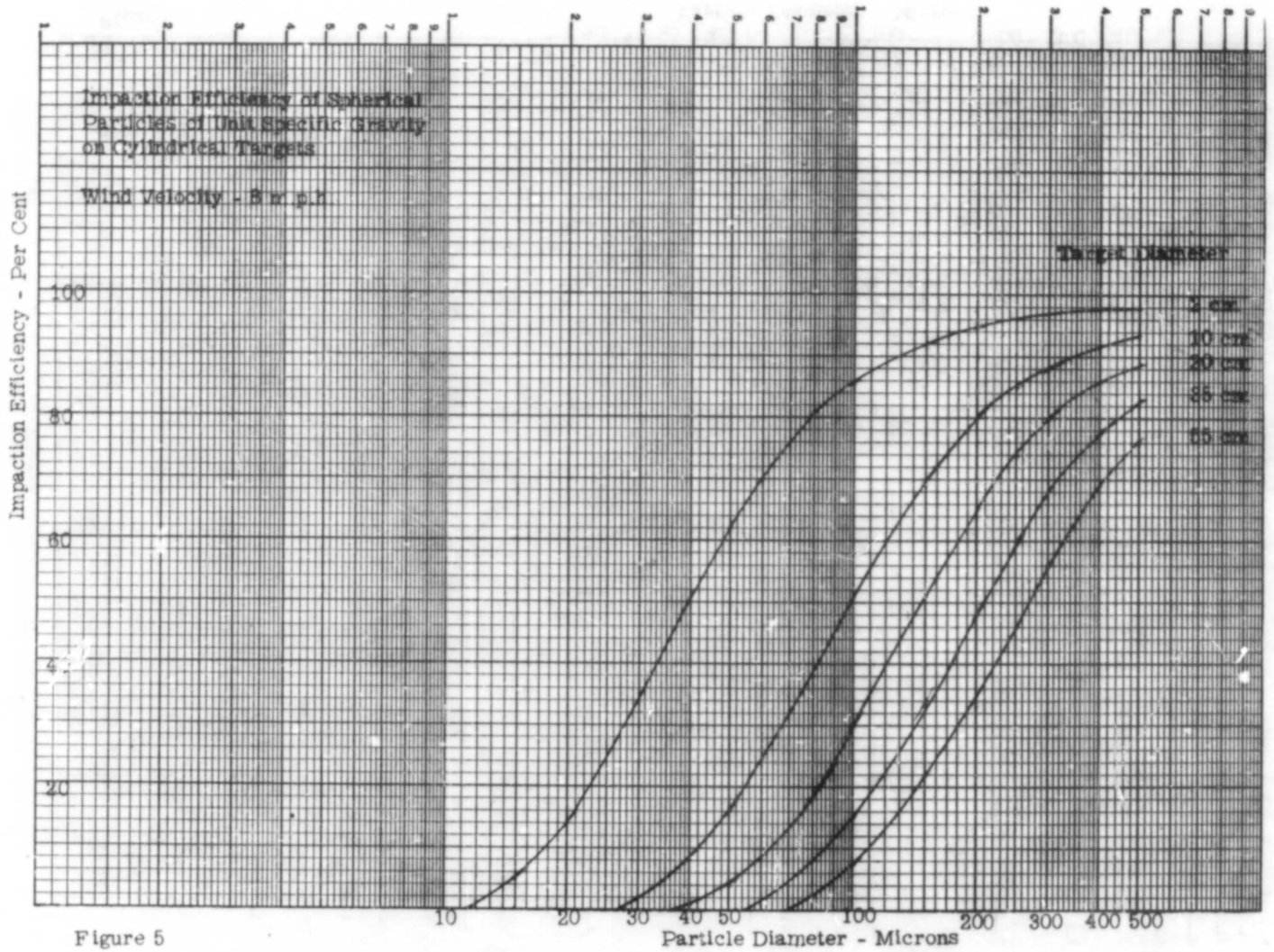
Impaction Efficiency of Spherical Particles of Unit Specific Gravity on Cylindrical Targets
Wind Velocity - 8 m p.h
Target Diameter
1 cm
10 cm
20 cm
35 cm
65 cm
Impaction Efficiency - Per Cent
100
80
60
40
20
10
20
30
40
50
100
200
300
400
500
Particle Diameter - Microns

Figure 5

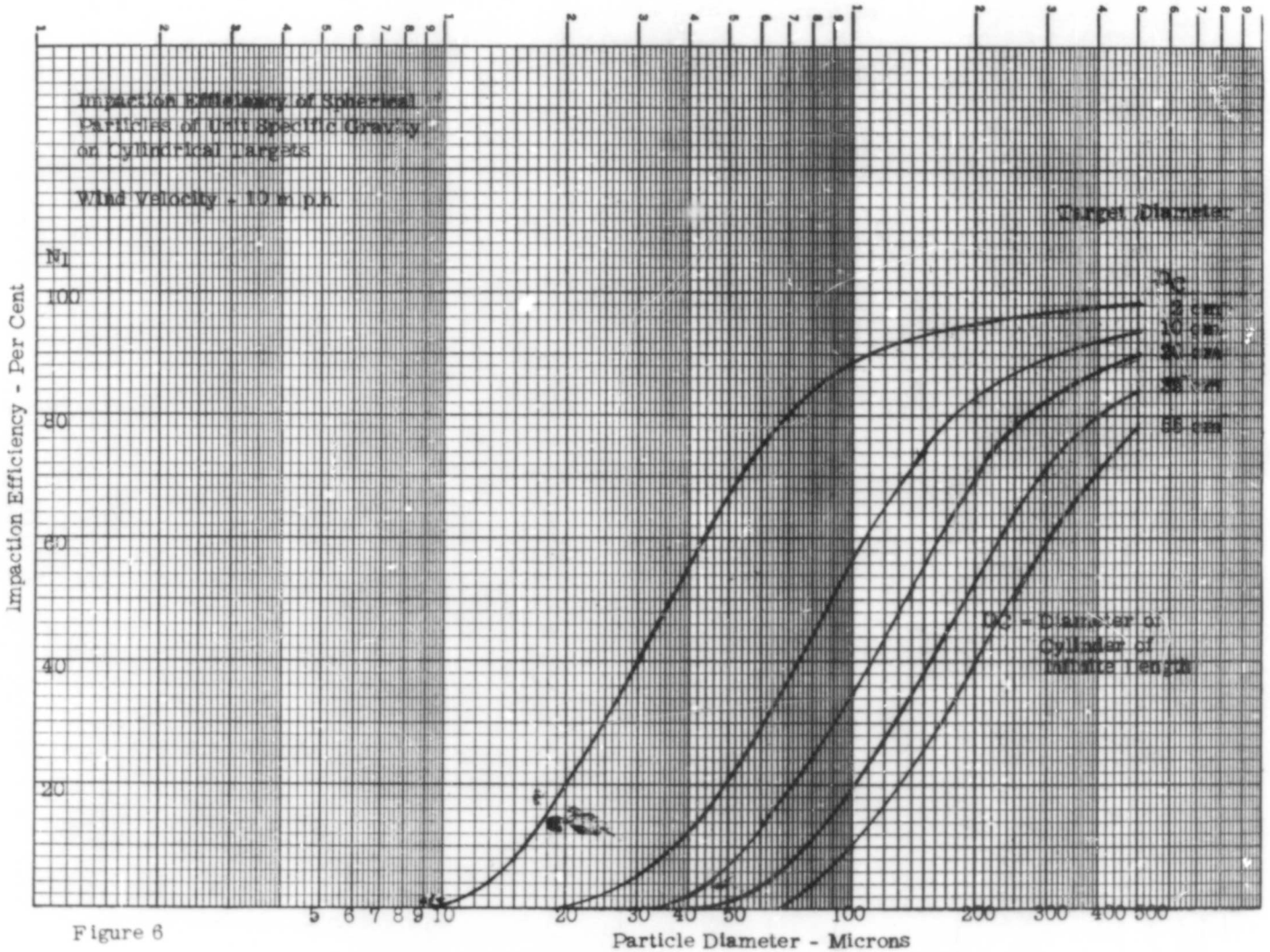
Impaction Efficiency of Spherical Particles of Unit Specific Gravity on Cylindrical Targets
Wind Velocity - 10 m. p.h.
Target Diameter
Impaction Efficiency - Per Cent
100
80
60
40
20
5 6 7 8 9 10 20 30 40 50 100 200 300 400 500
Particle Diameter - Microns
DC - Diameter of Cylinder of Infinite Length

Figure 6

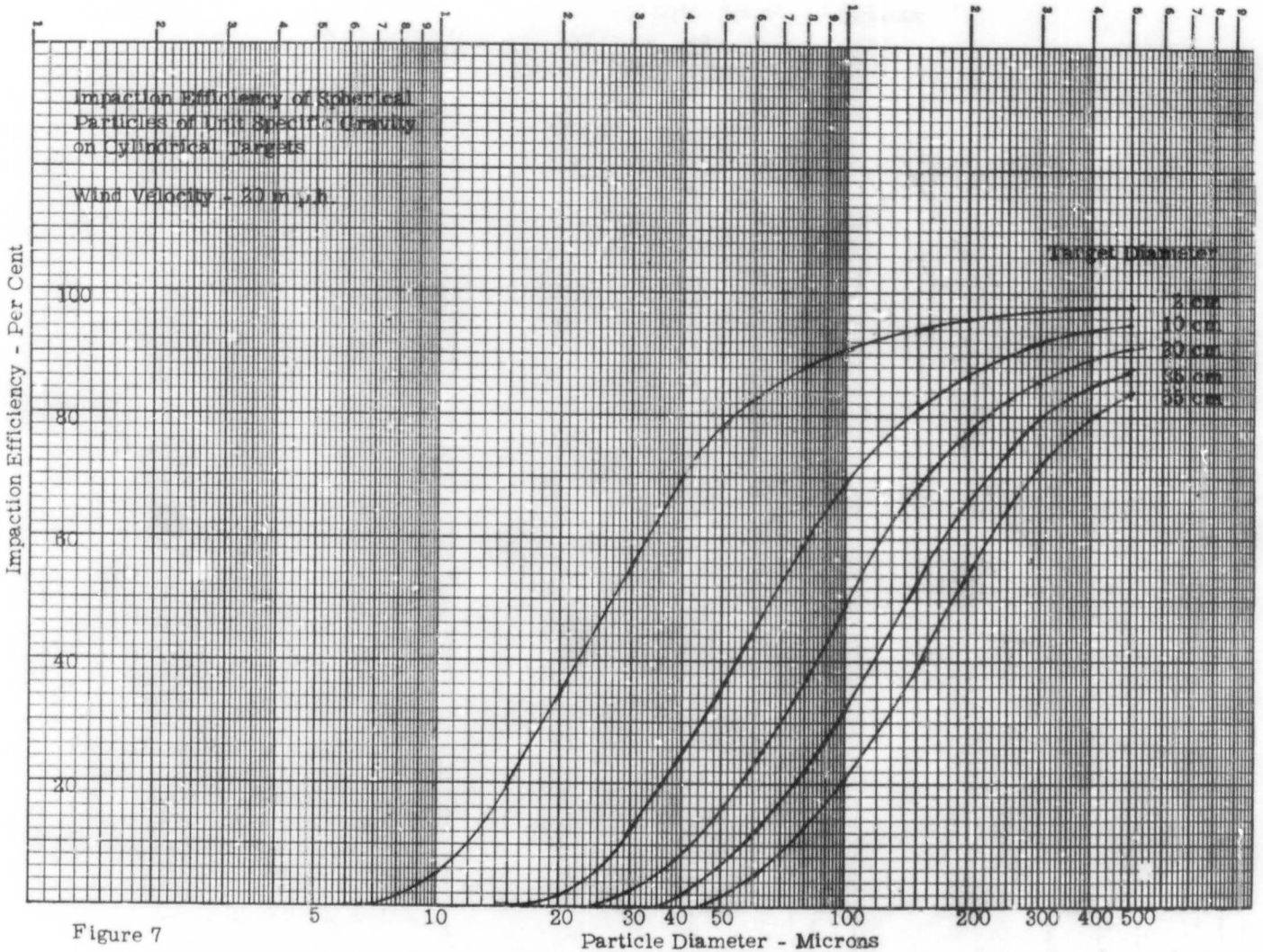
Impaction Efficiency of Spherical Particles of Unit Specific Gravity on Cylindrical Targets
Wind Velocity - 20 m.p.h.
Target Diameter
3 cm
10 cm
20 cm
36 cm
55 cm
Impaction Efficiency - Per Cent
100
80
60
40
20
5
10
20
30
40
50
100
200
300
400
500
Particle Diameter - Microns

Figure 7

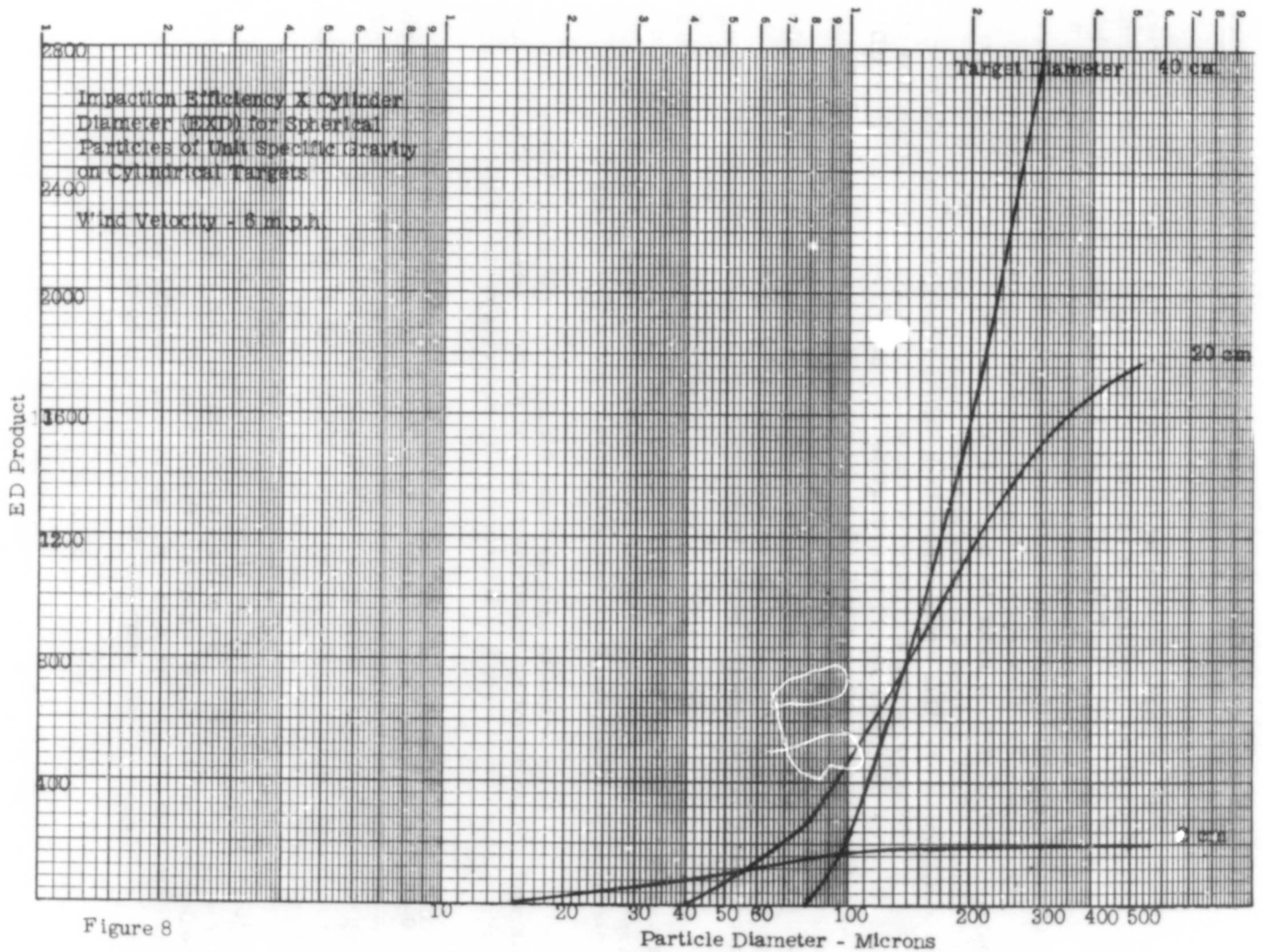
Impaction Efficiency X Cylinder Diameter (EXD) for Spherical Particles of Unit Specific Gravity on Cylindrical Targets
Wind Velocity - 6 m.p.h.
Target Diameter 40 cm.
30 cm
1 cm
ED Product
2800
2400
2000
1600
1200
800
400
10
20
30
40
50
60
100
200
300
400
500
Particle Diameter - Microns

Figure 8

B. Comparison of Calculated Impaction Efficiencies with Experimental Data.

Some impact studies by the Chemical Corps Medical Laboratories (ref. 2) covered the deposition of triphenyl phosphate aerosols on human arms at low wind velocities. In Table III of ref. 2, it was reported that the efficiency of impaction of triphenyl phosphate aerosol, velocity 5 m.p.h. and MMD 6.5 microns was 0.08 ± 0.14% on a hairless surface and 0.63 ± 0.14% on a hairy surface. However, reference to Figs. 3 and 4 of this report discloses that particles smaller than about 38 microns at 4 m.p.h. and particles smaller than about 28 microns at 6 m.p.h. show no impaction on a cylinder of 10-cm. diameter. One would expect then that if a hairless arm could be considered equivalent to a cylinder of the order of 10 cm., then impaction of 6.5 microns particles should be negligible. Actually, even though the MMD was 6.5 microns there was still 5% of the mass of the aerosol above 20 microns. In ref. 2, work with the Sinclair-LaMer Generator (which is designed to give uniform particle sizes) still shows that 5% of the mass of the aerosol has a diameter about three times the MMD and in another retort generator this ratio goes above 6 to 1.

In view of the fact that low impaction efficiencies are given in aerosols where over 5% of the mass had diameters 3 to 6 times the MMD, it appears likely that the impaction data cannot be interpreted from MMD data unless the particle size distribution is known or can be calculated.

Other reports such as those for field tests at Fort Belvoir and Camp LeJeune do not have sufficient data on particle size distributions to make any reliable comparisons with theoretically expected contaminations.

Tests on the impaction on man of large particles in the 100-to-500-micron range have been covered by a Porton report (ref. 6). In reference 6 it was reported that the collection efficiency for 100 micron droplets was approximately 0.1 in a wind speed of 5 m/sec (11 m.p.h.). Reference to Figs. 6 and 7 of this report shows that a 100 micron droplet would have a 0.1 impaction efficiency on a cylinder of 55 cm. in diameter and 0.2 impaction efficiency at 20 m.p.h. Since the variation is roughly linear with wind velocity in this range, then at 11 mph the impaction efficiency would be 0.11 for a 55-cm. cylinder. Since the size parameter varies inversely as the square root of the target diameter, then for an efficiency of 0.10 the target diameter would be $(1.1)^2$ X 55 cm., or 66 cm. The Porton report gives 35 cm. radius, or 70 cm. diameter as the equivalent cylinder to man.

Actually, however, from the standpoint of impaction, man is a composite of cylinders of several sizes from 2 cm. to 55 cm., and it is obvious that the over-all effectiveness will vary with particle size and wind velocity.

With both arms by the torso so that no air passes between the arms and torso, and with both legs together so that they act roughly as a single cylinder, the upper limit of the composite target would appear to be equivalent to a 40-to-45-cm. cylinder. However, if we can consider that the arms are outstretched so that they act as individual cylinders apart from the torso and that the legs are spread apart enough to act as two cylinders, then the average effect over the total projected area would have the same impaction efficiency as a cylinder approximately 20 cm. in diameter. Under most situations, conditions are usually somewhere in between these two extremes. In reference 6, the estimate of man as equivalent to a cylinder 70 cm. in diameter means than man, whose projected area is roughly equal to a cylinder of about 45 cm., has a higher impaction efficiency than a cylinder of 45-cm. diameter, and we must go to a cylinder of roughly 70-cm. diameter so that the total quantity on the projected area of the 70-cm. diameter cylinder will be equal to the total quantity impacted on man. However, in view of the fact that examination of Figs. 2 through 7 shows that the impaction efficiencies on cylinders from 10 cm. to 55 cm. are functions of the particle size and wind velocity, it appears that we may not be able to take a given cylinder diameter to represent man and that we should consider that the amount impacted on man will be some functions of the particle size distribution, the wind velocity, and the position of man. This subject requires further study to determine whether a more detailed mathematical relationship is required to describe the impaction on man.

IV. Discussion

The parameters mentioned in Section II are discussed, based on the calculations in the body and Appendix of this report.

1. Particle Size Distribution

Inasmuch as impaction data require knowledge of the particle size distribution and the MMD is not a sufficient criterion, it appears desirable to determine and record particle size distributions and to determine whether the

distributions encountered for MMD from five to several hundred microns can be described mathematically by the same type of equation. From independent studies on aerosols and finely divided matter, it appears that there is a trend for the standard deviation to increase as the MMD increases, but it is not at all certain whether there is any quantitatively useful correlation. However, it is clear that the impacted particles come mainly from that half of the mass which has diameters larger than the MMD, and that this distribution must be known for quantitative evaluation of impaction data.

2. Wind Velocity

The importance of wind velocity cannot be divorced from the size of the target and the particle diameter. Since all impaction efficiencies show an S-shaped curve, this means that at some low velocity the fractional change in impaction with velocity is small for any given particle diameter; that at some intermediate range there is a marked increase with increasing velocity; and that beyond a certain velocity range the fractional increase again becomes small (since it is near complete impaction).

3. Over-all Size of Target

A smaller target will always have a greater impaction efficiency than a larger target for the same external conditions. However, under certain circumstances the ratio of the impaction efficiency of the small target to the large target may be greater than the ratio of the diameter of the large to the small target. In this case, the small target will actually have more material impacted on it. The comparative impaction take-up is given in Fig. 8. One could interpret this as showing that under certain circumstances a free arm could have more impacted agent than a torso and that a small animal, due to size only and not to fur, could receive more agent by impaction than a larger animal.

4. Shape of Target and Roughness of Surface

The condition of turbulence around irregularly shaped objects can alter the impaction of particles. However, reference to Fig. 1 shows that the departure from Stokes' law behavior means a factor of not more than 2 to 1 in the impaction efficiency on cylinders between the lowest and highest $N_{\rho g}$ values. However, a variation in shape could mean a departure from the use of cylinders as a proper description. Reference 1 contains graphs on impaction efficiencies with other shapes, and the most marked variations come in the impaction efficiencies of recessed collectors and inverted troughs

In these cases, impaction efficiencies of 0.10 to 0.20 occur with size parameter values of 0.1 to 0.2, whereas impaction efficiencies on cylinders with these size parameters are negligible. From reports (refs. 2, 3, 5), variation in surface, such as a hairy or hairless arm is more important for small particles in the 5-to-10-micron range. For larger particles, the inertia effect becomes more important. Here again, a more critical evaluation of particle size distribution could clarify the data.

5. Activity and Position of Personnel

The activity of personnel could conceivably affect impaction in two ways. A person who is working is more likely to have his arms extended, and the arm acting as a cylinder of smaller diameter is a more efficient impactor than when the arms hang by the side of the body. Furthermore, a group of people standing exposed to a cloud moving at, say, 5 miles per hour could show a different impaction than a group moving in various directions at 5 miles per hour. In the latter case, there would be a range of effective velocities from 0 to 10 miles per hour.

People kneeling or lying on the ground would be more exposed to contamination through settling of particles. However, if the particles do not show any appreciable settling, then people on the ground may receive less agent by impaction because the wind velocity near the ground is lower.

6. Nature of the Agent in Relation to the Surface

The impaction calculations in this report assume that every particle touching the surface of the target will adhere. Data from some reports (ref. 5) indicate that small particles may not wet the surface well, and may give smaller impaction efficiencies than calculated. There are not sufficient data available to determine the quantitative significance and reasons for such deviations from calculated efficiencies. For example, the nature of the surface may be important in relation to the droplet to determine whether a drop will wet the surface, but it is not clear from this observation whether the viscosity of the droplet is also important, since the viscosity determines the amount of deformation of a droplet due to mechanical impact.

V. Literature Cited

1. William E. Ranz, Technical Report No. 1, Bulletin No. 66, Principles of Inertial Impaction, U. S. Public Health Service Research Grant S-19.

2. G. Asset, D. Pury, MLRR 306, Final Report, Deposition of Triphenyl Phosphate Aerosols on Human Arms at Low Wind Velocities, 1954.

3. B. P. McNamara, CWLR 2006, Chemical Warfare Casualty Production as Influenced by the Particle Size of Aerosol Clouds, 1956.

4. Eleventh Tripartite Conference on Toxicological Warfare, U. S. Progress Report on Medical Aspects, 1 July 1955-30 June 1956.

5. G. Asset, John E. Eipper, CWLR 2163, Deposition of Windborne Droplets of Dibutyl Phthalate Encoated Glass Microscope Slides, 23 August 1957.

6. K. Trouern-Trend, Porton Evaluation Group Note 10/56, Shell, Chemical, 25-Pr. B.E., Mk. 8 Charged V Agent; Hazard to Men Standing in the Open, 7 November 1957.

Appendix

A. Generalized Impaction Calculations

In a cloud of concentration C, moving at velocity V, the total mass passing through an area A, in time t, is

$$M = AVCt$$

This value of C covers the total concentration over all particle sizes. Since impaction efficiency on any given target and wind velocity is greatly dependent on particle size, any quantitative calculation on the total quantity of agent impacted will require knowledge of the particle size distribution. Let $\frac{dC}{C} = f_1(D)\, dD$. Here $\frac{dC}{C}$ is the fraction of the total concentration represented by particle diameters between D and D + dD.

Then $M_d = AV\, dC\, t$ is the mass of particles between diameters D and D + dD which pass through the area A in time t.

The theoretical impaction curves given in Figs. 2 through 7 give $N_I = \frac{m_d}{M_d} = f_2(N_D, N\rho_g)$. Here m_d is the mass of particles impacted divided by the total mass of particles passing through an area equal to the projected area of the target (for diameters between D and D + dD).

Multiplying the impaction efficiency for each diameter by the concentration of particles between D and D + dD gives

$$f_2(N_D, N\rho_g)\, dC = Cf_1(D) f_2(N_D, N\rho_g)\, dD.$$

The amount impacted on a given target is then

$$m = AVCt \int_o^\infty f_1(D) f_2(N_D, N\rho_g)\, dD$$

The integral as written covers diameters from 0 to ∞ but under most cases almost all the mass from the smallest diameter to the largest diameter is covered by a factor less than ten.

B. Calculation of Parameters in Range of Interest to Chemical Warfare

In Fig. 1 the fraction impacted is given as a function of the size parameter and the curve relating these two numbers consists of a family of curves which depends on a third parameter, the non-Stokes' law behavior.

N_1 = fraction of the total number of particles of size D_p which impact on the collecting surface.

$$N_D = (\rho_p V / 18_\mu D_c)^{1/2} D_p$$

N_D is called the size parameter and is dimensionless. It is equal to the square root of the ratio of the Stokes' law stopping distance to a characteristic linear dimension of the target upon which impaction occurs. The stopping distance is the distance a particle of diameter D_p and density ρ_p at an initial velocity V will travel until it comes to rest in still air. N_D is also the ratio of the force required to stop the particle with initial velocity V in the distance $D_c/2$ to the Stokes' law fluid resistance at a relative particle velocity of V.

By substituting $\mu = 1.8 \times 10^{-4}$ poise (gm/cm sec.),

Velocity = Vm.p.h. X 44.70cm/sec.m.p.h.

$\rho_p = 1$ gm/cm^3

Diameter particle = D_p microns X 10^{-4} cm/micron into the formula for the size parameter the following expression is obtained:

$$N_D = .0118 \left(\frac{V}{D}\right)^{1/2} D_p$$

Here V must be given in miles per hour, D_c in centimeters, and D_p in microns.

$$N_{\rho g} = 9\rho_g{}^2 V D_c / \rho_p{}_\mu$$

This is the parameter accounting for gas inertia effects during those times and under those conditions when Stokes' resistance law does not apply to the particle's motion. This third parameter describes the condition of turbulence of the air and is not dependent on particle size.

$$\text{Substituting } \rho_g = 1.2\text{X}10^{-3} \text{ gm./cm.}^3$$

$$\rho_p = 1 \text{gm./cm.}^3$$

$$\text{and } \mu = 1.8\text{X}10^{-4} \text{ gm./cm.sec.}$$

the following expression is obtained:

$$N_{\rho_g} = 3.22VC_c.$$

Here V is in miles per hour and D_c in centimeters.

With N_D and N_{ρ_g} now expressed in terms of V, D_c and D_p in m.p.h., centimeters and microns, we can now insert the values of chemical warfare interest into the formulas and obtain the values of the impaction efficiencies from the curves.

For velocity values, most meteorological conditions are covered by wind velocities between 4 and 10 m.p.h., but this is broadened to a range of 2 m.p.h. to 20 m.p.h. to cover the complete range of probable velocities.

For D_c, the target size, approximate diameters of cylinders of 2 cm. (fingers), 10 cm. (arms), 20 cm. (legs), 35 cm. (body) and 55 cm. (body and both arms at side of body so that no air moves between the arms and the body) were taken. Many of the conditions are idealized. Ordinarily fingers are not spread so that each finger acts as a target and the hand is not usually held in a manner that would give the maximum projected area perpendicular to the wind velocity. However, the average effect of man in various positions may be able to be characterized as equivalent to cylinders of the assumed diameters.

The particle size range is taken between 5 microns and 500 microns. In the large particle size range, a large fraction of the particles on the target may be due to settling rather than impaction caused by the momentum acquired through wind velocity. This is an additional complication which has to be considered but is not covered in this report.

C. Validity of Impaction Curves in Range of Chemical Warfare Interest

Fig. 1 as taken from ref. 1 cannot be applied to systems where the Reynolds' number of the gas flow, $D_c \rho_g V/\mu$, is less than 10^3. In this paper the lowest Reynolds' number is 2 cm. X $1.2X10^{-3}$ gm./cm.^{3} X 2 m.p.h. X 44.7cm./sec.m.p.h. = $2.3X10^3$. This applies to a cylinder of 2 cm. in diameter at 2 miles per hour. Therefore, we are in the range where the curves are applicable as given in Fig. 1.

D. Assumption of Constant Viscosity of Air and Density of Particles

The viscosity of air at 20°C. (68°F) is $1.8X10^{-4}$ poise. This varies from $1.7X10^{-4}$ poise at 0°C. (32°F.) to $1.9X10^{-4}$ poise at 40°C. (104°F.). This variation is approximately 5% of the value of $1.8X10^{-4}$ poise, which is valid under most conditions. The correction for temperature could be put in but it is questionable whether turbulent conditions are known with sufficient accuracy or impaction measurements made with sufficient accuracy to justify this correction.

A specific gravity of one for the particles was taken for convenience. Impactions for particles of any other density can be determined since the impaction efficiency is directly proportional to the square root of the density of particles.

E. Tabulation of Impaction Data

By inserting the values of D_c, V and D_p into the formulas for N_D and N_{ρ_g}, the dimensionless size parameter and parameter for gas inertia effect were calculated. The values for the impaction efficiency were then read from the curves in Fig. 1. In many of the cases the value for various N_{ρ_g} values had to be obtained by interpolation. This was considered satisfactory since an interpolated value of, say, 21% could have been 20% or 22%. In view of the uncertainties in the quantitative validity of the formulas to describe a condition of turbulence under experimental conditions, this interpolation was considered adequate. Table 1 gives the values of N_D and N_{ρ_g} calculated from the formulas and also the values of N_I which were read from the curves directly or by interpolation.

Table 1

Impaction Efficiencies of Liquid Particles as a Function of Diameter of Droplets, Characteristic Diameter of Cylinder and Wind Velocity

Target Diameter (mm.)		2						10					
Wind Velocity (miles per hr.)		2	4	6	8	10	20	2	4	6	8	10	20
φ		13	26	39	52	65	130	65	130	195	255	325	650
Particle Diameter (microns) 5	E_2	.059	.083	.10	.12	.13	.19	.096	.077	.064	.053	.059	.083
	E_1	-	-	-	-	-	-	-	-	-	-	-	-
10	E_2	.12	.17	.20	.26	.26	.27	.052	.076	.097	.11	.12	.17
	E_1	-	-	-	-	(.001)	.05	-	-	-	-	-	-
15	E_2	.18	.25	.31	.35	.40	.58	.078	.11	.14	.16	.18	.25
	E_1	-	(.001)	.018	.06	.08	.2	-	-	-	-	-	(.001)
20	E_2	.26	.33	.41	.47	.53	.75	.10	.15	.18	.21	.26	.33
	E_1	(.002)	.087	.10	.12	.20	.36	-	-	-	-	(.001)	.015
25	E_2	.33	.50	.61	.71	.79	1.1	.18	.22	.28	.32	.35	.50
	E_1	.06	.18	.25	.35	.40	.55	-	-	(.005)	.02	.06	.13
30	E_2	.57	.82	.97	.96	1.56	1.50	.21	.30	.37	.42	.47	.66
	E_1	.47	.11	.53	.50	.56	.70	-	(.01)	.06	.08	.11	.29
35	E_2	.52	.81	1.08	1.18	1.32	1.72	.26	.37	.46	.51	.59	.81
	E_1	.28	.45	.56	.62	[illegible]	[illegible]	(.001)	[illegible]	[illegible]	[illegible]	[illegible]	[illegible]
40	E_2	.71	.99	1.27	1.51	1.59	[illegible]	[illegible]	[illegible]	[illegible]	[illegible]	[illegible]	[illegible]
	E_1	.34	.55	.62	.70	[illegible]	[illegible]	[illegible]	[illegible]	[illegible]	[illegible]	[illegible]	[illegible]
50	E_2	.96	1.31	1.53	1.89	2.11	[illegible]	.37	.53	.66	.76	.83	1.18
	E_1	.53	.65	.74	.81	.84	.88	.15	[illegible]	.36	[illegible]	[illegible]	[illegible]
100	E_2	1.13	1.60	2.06	2.38	2.66	3.76	.52	.74	.91	1.06	1.18	1.66
	E_1	.41	.78	.84	.86	.89	.91	.19	.32	.43	.50	.56	.69
150	E_2	1.77	2.49	3.06	3.54	3.96	5.61	.78	1.11	1.38	1.59	1.77	2.47
	E_1	[illegible]	[illegible]	.92	.93	.935	.96	.39	.56	.64	.70	.75	.87
200	E_2	2.56	1.37	4.08	4.77	5.28	7.68	1.04	1.48	1.84	2.12	2.36	3.32
	E_1	.88	.77	[illegible]	[illegible]	.95	[illegible]	.52	.69	.76	.80	.84	.88
300	E_2	2.95	4.15	5.1	5.9	6.60	9.35	1.30	1.85	2.30	2.65	2.95	4.15
	E_1	[illegible]	.86	.95	.96	.96	.965	.62	.77	.80	.85	.87	.90
400	E_2	3.56	4.96	6.13	7.08	[illegible]	11.2	1.58	2.22	2.75	3.18	3.56	4.96
	E_1	.86	.96	.965	.97	.97	.97	[illegible]	.87	[illegible]	[illegible]	.91	[illegible]
500	E_2	4.77	6.64	8.16	9.44	10.6	15.0	2.08	2.96	3.68	4.35	4.77	6.46
	E_1	.95	.975	.975	.975	.98	.98	.94	.88	.90	.91	[illegible]	.96
600	E_2	5.90	8.30	10.2	11.8	13.2	26.7	2.40	3.70	4.60	5.20	5.90	8.30
	E_1	.975	.975	.98	.98	.98	.98	.88	.91	[illegible]	.975	[illegible]	.95

Target Diameter (mm.)		20						35						55					
Wind Velocity (miles per hr.)		2	4	6	8	10	20	2	4	6	8	10	20	2	4	6	8	10	20
φ		130	260	390	520	650	1300	227	455	683	909	1140	2300	358	716	1070	1433	1791	3580
Particle Diameter (microns) 5	E_2	.013	.026	.032	.037	.047	.059	.014	.020	.024	.028	.031	.044	.011	.018	.020	.023	.024	.037
	E_1	-	-	-	-	-	-	-	-	-	-	-	-	-	-	-	-	-	-
10	E_2	.04	.05	.06	.07	.08	.12	.03	.04	.04	.04	.05	.06	.02	.03	.04	.04	.04	.05
	E_1	-	-	-	-	-	-	-	-	-	-	-	-	-	-	-	-	-	-
15	E_2	.06	.08	.10	.11	.12	.15	.04	.06	.07	.08	.09	.13	.03	.05	.06	.07	.08	.12
	E_1	-	-	-	-	-	-	-	-	-	-	-	-	-	-	-	-	-	-
20	E_2	.07	.10	.12	.13	.17	.24	.06	.08	.10	.11	.13	.18	[illegible]	[illegible]	[illegible]	[illegible]	[illegible]	[illegible]
	E_1	-	-	-	-	-	(.002)	-	-	-	-	-	-	-	-	-	-	-	-
25	E_2	.12	.16	.19	.20	.25	.35	.08	.12	.14	.17	.19	.26	.07	.09	.12	.14	.16	.21
	E_1	-	-	-	-	(.002)	.005	-	-	-	-	-	(.002)	-	-	-	-	-	-
30	E_2	.15	.21	.26	.30	.33	.47	.11	.16	.19	.22	.25	.32	.09	.12	.15	.17	.19	.27
	E_1	-	-	(.002)	(.01)	[illegible]	[illegible]	-	-	-	-	[illegible]	[illegible]	-	-	-	-	-	-
35	E_2	.19	.26	.32	.37	.42	.59	[illegible]	[illegible]	[illegible]	[illegible]	[illegible]	[illegible]	[illegible]	[illegible]	[illegible]	[illegible]	[illegible]	[illegible]
	E_1	[illegible]	[illegible]	[illegible]	[illegible]	[illegible]	[illegible]	[illegible]	[illegible]	[illegible]	[illegible]	[illegible]	[illegible]	[illegible]	[illegible]	[illegible]	[illegible]	[illegible]	[illegible]
40	E_2	[illegible]	[illegible]	[illegible]	[illegible]	[illegible]	[illegible]	[illegible]	[illegible]	[illegible]	[illegible]	[illegible]	[illegible]	[illegible]	[illegible]	[illegible]	[illegible]	[illegible]	[illegible]
	E_1	[illegible]	[illegible]	[illegible]	[illegible]	[illegible]	[illegible]	[illegible]	[illegible]	[illegible]	[illegible]	[illegible]	[illegible]	[illegible]	[illegible]	[illegible]	[illegible]	[illegible]	[illegible]
50	E_2	[illegible]	[illegible]	[illegible]	[illegible]	[illegible]	[illegible]	[illegible]	[illegible]	[illegible]	[illegible]	[illegible]	[illegible]	[illegible]	[illegible]	[illegible]	[illegible]	[illegible]	[illegible]
	E_1	.10	[illegible]	[illegible]	[illegible]	[illegible]	[illegible]	[illegible]	[illegible]	[illegible]	[illegible]	[illegible]	[illegible]	[illegible]	[illegible]	[illegible]	[illegible]	[illegible]	[illegible]
100	E_2	.37	.52	[illegible]	[illegible]	[illegible]	[illegible]	[illegible]	[illegible]	[illegible]	[illegible]	[illegible]	[illegible]	[illegible]	[illegible]	[illegible]	[illegible]	[illegible]	[illegible]
	E_1	[illegible]	[illegible]	[illegible]	[illegible]	[illegible]	[illegible]	[illegible]	[illegible]	[illegible]	[illegible]	[illegible]	[illegible]	[illegible]	[illegible]	[illegible]	[illegible]	[illegible]	[illegible]
150	E_2	.56	.73	.96	1.11	1.25	1.77	[illegible]	[illegible]	[illegible]	[illegible]	[illegible]	[illegible]	[illegible]	[illegible]	[illegible]	[illegible]	[illegible]	[illegible]
	E_1	[illegible]	[illegible]	[illegible]	[illegible]	[illegible]	[illegible]	[illegible]	[illegible]	[illegible]	[illegible]	[illegible]	[illegible]	[illegible]	[illegible]	[illegible]	[illegible]	[illegible]	[illegible]
200	E_2	.75	[illegible]	[illegible]	[illegible]	[illegible]	2.36	[illegible]	[illegible]	[illegible]	[illegible]	[illegible]	[illegible]	[illegible]	[illegible]	[illegible]	[illegible]	[illegible]	[illegible]
	E_1	.36	.50	[illegible]	.65	.72	.77	[illegible]	[illegible]	[illegible]	[illegible]	[illegible]	[illegible]	[illegible]	[illegible]	[illegible]	[illegible]	[illegible]	[illegible]
300	E_2	.93	1.30	1.60	1.85	2.09	2.95	[illegible]	[illegible]	[illegible]	[illegible]	[illegible]	[illegible]	[illegible]	[illegible]	[illegible]	[illegible]	[illegible]	[illegible]
	E_1	.45	.61	.69	.74	.79	.875	[illegible]	[illegible]	[illegible]	[illegible]	[illegible]	[illegible]	[illegible]	[illegible]	[illegible]	[illegible]	[illegible]	[illegible]
400	E_2	1.11	1.56	[illegible]	2.22	2.50	[illegible]	[illegible]	[illegible]	[illegible]	[illegible]	[illegible]	[illegible]	[illegible]	[illegible]	[illegible]	[illegible]	[illegible]	[illegible]
	E_1	.51	.59	[illegible]	[illegible]	[illegible]	[illegible]	[illegible]	[illegible]	[illegible]	[illegible]	[illegible]	[illegible]	[illegible]	[illegible]	[illegible]	[illegible]	[illegible]	[illegible]
500	E_2	1.49	2.08	[illegible]	[illegible]	3.35	4.77	1.17	[illegible]	[illegible]	[illegible]	[illegible]	[illegible]	[illegible]	[illegible]	[illegible]	[illegible]	[illegible]	[illegible]
	E_1	.62	.79	[illegible]	[illegible]	.87	.89	[illegible]	[illegible]	[illegible]	[illegible]	[illegible]	[illegible]	[illegible]	[illegible]	[illegible]	[illegible]	[illegible]	[illegible]
600	E_2	1.86	2.4	3.2	3.70	4.18	5.90	1.41	1.96	2.46	2.80	3.14	4.4	1.10	1.57	2.08	2.26	2.53	3.1
	E_1	.77	[illegible]	.875	[illegible]	.90	[illegible]	[illegible]	[illegible]	[illegible]	[illegible]	[illegible]	[illegible]	[illegible]	[illegible]	[illegible]	[illegible]	[illegible]	[illegible]

EVAPORATION OF LIQUID DROPLETS FALLING AS A CLOUD

Albert Pfeiffer

Research Directorate
U. S. Army Chemical Warfare Laboratories
Army Chemical Center, Md.

I. INTRODUCTION

The evaporation of particles falling as a cloud is important in the application of insecticides and herbicides in the form of spray clouds, and in studies in meteorology, as well as in the field of chemical warfare.

The term "falling as a cloud" is used in this paper to describe the behavior of particles falling under the influence of mass subsidence. Mass subsidence occurs when a population of particles falls faster than the single particles would fall under the same conditions.

The basic condition required for mass subsidence is expressed by the equation for the velocities of two adjacent particles:

$$v_I \leq \left(v_a + v_{IIa}\right) \tag{1}$$

where v_I is the velocity of fall of particle I relative to the earth, v_a is the velocity of air following particle I relative to the earth, and v_{IIa} is the velocity of particle II relative to the moving air. These relationships are shown in figure 1.

The evaporation of particles falling as a cloud can be considered by assuming, first, that vapor stagnation exists, and second, that air streams carry away the stagnated vapor. The problem is complicated by the different values of vapor stagnation at different levels of the falling cloud in which the particle is located and other special conditions of evaporation existing in a falling cloud. Therefore the subsiding cloud is studied first in order to permit subsequent calculation of the evaporation rate of the particles falling as a cloud.

II. EVAPORATION CONDITIONS IN THE FALLING CLOUD

1. The wind velocity relative to a particle falling with other particles in a cloud is the normal velocity of fall of the particular

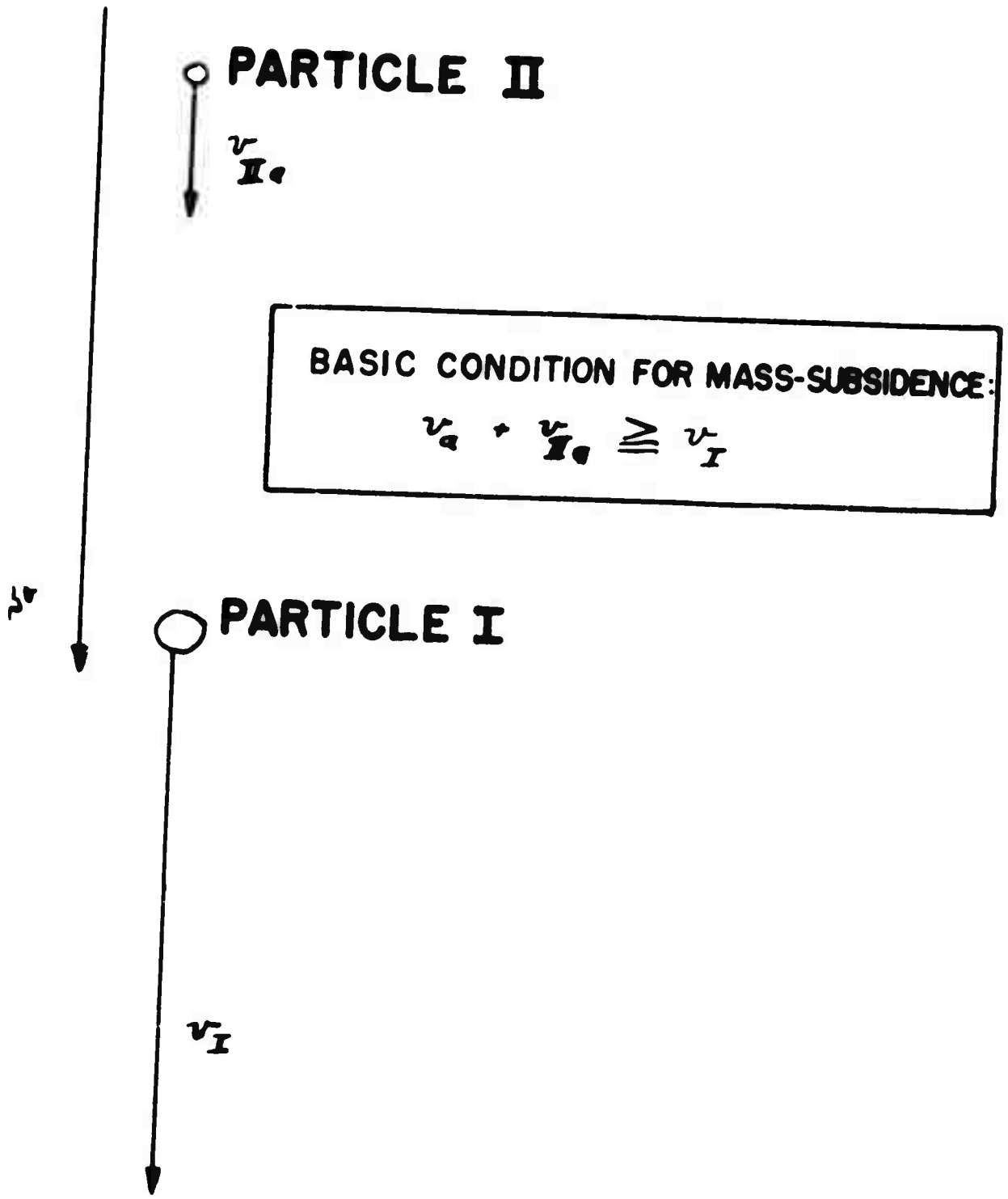

BASIC CONDITION FOR
MASS-SUBSIDENCE
FIGURE 1.

particle in still air of the same density and temperature, because the relative velocity of the falling particle with respect to the surrounding air is such that the force of resistance of the air acting upon the falling particle is equal to the force of gravity. Since the ventilation of the falling particle increases the evaporation rate, Froessling's wind factor f, or better, a corrected wind factor f_c, has to be calculated for the velocity of fall of the particular particle in still air, if an estimate of the evaporation rate of the falling drop is desired.

2. The falling cloud is ventilated by an air stream having the velocity v_i relative to the falling cloud. This ventilation stream and the sum of the evaporation rates of all particles control the value P_2 of the stagnation pressure of the vapor, which is important in determining the overall evaporation rate. But since we have to calculate v_i to know the stagnation pressure P_2 we should know how v_i and the velocity of fall of the complete cloud are related to each other.

3. In mass subsidence, the smaller particles fall in the air stream produced by the larger particles. The largest particles remaining in the cloud fall with a velocity relative to the ventilation wind which is equal to the velocity of fall of these particles in still air. But it is evident that the velocity of fall, relative to the earth, of the largest particles remaining in the cloud is equal to the velocity of fall, v, of the complete cloud relative to the earth. Therefore, the vertical velocity of the ventilation wind relative to the cloud is equal to the velocity of fall of the largest particles remaining in the cloud in still air. Consequently, in the falling cloud air moves with the velocity v_a relative to and in the direction of the earth and therefore

$$v_a = v - v_i \tag{2}$$

Experiences with clouds falling in the manner of "mass subsidence" show that not infrequently the following equation is fulfilled

$$v = 100\, v_i \tag{3}$$

An extreme example of the effect of a falling cloud upon the atmosphere is available in the case of avalanches of stone which can cause such violent air movements near the avalanche that houses are destroyed, as experiences in the Alps have shown.

For the present problem of evaporation of particles falling as a cloud, the value of v_i can be calculated from (2) since v and v_a can be measured. Alternatively, if one knows the size of the largest particles

remaining in a cloud, the velocity of the fall in still air (which is equal to v_i) can be calculated from Stoke's Law.

4. Because in every case

$$v_i < v$$

an air stream moves parallel to the bottom of the cloud and at the side of the cloud opposite to the direction of fall. It is easy to see that this air stream causes a circulation stream in the cloud as figure 2 shows. This circulation stream is important for the evaporation of the particles in a falling cloud because it almost completely and continuously mixes the particles with the air in the cloud. This mixing process is accompanied by another which is caused by particles falling with different velocities relative to the cloud. Still another mixing effect is produced by whirls in the cloud established by the different velocities of fall of the particles relative to the cloud and by the winds of velocities v_i and v.

III. THE EVAPORATION PROCESS

1. Temperature Lowering by Evaporation of Particles

The rate of evaporation is proportional to the rate at which the particle surface is heated. The amount of heat going to the evaporating particle per unit time at normal temperature and under normal conditions is not significantly influenced by radiation if the particle is heated by contact with the surrounding air and the air around the particle is in motion. The diffusion of heat from the surrounding air to the particle obeys the same law as the diffusion of vapor from the evaporating particle to the surrounding air. Therefore an equilibrium exists between both heat transfer and evaporation, and the temperature at the surface of the evaporating body has an almost constant value during the evaporation if radiation can be neglected. In this paper it is proposed that the influence of radiation upon evaporation can be neglected.

The overall evaporation process can be considered to occur in 3 steps, namely, ejection, absorption, and diffusion, as presented in the following paragraphs.

2. Ejection

From a very thin zone under the surface of the liquid drop which is called "subsurface" (figure 3) liquid molecules are ejected at a rate $\frac{dm_E}{dt}$ which is referred to as "ejection rate". This rate is equal to

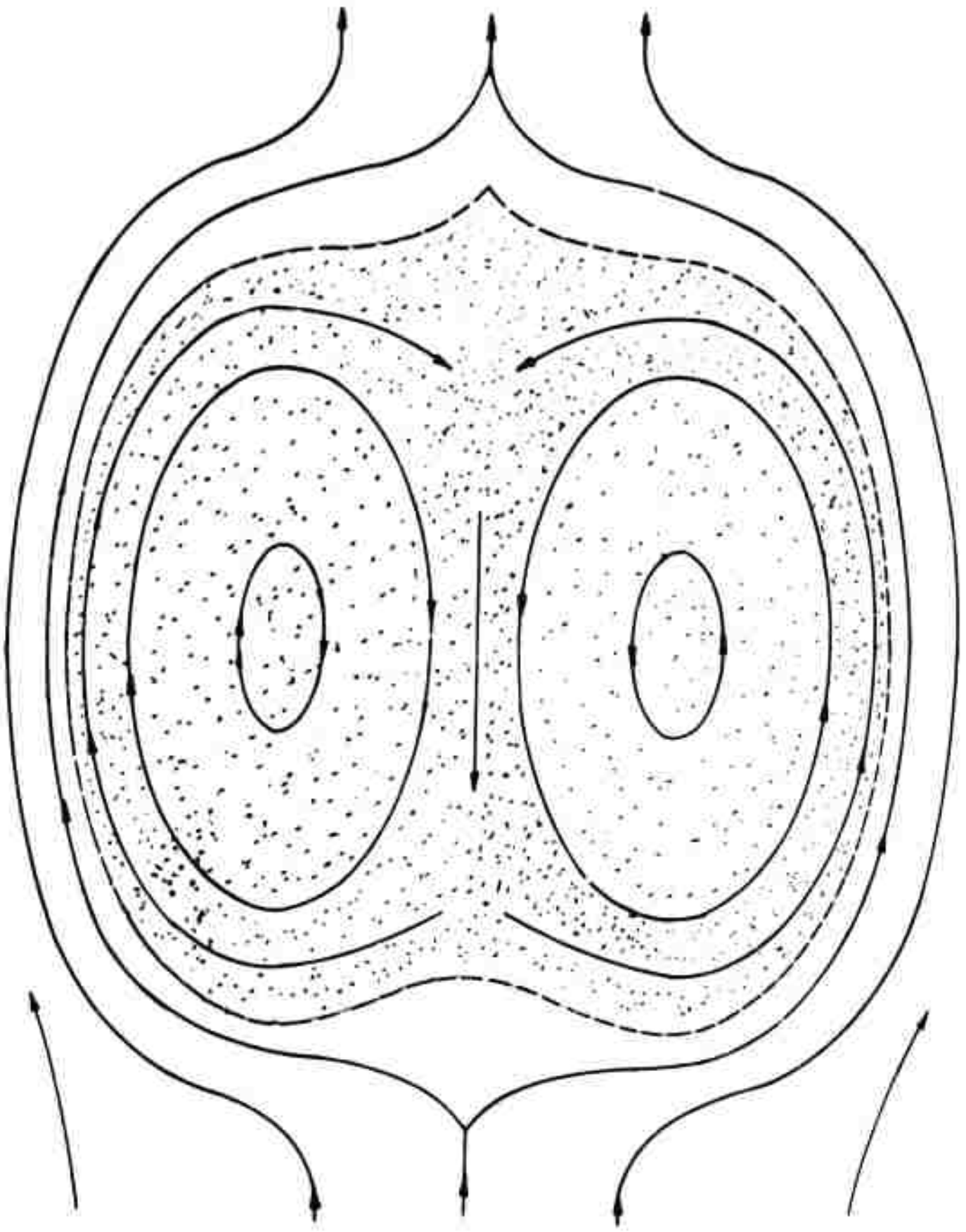

CIRCULATION STREAMS IN FALLING CLOUDS

FIGURE 2

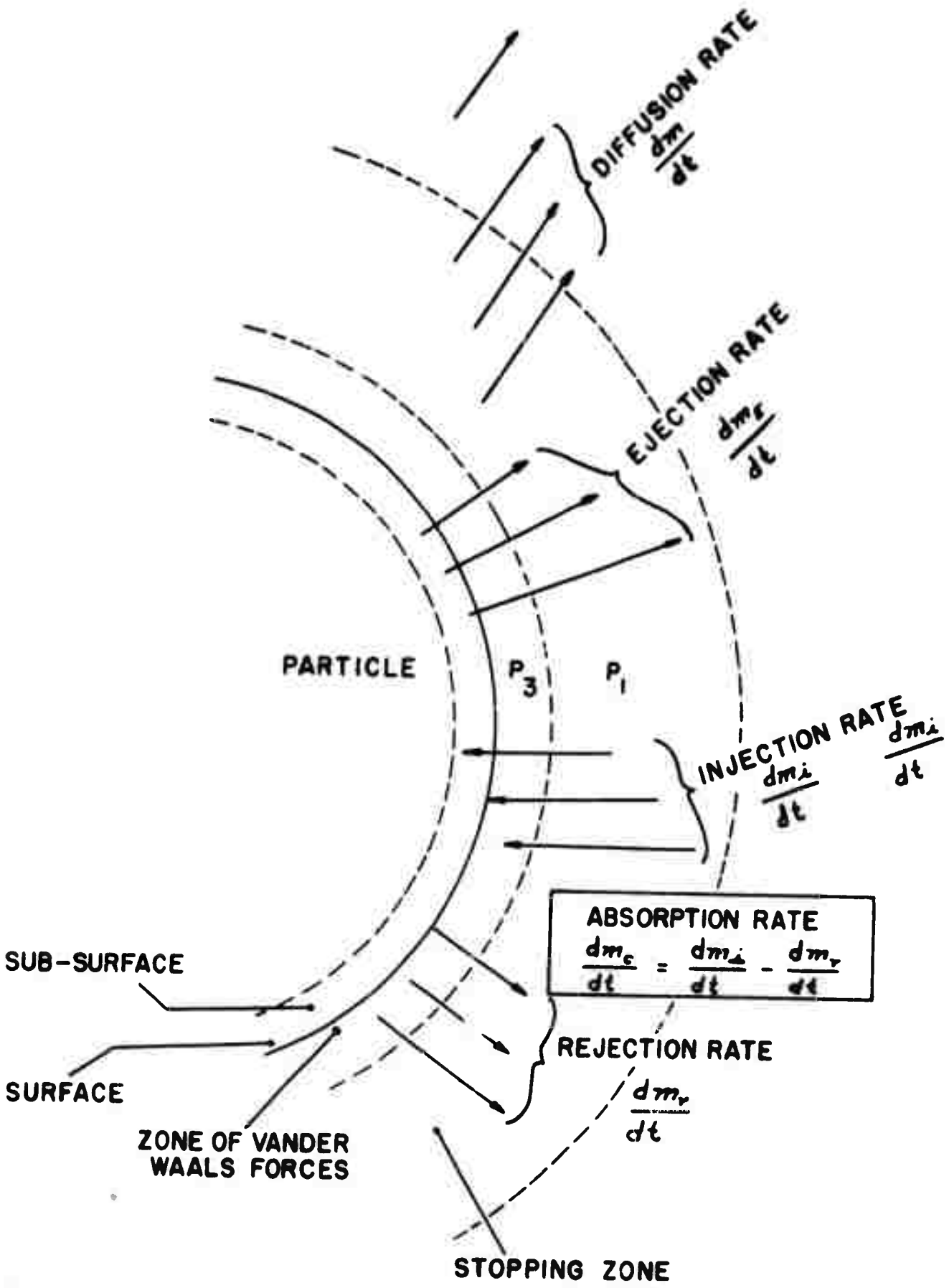

SCHEMATIC OF MOLECULAR EXCHANGE BETWEEN DROP AND VAPOR CLOUDS

FIGURE 3

the "maximum possible evaporation rate" $\left(\frac{dm}{dt}\right)^{max}$ because the mass of molecules which evaporates in a certain time cannot be larger than the amount of particles which is ejected in the same time. This "ejection rate" or "maximum possible evaporation rate" can be measured using a new method which will be described in a separate paper. The ejection rate is a typical molecular constant of the particular evaporating material, as is, for instance, the vapor pressure.

For liquid drops the "ejection rate" equals the "maximum possible evaporation rate" developed by Penner (1947):

$$-\left(\frac{dm}{dt}\right)^{max} = 4\pi a^2 \sqrt{\frac{2\,[\Delta H_{vap}]}{RT\gamma}} \cdot \text{ue}^{-\frac{[\Delta H_{vap}]}{RT}}$$

It was mentioned that

$$\frac{dm_E}{dt} = \left(-\frac{dm}{dt}\right)^{max}$$

and therefore

$$\frac{dm_E}{dt} = 4\pi a^2 \sqrt{\frac{2\,[\Delta H_{vap}]}{RT\gamma}} \cdot \text{ue}^{-\frac{[\Delta H_{vap}]}{RT}}$$

The ejected vapor molecules of course, stop in a zone lying directly at the surface of the evaporating particle. This zone is called the "stopping zone."

3. Absorption

From the zone in which the ejected vapor molecules stop, some vapor molecules are moved by normal gaseous molecular motion directly back into the subsurface of the liquid drop and into the zone of van der Waals forces. Only molecules having a distance from the zone of van der Waals forces of the drop surface smaller than about two times the mean free path of the vapor molecules in the "stopping zone" can move back directly into the "subsurface" or into the zone of van der Waals forces.

In the subsurface, vapor molecules coming back from the "stopping zone" are completely or partly absorbed and therefore become liquid again. The rate at which vapor molecules are absorbed is without doubt proportional to the rate at which vapor molecules strike the zone of van der Waals forces at the surface of the evaporating particle. How many of these molecules striking the zone of van der Waals forces enter the subsurface and stick there can be expressed by an absorption constant, R_R. Using Langmuir's formula

(1915) for the mass of gas molecules striking a surface situated in the gas, and R_R, one obtains the following equation for the absorption rate $\frac{dm_c}{dt}$:

$$\frac{dm_c}{dt} = R_R P_1 S \sqrt{\frac{m}{2\pi RT}}$$

R_R is described in more detail in a separate paper and is defined as $\frac{P_1 - P_3}{P_1} = R_R$ where P_3 is the partial pressure of vapor in the zone of van der Waals force at the evaporating surface. R_R is a typical constant of the evaporating substance but dependent on the gas in which the evaporation takes place.

R_R can be calculated from the measured ejection rate $\frac{dm_E}{dt}$ and evaporation rate $\frac{dm}{dt}$ as will be shown later when the formula for $\frac{dm}{dt}$ is developed.

In the "stopping zone" the partial pressure of the vapor is almost uniform because of the rapid motion of the vapor molecules (average velocity in the order of about 600 meters per second) and the very small depth of the "stopping zone" (about 2 mean free paths of the vapor molecules). P_1 is the "average value of the partial pressure in the "stopping zone."

4. Diffusion

From the stopping zone, the vapor molecules diffuse into the atmosphere of the surrounding space, forming a "vapor cloud". The partial pressure P_1 varies of course with the radius r_{max} of the vapor cloud. For a constant or almost constant r_{max} and a stationary or quasi-stationary diffusion, the following equation, expressing the first diffusion law of Fick in a new way, is valid:

$$\frac{dm}{dt} = S \cdot L \sqrt{\frac{m}{2\pi RT}} \cdot \frac{dP}{dr}$$

The constant L is defined by

$$L = \delta \cdot \beta$$

δ is the mean free path of the diffusing molecules in the path of diffusion and β is a constant of proportionality. L has therefore the dimension of length. Between L and the normally used diffusion constant D exists the

following relation:

$$\frac{D}{L} = \sqrt{\frac{RT}{2\pi M}}$$

where D is the diffusion coefficient, L is the diffusion conductivity of the vapor, and the remaining symbols have their usual meaning. The development of the new diffusion equation is described in a separate paper entitled "Diffusion Seen From a New Viewpoint" to be published in the near future, in which it is assumed that a part of the molecules striking an imaginary lamina may penetrate and another part may return. The diffusing molecules are the penetrating portion.

For relatively highly volatile substances it is proposed that the diffusion is non-stationary, because there is a delay in establishing the dynamic vapor concentration equilibrium in the diffusion path. These delayed equilibria caused by continuous decrease of the particle surface by evaporation delay the decrease of the P-values of the P-Radius curve. The reason for this delay is that the diffusion path contains a certain amount of vapor which requires a finite time to diminish to the new P-values along the radius of the vapor cloud. Therefore, the real values of the decreasing P_1 are higher than they would be in the case of stationary diffusion. But because the evaporation experiments show that the surface-time curve of a particle is a straight or almost straight line for relatively high-volatile as for low-volatile materials, the mathematical law of the P-Radius curve for the vapor cloud around a single drop cannot be changed significantly by the continuous decrease of the magnitude of the particle surface during evaporation. Therefore the P-values calculated using the formula for stationary diffusion have to be multiplied by a delay factor $\theta > 1$ to express the higher P-values for the non-stationary diffusion. In this way the delay factor θ does not change the mathematical law of the P-radius curve. These considerations, of course, cannot be applied without some limitation upon the evaporation of extremely small particles, for instance for particles smaller than 0.1 micron, in which the curvature of the particle surface influences the ejection rate.

Based on the considerations above one obtains for P_1 the equation:

$$P_1 = \frac{dm}{dt} \cdot \frac{1}{\sqrt{\frac{M}{2\pi RT}} \cdot 4\pi L} \cdot \frac{n-1}{n(a+2\delta)} \cdot \theta$$

This value of P_1 inserted in the equation

$$\frac{dm}{dt} = \frac{dm_E}{dt} - P_1 \cdot S \sqrt{\frac{M}{2\pi RT}} \cdot R_R$$

if S for a sphere is replaced by $4\pi a^2$ gives the following equation for the evaporation of spheres under the assumed conditions:

$$\frac{dm}{dt} = \frac{dm_E}{dt} : \frac{1}{1 + \frac{(n-1)\,a^2}{n \cdot L\,(a + 2\delta)} \cdot \theta \cdot R_R}$$

n is related to the diameter r_{max} of the vapor cloud around a single particle and to $a + 2\delta$ by the following equation:

$$n = \frac{r_{max}}{a + 2\delta}$$

5. Vapor Stagnation

In the case of vapor stagnation the value of the partial pressure is $P_1 + P_2$. The value P_2 is the partial pressure which is caused by stagnation. Therefore the equation for $\frac{dm_c}{dt}$ is

$$\frac{dm_c}{dt} = (P_1 + P_2) \cdot S \cdot \sqrt{\frac{M}{2\pi RT}} \cdot R_R$$

If one inserts into this equation the expression found for P_1, the following equation is obtained for a sphere with vapor stagnation:

$$\frac{dm}{dt} = \frac{\frac{dm_E}{dt} - P_2 4\pi a^2 \sqrt{\frac{M}{2\pi RT}} \cdot R_R}{1 + \frac{(n-1)a^2}{Ln\,(a + 2\delta)} \cdot \theta R_R}$$

6. Influence of Wind

The influence of wind changes the size of the vapor cloud and this effect can be expressed by the wind factor, f, of Froessling. For f, these equations are used:

$$f = 1 + k\sqrt{Re}$$

$$Re = \frac{\rho U 2a}{\eta}$$

$$k = \sim \frac{0.276}{\sqrt[3]{\sigma}}$$

The wind factor expresses the change of the evaporation rate by wind and is used by Froessling in connection with Langmuir's formula. Langmuir's formula proposes $r_{max} \gg a$ (compare the form factor in the development of the Langmuir equation). Therefore $\frac{n-1}{n}$ has to be replaced by

$$\frac{n-1}{n} \cdot F = f$$

where F is the wind factor correcting $\frac{n-1}{n}$ for $n \gg 1$. When the particles are closer than two times the thickness of the boundary layer of vapor atmosphere around a single falling particle at the given wind speed, Froessling's wind factor f is no longer applicable and has to be either calculated for the special conditions or experimentally determined. Inserting the corrected wind factor f_c into the evaporation equation for stagnating vapor produces the following evaporation formula for a single drop in a vapor cloud with the stagnation pressure P_2:

$$\frac{dm}{dt} = \frac{\frac{dm_E}{dt} - P_2 \cdot 4a^2\sqrt{\frac{M}{2\pi RT}} \cdot R_R}{1 + \frac{a^2}{f_c \cdot L(a + 2\delta)} \cdot \theta R_R}$$

7. The Stagnation Pressure P_2

From the preceding formula the value of $\frac{dP_2}{dt}$ in a differential thin lamina of the airstream situated perpendicular to the direction of the airstream and moving with the airstream can be calculated (figure 4). The stagnation pressure P_2 in the moving lamina increases in time proportional to m; therefore, $\frac{dP_2}{dt} \propto \frac{dm}{dt}$. The formula

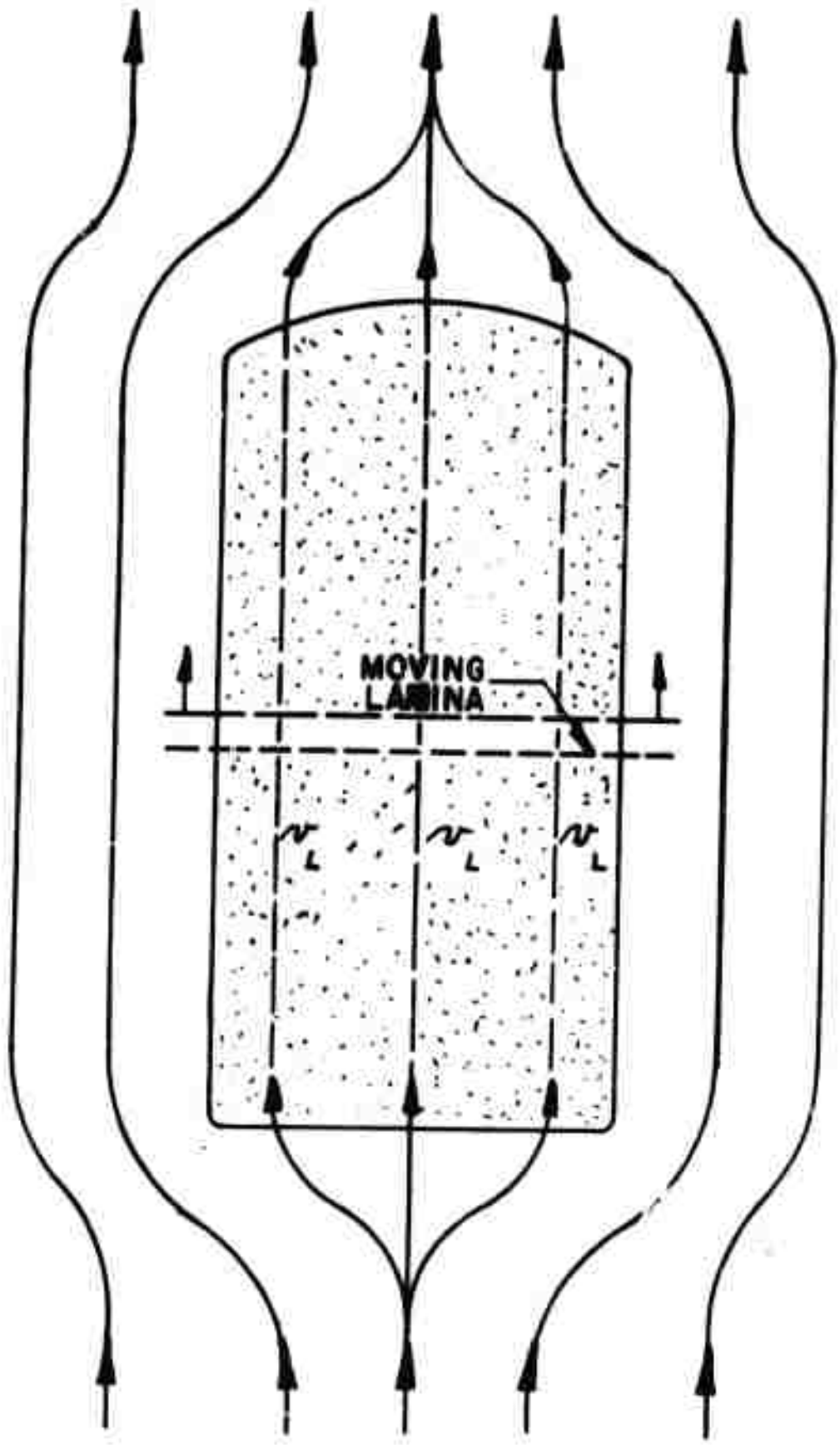

VENTILATING AIRSTREAM THROUGH A CLOUD

FIGURE 4

$$\frac{dP_2}{dt} = \frac{c^2}{V} \cdot \sum_{1}^{n} \frac{\left(\frac{dm_E}{dt} - P_2 4\pi a^2 \sqrt{\frac{M}{2\pi RT}} R_R\right)}{\frac{a^2}{f_c \cdot L \cdot (a + 2\delta)} R_R}$$

is valid for every location in the cloud because the cloud can be considered as almost completely mixed. The value of V is 1 if one takes for V a unit volume of the cloud. From the above equation can be obtained the value of t by integration. In the case of mono-dispersed aerosol and a particle number N, one obtains the following integral because $\frac{dm_E}{dt}$ is constant.

$$t = \int \frac{V \cdot a^2 R_R \cdot dP_2}{c^2 N \left(\frac{dm_E}{dt} - P_2 4\pi a^2 \sqrt{\frac{M}{2\pi RT}} \cdot R_R\right) f_c \cdot L \cdot (a + 2\delta)}$$

the value of a is assumed to be constant during the time the lamina is moving through the cloud (almost complete mixing). In this time the airstream moves a distance

$$h = v_i t$$

through the cloud. The height of the cloud required to give the stagnation pressure P_2 in the air coming out of the top of the cloud is h. The mass of vapor coming out of the top of the falling cloud in time t, is:

$$m = 3 \frac{v_i \cdot t \cdot P_2 \cdot Q}{c^2}$$

Therefore, the evaporation rate of the cloud is

$$\left(\frac{dm}{dt}\right)_2 \text{cloud} = 3 \frac{v_i \cdot P_2 \cdot Q}{c^2}$$

GLOSSARY OF SYMBOLS NOT EXPLAINED IN TEXT

a = radius of evaporating sphere

c = average velocity of vapor molecules

γ = specific heat ratio of evaporating liquid

D = diffusion coefficient

δ = mean free path of vapor molecules

$[\Delta H_{vap}]$ = heat of evaporation

e = base of natural logarithms

η = viscosity of air

m = mass of molecules evaporated

M = mass of evaporating molecule

m_c = mass of absorbed vapor molecules

m_E = mass of molecules ejected

P_1 = average value of the partial pressure of vapor in the stopping zone

Q = horizontal cross section of the cloud

R = universal gas constant

Re = Reynold's number

ρ = density of air

S = surface of evaporating particle

$\sigma = \frac{D}{R}$

t = time

T = temperature, °K

u = velocity of sound in the liquid

U = relative velocity of drop and air

TRAVEL OF DROPLETS IN TURBULENT STREAM

by

Gabrielle Asset
Directorate of Research
U. S. Army Chemical Warfare Laboratories
Army Chemical Center, Maryland

Particle travel in the atmosphere is influenced by several factors. The path of the particles depends upon gravity, wind velocity, wind profile, convective currents and wind turbulence. If the path of particles were known it would be possible to compute downwind concentrations of an agent disseminated from a plane or by means of an explosive on the ground. Equations have been derived by Sutton (1) and Gifford (2) to predict downwind concentration of aerosols of droplets. These equations take into account wind velocity profiles, and also turbulence to the extent that a coefficient for turbulent diffusion appears as a factor. Tank (3) (4) derived equations to predict the area and the shape of the surface deposit of droplets dispersed through the atmosphere and deposited on the ground. In this derivation diffusion parameters due to turbulence are employed, but their values are estimated.

In this paper we shall discuss the effect of turbulence on particle travel. Turbulence is present in the atmosphere nearly all the time. It is characterized by the presence of randomly fluctuating velocities superimposed on the general wind velocity. Figure 1 is a graph of wind measurements made by Gill and Cramers (5) over a period of 2 minutes. The fluctuating nature of the wind velocity is apparent. The velocity in such measurements is denoted by a mean, and the measure of the fluctuation by the root mean square of the fluctuations, i.e., the standard deviation of the average. It has been shown experimentally that the frequency of occurrence of these standard deviations is the same as that of a random phenomenon. In the atmosphere these fluctuations take place in all three directions even though the mean wind trajectory is horizontal. The ratio of the root mean square of the fluctuating velocity to the mean wind velocity, $\sqrt{\overline{v^2}} / \overline{v}$, is a measure of intensity of

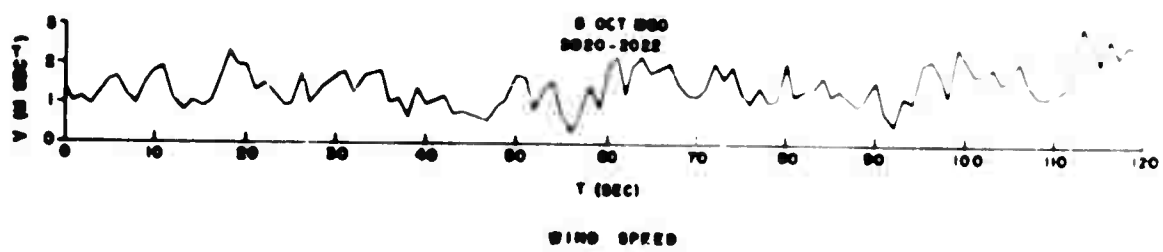

FIGURE 1

FLUCTUATIONS OF WIND VELOCITY (FROM CRAMERS AND GILL)

turbulence. The fluctuating velocities at two different points in space are correlated to each other if the two points are sufficiently close together. The correlation coefficient of the fluctuating velocities is expressed in the usual statistical way:

$$R_x = \overline{v_{x_o} v_{x_1}} \Big/ \sqrt{\overline{v_{x_o}^2}} \sqrt{\overline{v_{x_1}^2}}$$

The correlation coefficient is unity when x_o and x_1 are close together; but it falls to zero as they become farther apart. The integral $\int R_x dx$ is a length which defines the Eulerian scale or the size of turbulence.

According to the modern view, a turbulent flow may be considered as the movement of parcels or eddies of air, irregular in shape, size, and in angular velocity. The average distance by which these parcels are displaced is given by

$$\overline{Y^2} = \overline{V^2} \int_o^t \int_o^T R_\tau d_\tau dt$$

where $\overline{Y}$ is average distance, $\overline{V}$ is the average of the fluctuating velocities of the parcel in the direction of the displacement. R is the Lagrangian correlation coefficient. This correlation coefficient is different from the one which has been previously mentioned which is commonly measured. Figure 2 shows the position of a parcel of air at times, τ. The correlation between the velocity at time $\tau = 0$ at some other time $\tau = \tau_n$, is the Lagrangian correlation. To obtain this correlation we must study the fluctuating velocities of the parcel along its path. The Lagrangian correlation is a difficult one to measure, as it is impossible to follow a parcel of air and probably it keeps its velocity only a short time. Some workers have used tracers and measured their velocities and their positions at successive time intervals in the air. Smoke puffs, soap bubbles, thistledown and spores, have commonly been used.

What are the effects of turbulence on the travel of aerosol? Turbulence causes a cloud of aerosol to spread in all directions and to become dilute. A continuous cloud such as generated by a smoke generator spreads laterally, vertically, and longitudinally as it moves down stream and becomes more dilute. Figure 3 illustrates the spread of the cloud. Smoke issuing from a smoke pot spreads vertically and laterally.

PATH OF A PARCEL OF AIR IN TURBULENCE

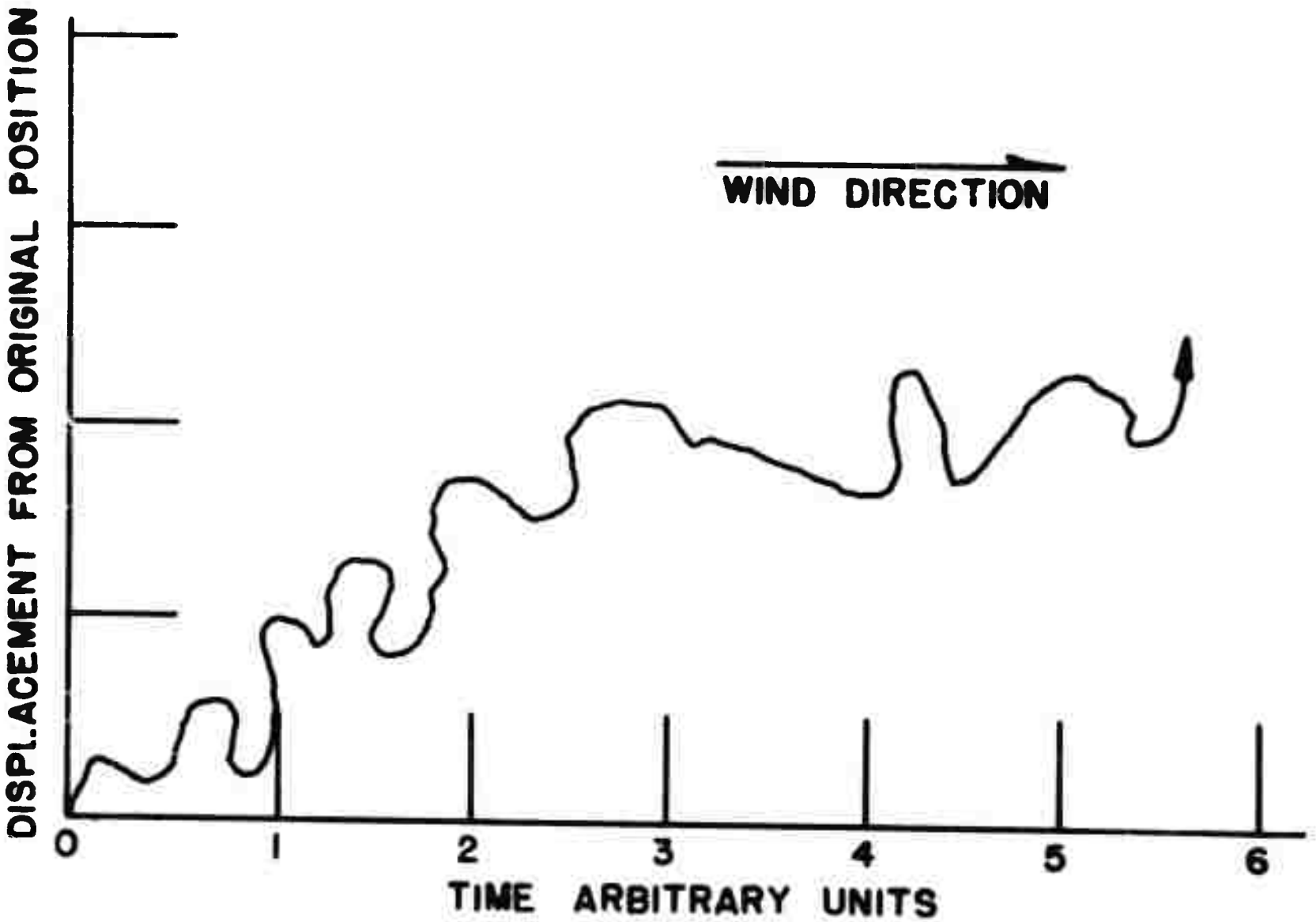

FIGURE 2

FIGURE 3

AN ILLUSTRATION OF THE LATERAL AND VERTICAL SPREAD OF A SMOKE CLOUD

Now let us consider the motion of individual drops or particles suspended in a parcel or eddy of turbulent air. Figure 4 shows a diagram of a particle suspended in an eddy. As the eddy moves in an irregular path small droplets of one micron will probably follow the motion of the parcels as they twist and turn under the influence of the fluctuating velocities of the other parcels. However, large heavy droplets will not be able to follow the changing fluctuating velocities. If the parcel moves or twists too fast the heavier particle continues to move at its own velocity, thereby developing a velocity relative to that of the air. Another parcel or eddy may catch up with it. On the other hand, if the parcel slows down the drop moves relatively faster and slips into another eddy. From these considerations it is obvious that the drop may not necessarily follow path motion of the parcel or eddies of air. Friedlander estimated the relative velocities of aerosol particles in turbulent flows. Figure 5 shows some of his results. According to these estimates particles of 5 microns acquire very little relative velocities and therefore follow the motion velocities of the eddies, whereas particles of 100 microns move at large relative velocities and therefore are independent of some fluctuations.

These values indicate that data from field studies done with 5 micron particles will not apply to particles of 100 microns. The smaller one will be spread laterally at the same rate as gases but drops of 100 microns will spread to a lesser or greater rate. It is necessary to know the relationship of the rate of spread of the aerosol or drops with the particle size and with the properties of turbulence. With this kind of knowledge more accurate predictions may be made for the diffusion of aerosols and the ensuing concentration and deposition.

DISPLACEMENT OF PARTICLES IN TURBULENCE

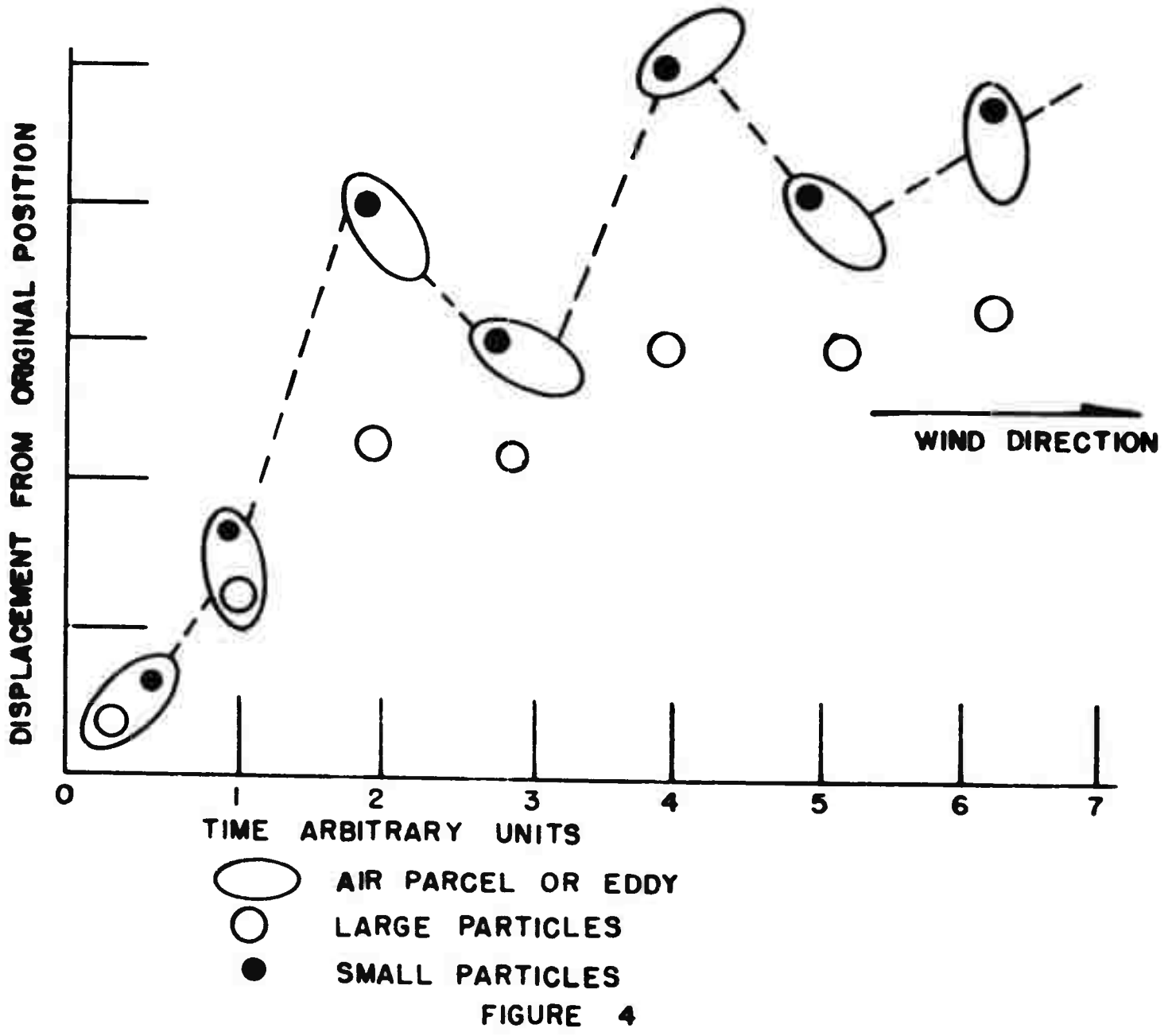

FIGURE 4

RELATIVE VELOCITIES OF AEROSOL PARTICLE AND AIR PARCEL. (FROM FUCHS AND SUTUGIN)

PARTICLE DIAMETER microns	RELATIVE VELOCITY $\overline{(V_p - V_A)^2} / \overline{V_A^2}$
5	.02
10	.05
20	.22
30	.35
100	.90

FIGURE 5

BIBLIOGRAPHY

1. Sutton, O. G., Micrometeorology, p. 110 New York: McGraw-Hill (1953).

2. Gifford, Frank, Jr., Atmospheric Diffusion from Volume Sources. J. Meteor. 12, 245 (1955).

3. Tank, William G., The Use of Large-Scale Parameters in Lower Level Diffusion Computations. Dugway Proving Ground. Cloud Physics Scientific Report No. 4 (1956).

4. Tank, W. G., The Consideration of Nonisotropic Turbulence. DPGRR 113 (1957), (Dugway Proving Ground).

5. Cramer, H. E., Gill, G. C., and Record, F. A., Research on Atmospheric Turbulence and Associated Diffusion of Aerosols and Gases near the Earth's Surface. Contract AF19(604)-145 Air Force Cambridge Research Center, 15 June 54.

6. Friedlander S. V., Behavior of Suspended Particles in a Turbulent Fluid. AIChE Journal 3, 381, 1957.

MODELS FOR COMPUTING CONTAMINATION EXPECTED FROM AIRCRAFT SPRAY

John Rosinski, Richard H. Snow, and Fred B. Smith

Armour Research Foundation,
Illinois Institute of Technology,
Chicago 16, Illinois

The work leading to this paper was performed under several task assignments of Contract No. DA 18-108-CML-5507, entitled Analysis of Selected Dissemination and Design Problems. Technical supervision of the contract was provided by the Weapons Research Division, Research Directorate, U. S. Army Chemical Warfare Laboratories. Since reports covering all task assignments have been issued, this is neither a summary of work performed, nor a presentation of results. We discuss equations describing the motion of particles through the atmosphere, and indicate how simplifying assumptions influence the fit of physical models to experimental data.

I. DRIFT EQUATION

When a liquid is discharged into the atmosphere, droplets are formed. These droplets will drift with the wind during the time that it takes for them to fall to the ground. The simplest case is when the dispersion due to atmospheric turbulence is unimportant. For this case, the effective density of droplets on the ground is:

$$D_e = Q \frac{dM}{d(d)} \left| \frac{d(d)}{dy} \right| \qquad (1)$$

where

D_e = effective density of droplets at a point on the ground, g/m^2

Q = mass of agent released per meter, g/m

(d) = droplet diameter, mm

y = distance from release point measured on the ground, m

$dM/d(d)$ = drop size distribution, g/mm size range - g released, in the size range (d) + d(d)

$d(d)/dy$ = size range of droplets falling in an increment of distance from the release point, mm/m

This equation shows that the spread of droplets is determined by the drop size distribution, $dM/d(d)$, and the drift, $d(d)/dy$.

The meaning of Q becomes apparent when the method of releasing the liquid is considered. If the liquid is released in a plume from an aircraft flying a straight and level path across wind, Q represents the mass released per meter of plume length.

Previous speakers in this symposium have indicated the extreme complexity of the mechanics of breaking of liquids and formation of droplets. At present, it is necessary to resort to empirical investigations to ascertain the drop size distributions which may be expected from operational spray devices. Applicable experimentally determined drop size distributions were not available for our study. Therefore, an arbitrary size distribution fitting an equation of the form proposed by Nukiyama and Tanasawa[1], and by Mugele and Evans[2], was assumed.

$$\frac{dM}{d(d)} = 0.046\,(d)^3 \exp\left[-1.47\sqrt{\frac{(d)}{6-(d)}}\right] \qquad (2)$$

This distribution is shown in Fig. 1.

In the absence of atmospheric turbulence, droplets of one size fall at the same rate, and encounter the same winds. That is, droplets of the same size, released from the same point, at approximately the same time, would arrive at the same point on the ground. Smaller droplets would drift greater distances than larger ones, but there would be no overlapping of droplet sizes.

Droplets of one to three mm diameter quickly attain their terminal velocity in air. These terminal settling velocities may be computed from the empirical equations derived by Best[3]. For the International Commission for Air Navigation standard atmosphere:

$$v_z = 9.32\left\{1 - \exp\left[-\left(\frac{(d)}{1.77}\right)^{1.147}\right]\right\}\exp\left(4.05 \times 10^{-5} z\right) \qquad (3)$$

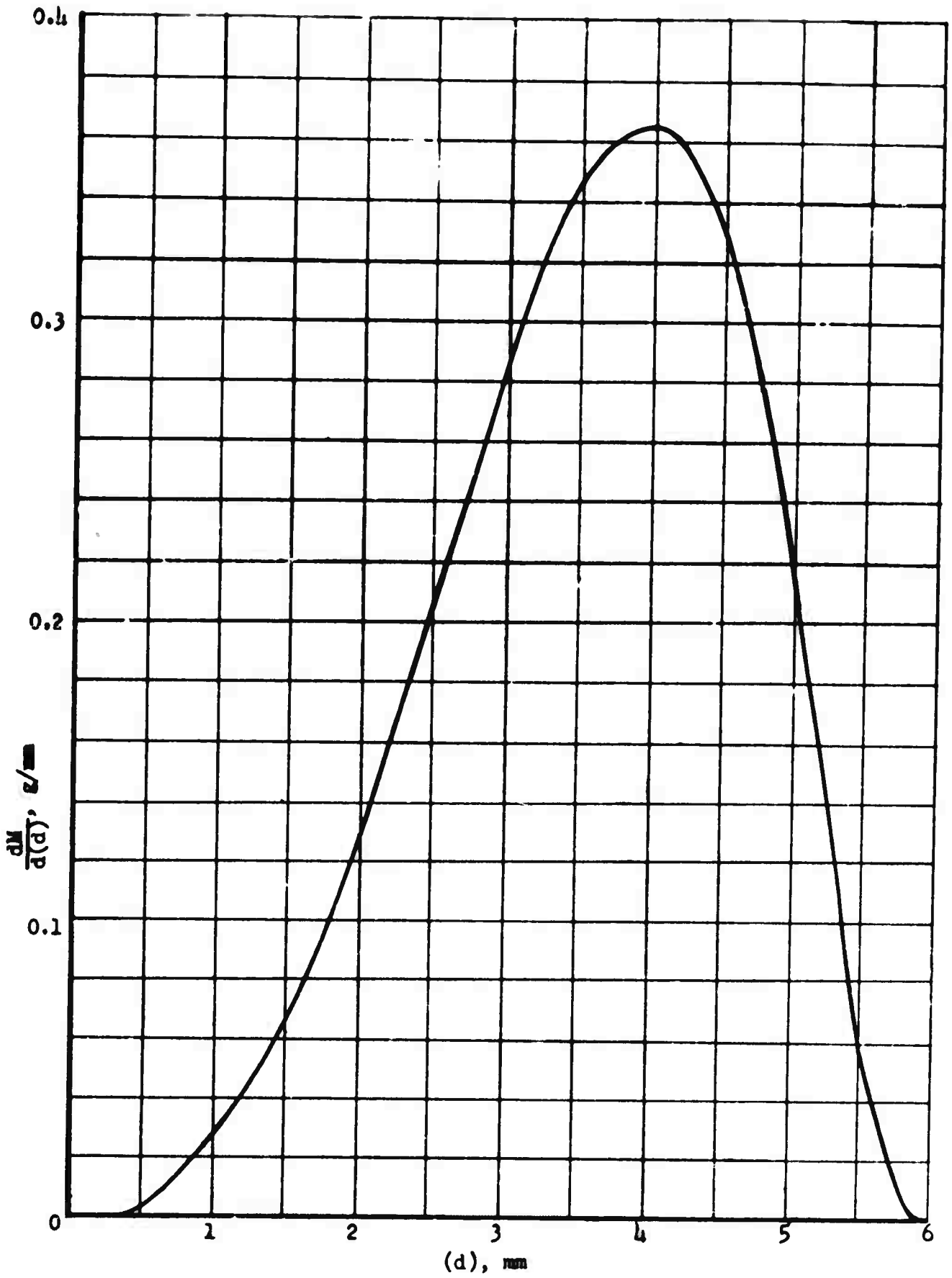

FIGURE 1

DROP SIZE DISTRIBUTION USED IN EXAMPLES

For the Summer Tropical standard atmosphere

$$v_z = 9.58 \left\{ 1 - \exp \left[- \left(\frac{(d)}{1.77} \right)^{1.147} \right] \right\} \exp (3.54 \times 10^{-5} z) \qquad (3')$$

where

z = height, m

v_z = terminal velocity of drop, m/sec

(d) = drop diameter, mm

The horizontal component of droplet displacement is determined by the wind velocity profile. Under usual conditions, the wind velocity at any level up to 400 meters in height is approximated closely enough by the empirical equations developed by Chapman, by Hellman, or by Ekman. Chapman's equation was used in this work. It is:

$$v_x = a \log_{10} z + b \qquad \text{(See Fig. 2)} \qquad (4)$$

The variation of wind velocity with height above 400 meters changes with synoptic and local meteorological conditions, terrain, latitude, season, etc. This is a subject being continually studied by meteorologists, and is one of the areas being intensively investigated during this Geophysical Year. Means exist for determining wind profile above 400 meters by direct measurement. Statistical surveys have been conducted for some areas. For comparing munitions, it is reasonable to assume that winds above 400 meters have the same speed and direction as the wind at 400 meters. This assumption was made in our analyses.

Combining the expressions for wind velocity and settling velocity gives the expression for the drift distance of a droplet:

From 400 m height:

$$y = \frac{1}{v_z}(867a + 400b) \qquad (5)$$

From 5000 m height:

$$y = \frac{867a + 400b + 4170v_x}{v_z} \qquad (5')$$

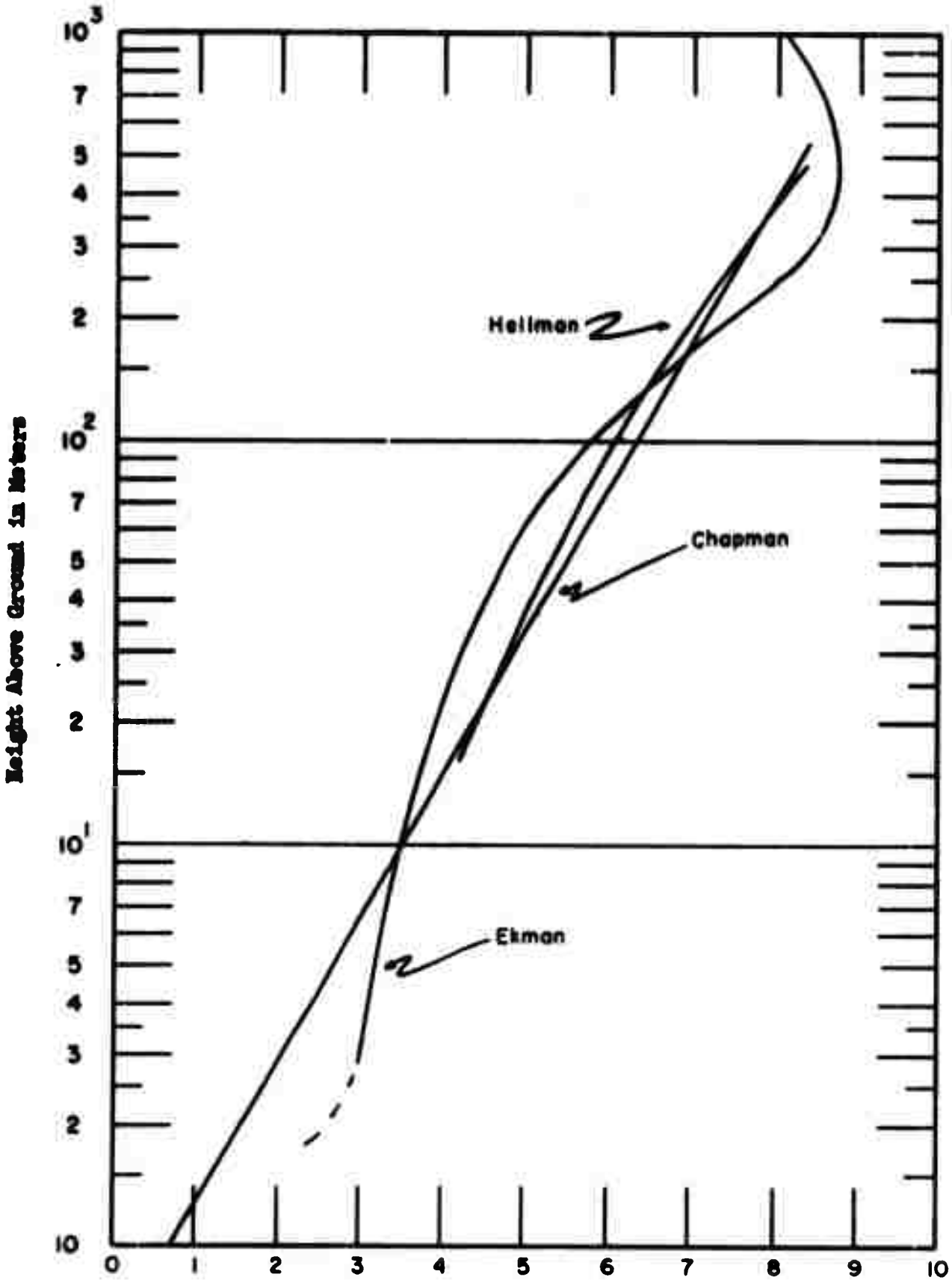

FIGURE 2

COMPARISON OF WIND PROFILE RELATIONSHIPS

where

y = drift, m

Since these equations are functions of droplet diameter, we differentiate with respect to y to find the size range of droplets falling per meter at a distance y from the release point.

From 400 m height:

$$\frac{d(d)}{dy} = \frac{-0.165 v_z^2}{(867a + 400b)\left(\frac{(d)}{1.77}\right)^{0.147}\left(\exp\left[-\left(\frac{(d)}{1.77}\right)^{1.147}\right]\right)} \tag{6}$$

From 5000 m height:

$$\frac{d(d)}{dy} = \frac{-0.165 v_z^2}{(867a + 400b + 4170 v_x)\left(\frac{(d)}{1.77}\right)^{0.147}\left(\exp\left[-\left(\frac{(d)}{1.77}\right)^{1.147}\right]\right)} \tag{6'}$$

Equation (1) has been programmed for the IBM 650 digital computer, and a number of cases have been solved. Fig. 3 shows the time of fall of drops through the ICAN atmosphere, and Fig. 4 shows the drift of drops falling through the same atmosphere. The model represented by the drift equation, without consideration of turbulence, is useful for estimating ground contamination caused by large drops disseminated from low heights, when the spray is horizontal and normal to the wind.

II. DISPERSION CAUSED BY TURBULENCE

When the liquid is ejected in a plume parallel to the wind direction, the segregation of particle sizes by the mean wind is not important. This is quite apparent when we consider that drift alone will cause no increase in width of pattern over the width of the initial plume. Segregation due to drift with the mean wind occurs only at the ends of the contaminated area. At intermediate points, there is a complete spectrum of particle sizes. However, particles of different sizes originate at different points in the plume. When the liquid is discharged in a plume parallel to the wind direction, the density of contamination on the ground may usually be represented by:

$$D'(Z) = \sum Q \frac{dM}{d(d)} \frac{1}{\sqrt{\pi}\, CL^{m/2}} \exp\left[-\frac{Z^2}{C^2 L^m}\right] \Delta(d) \tag{7}$$

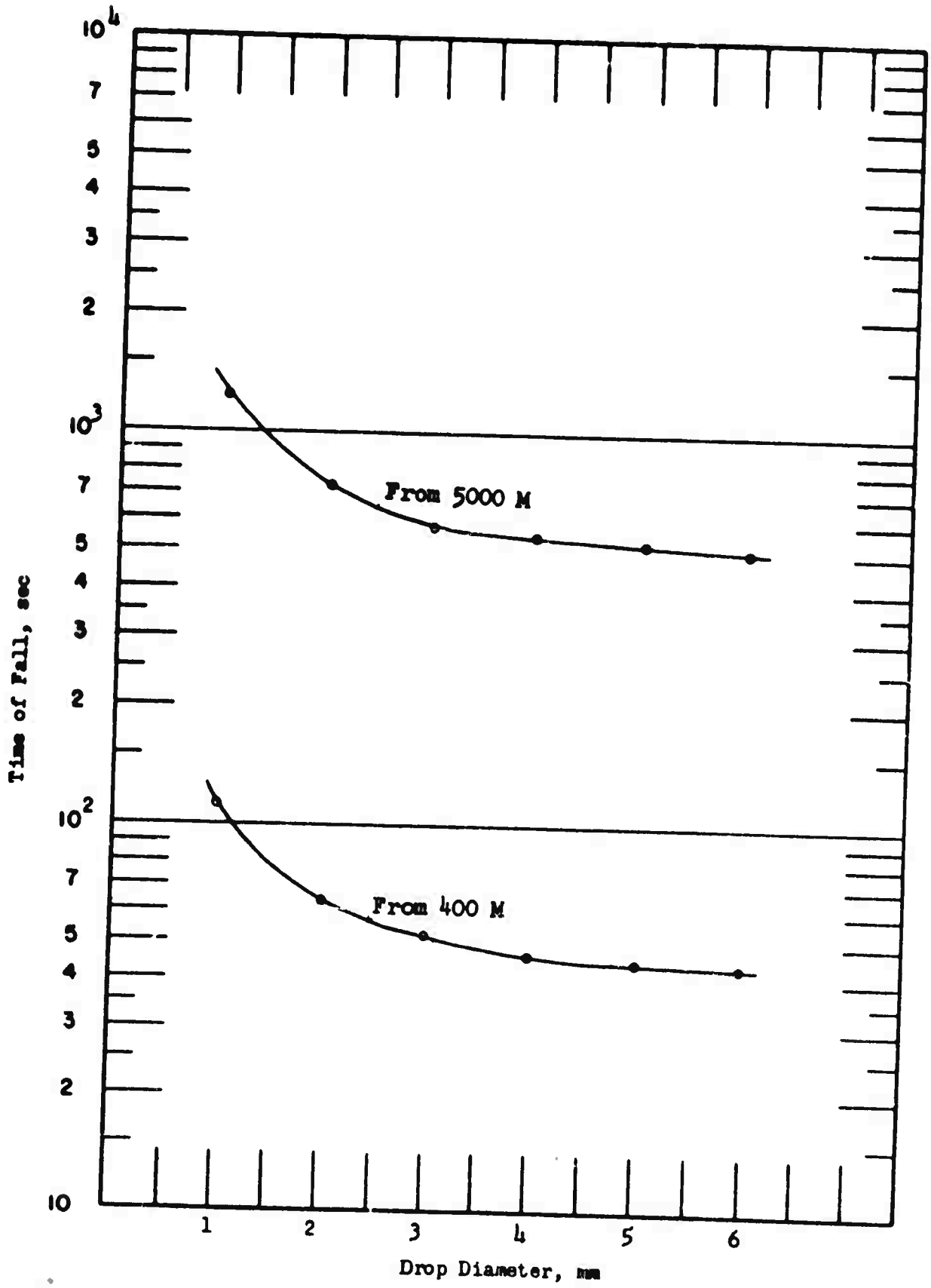

FIGURE 3

TIME OF FALL OF DROPS THROUGH THE ICAN ATMOSPHERE

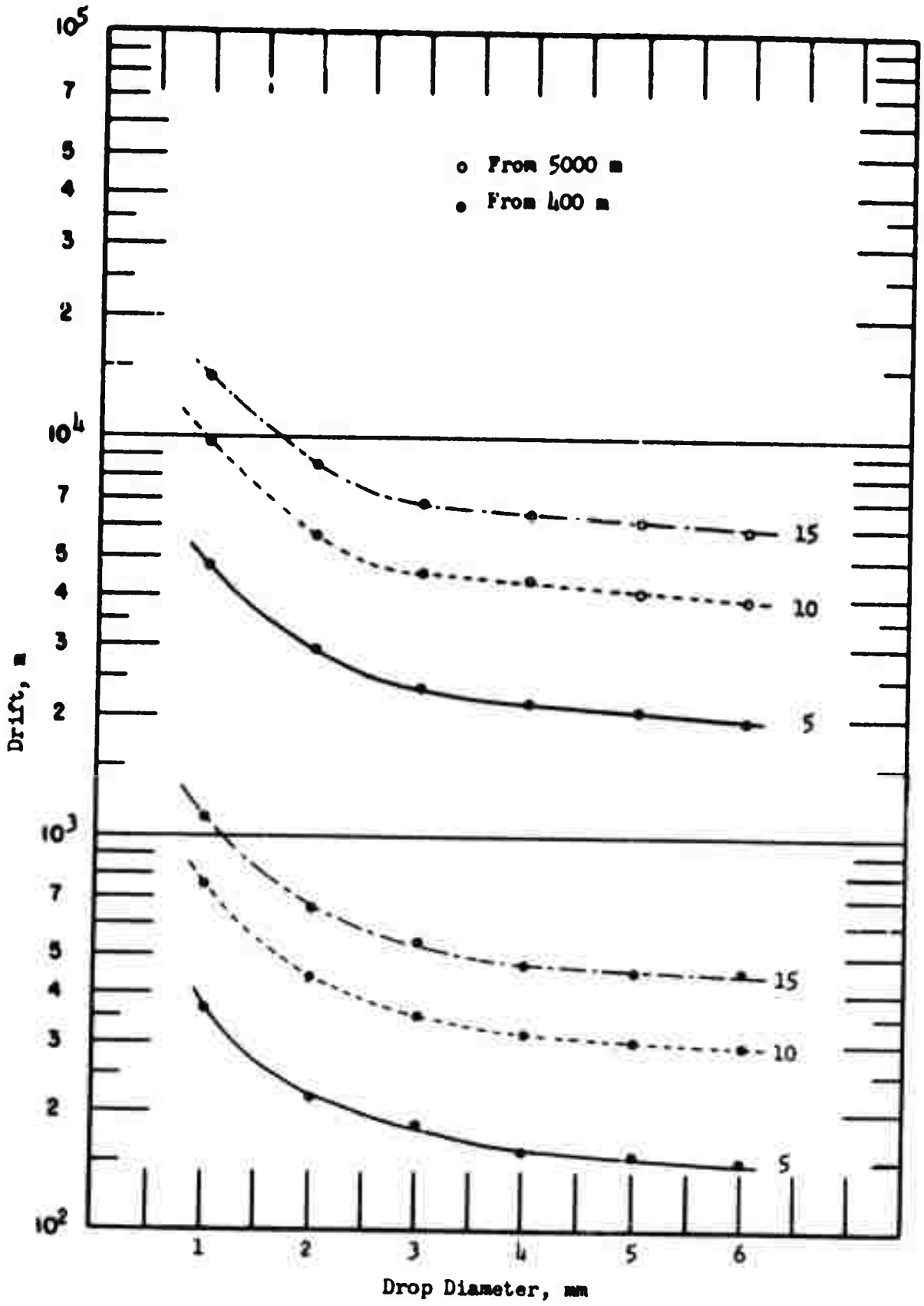

FIGURE 4

DRIFT OF DROPS FALLING THROUGH THE ICAN ATMOSPHERE

where

$D'(Z)$ = density of droplets on the ground at Z, g/m^2

Z = distance from the center line of the contaminated area, m

$L = \sqrt{H^2 + y^2}$

H = height of fall, m

C = empirical constant, $m^{0.125}$

m = empirical constant, 1.75

The summation is carried out over all effective particle sizes in increments of diameter, Δ (d).

Equation (7) is very similar to equation (1), but it includes a factor to account for atmospheric dispersion, and omits the factor d(d)/dy that expresses drift. This expression is summed over the increments of diameter, because all droplet sizes are found at each increment of area on the ground.

This dispersion factor was first used by Davies[4], who presented experimental values of the coefficients C and m. He derived equation (8), for computing the density of contamination at a point on the ground produced by the instantaneous release of droplets of the same size from a point in air.

$$D'(Y, Z) = \left(\frac{Q}{\pi C^2 L^m}\right) \exp\left[-\frac{Y^2 + Z^2}{C^2 L^m}\right] \qquad (8)$$

Davies identified m with the exponent in the equation relating relative wind velocities at different heights. For adiabatic conditions m has the value 1.75. He presented a chart giving values of C for various drop diameters and heights of fall. In some of our work, the average values of C between the height of release and the ground were obtained from Davies' chart by graphical methods. We have converted the units of C to the 0.125 power of meters.

III. COMBINED DRIFT AND DISPERSION OF DROPLETS

A. Example

In this example, it is assumed that 350 gallons of liquid is released at a point in the atmosphere from a tank or device that suddenly

AD205196

opens. We shall not attempt to define this device other than to make general remarks about some of its attributes. The device is designed to release the liquid as a coherent mass. It does not impose surface forces or accelerations which tend to disrupt the liquid body. It does not deflect, support, or cause flow after it functions to release the liquid. Its net effect is to provide a body of liquid at rest or falling freely through the air.

The liquid mass will break from stresses caused by drag forces between the air and the liquid, stresses set up by motion within the liquid, or both. We know that the large body will accelerate until pressure differences cause appreciable deformations, which tend to increase pressure differences, and cause internal circulation of the liquid, thus increasing total internal strains. In short, this is an unstable situation in which stresses build up until they are released by fracture. Fractures and separation of parts of the system set up further oscillations in the resulting pieces. So, we have the formation of filaments, the separation of droplets, the impingement and capture of material, etc. which were discussed in yesterdays sessions. These processes may be ignored for a first approximation to the solution of this problem. It suffices to know that there is a maximum drop size which is stable in free fall through the air. Droplets larger than the maximum stable size will eventually break up. Large droplets acquire a greater terminal velocity than small droplets, and they are subjected to greater drag forces as they fall through the air. The ratio of surface to mass is greater for small droplets than it is for larger ones.

As a gross result of these phenomena not clearly understood nor adequately described, the mass of liquid will produce a column of spray which drifts down to the ground. The larger unstable masses of liquid will fall much faster than droplets small enough to be stable. A whole column of stable droplets will be formed before the droplets at the top of the column have time to drift very far. Relatively large masses of liquid will shatter at all heights of the column, leaving a spectrum of small stable droplets that are quickly slowed to mere drift velocities. There will be impingements and collisions until the complete size distribution in a column falling through the air is produced. The size distribution function that describes the number of droplets produced is not known. The variation of concentration with height or the resulting concentration at each height in the column is also unknown. The problem is estimate the contamination produced on the ground by this device.

In an actual case, the size distribution pattern produced on the ground, and the ground contamination density pattern would be measured. The height of column and concentration of liquid at each height would also be determined in these experiments. Suitably designed experiments conducted under measured conditions would yield the important information.

In this example, it is assumed that the height of the column of drops is 300 m and that the concentration is uniform throughout this height. At the time the column of spray is formed, the top of the column is at height Z = 1000m, and the column extends downward to height Z = 700 m. This is shown in Fig. 5. The wind is in direction y. As the droplets settle, they drift with the wind and are dispersed in directions x, -x, perpendicular to the wind by atmospheric turbulence.

The size distribution of equation (2) is assumed. This is shown in Fig. 1. The distribution on the ground can be calculated by dividing the column into increments of height, and making the assumption that all agent from each increment falls from the center of that increment. Then we sum the contributions from each increment at each unit area on the ground. By means of this approximation, the column problem is reduced to a number of point source problems.

B. Equation of Drift and Dispersion of Droplets

The equation for the density of droplets on the ground contains the factors for both drift and dispersion, which were discussed when we considered the previous models.

$$D(x, y) = \sum_{L} Q'' \frac{dM}{d(d)} \left| \frac{d(d)}{dy} \right| \frac{1}{\sqrt{\pi}\, C L^{m/2}} \exp\left[- \frac{x^2}{C^2 L^m} \right] \qquad (9)$$

where

$D(x, y)$ = density on the ground at (x, y), g/m^2

Q'' = quantity of liquid in an increment of column, g

L = position along column height

Dispersion also occurs in the direction parallel to the wind, although it has been neglected in this equation. In the derivation of this equation, it was assumed that spreading from drift in the wind direction is far more important than dispersion in this direction due to turbulence. This simplification may be justified if the height of fall is small, and only if the fraction of liquid of interest is contained in the large drops. A more refined solution, applicable to distributions containing a larger mass fraction of fine particles by including the factor for atmospheric dispersion in the wind direction. However, additional work is required to add this correction.

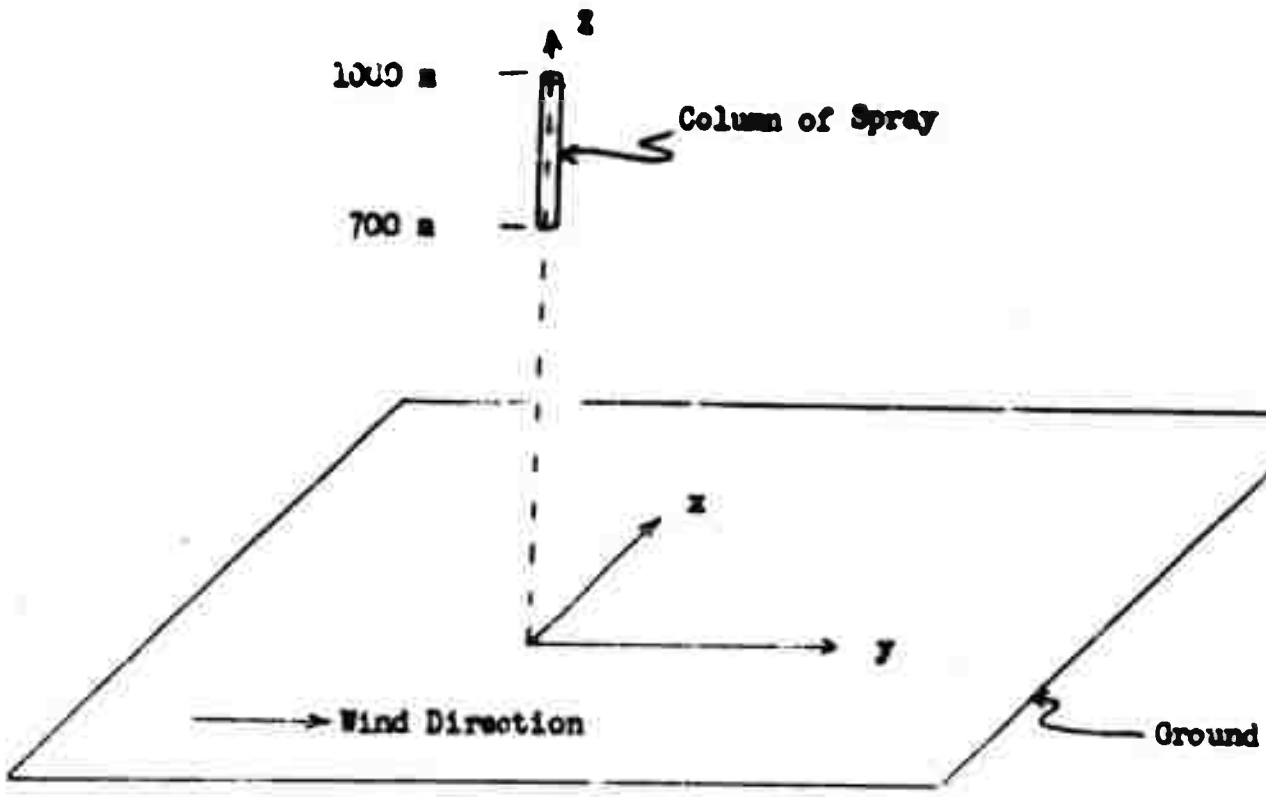

FIGURE 5

ILLUSTRATION OF COLUMN PROBLEM

IV. DISCUSSION

The models presented are useful for studying the influence of some important variables upon the distribution of ground contamination produced by some spray processes. It is necessary to distinguish between primary variables which exert a major influence on density at ground level, and secondary variables which may be neglected without altering the essential features of the problem. Considerable judgment must be exercised in determining what factors may safely be neglected. The final justification can only be in experimental results. Refinement may be achieved by including secondary variables, but the practical value of refinements is limited by the uncontrollable elements in the problem: for example, transient variations in meteorological conditions, variations in functioning of the device which alter jet breakup, unpredictable motions within the fluid caused by uncontrollable operational factors, etc. The main difficulty in selecting descriptive models for evaluating devices or selecting operating conditions, is the lack of complete experimental data on previous test of similar equipments. These are of some use to those responsible for establishing operating criteria and selecting design characteristics.

REFERENCES

1. Nukiyama, S. and Tanasawa, Y. Trans. Soc. Mech. Engrs. (Japan) 4, No. 14, 86, 1938; 5, No. 15, 138, 1939; 6 No. 18, 63, 68, No. 22, II-7, No. 23, II-8, 1940.

2. Mugele, R. A. and Evans, H. D. Ind. Eng. Chem. 43, 1317-24, 1951

3. Best, A. C. Quart. J. Roy. Meteorol. Soc. 76, 302-11, 1950

4. Davies, D. R. Proc. Cambridge Phil. Soc. 46, Part III, 1950

5. ARF Rept. No. 14, Cont. No. DA 18-108-CML-5507, Jan 1956 (S)

6. ARF Task IX Rept., Cont. No. DA 18-108-CML-5507, Sept 1957 (C)

7. ARF Task XII Rept., Cont. No. DA 18-108-CML-5507, Oct 1957 (S)

TECHNIQUES FOR THE DETERMINATION OF DROPLET SIZES IN SPRAY

A. L. Woolridge

Development Directorate,
U. S. Army Chemical Warfare Laboratories
Army Chemical Center, Md.

Spray systems are developed largely from certain basic assumptions and theoretical considerations, and from the performance of laboratory models constructed to conform to these considerations. In the final analysis these systems must be field tested to achieve a complete evaluation. We have heard from several speakers here that the droplet sizes produced by a spray system are of paramount importance. Therefore, it is necessary to have some method of estimating the drop size distribution in a spray.

There are many methods in the literature which deal with the determination of the sizes of air-borne or falling droplets. Some of these work well in the laboratory where conditions can be readily controlled. They may involve the use of intricate apparatus requiring rigid controls which make them impractical for field use. However, there are less complicated methods whereby drop sizes are estimated from the spots they produce on surfaces of contrasting colors. These methods are more specific for the agent being sampled and we have found that they lend themselves more readily to field testing.

The purpose of this presentation is to describe to you some of the techniques we use here at the Army Chemical Center to determine the sizes of droplets in sprays.

Our usual starting point is the particular agent or simulant to be disseminated, and our first consideration is the discovery of a suitable surface on which the droplets can be collected and examined.

The agent must, on contact with the surface, make an easily visible spot whose diameter is proportional to the diameter of the drop. This spot should spread but it should reach a limit of spread in a relatively short period of time. The ratio of spot size to drop size should be large enough to give the desired accuracy of measurements but not so large as to produce tremendous over-sampling from moderately concentrated clouds.

In selecting a sampling surface the characteristics of the agent itself must be considered. Certain surfaces will require that the agent be dyed in order to make the spots visible, or the surface may require a solvent effect from the agent to produce a spot, or the surface may be sensitized so that a color change takes place on contact with certain liquids.

Four sampling surfaces are most prominent in our work here. They are:

1. Jump cards, made of compressed paper, usually white, for which the agent must be dyed. The drop falling on the card is absorbed and spreads, producing a colored spot which can be seen and measured. Figure 1. shows a 6" x 6" jump card with spots produced by 225-micron droplets of bis-(2-ethylhexyl) hydrogen phosphite (BIS) dyed with FD&C No. 32.

2. A plastic film (polyvinyl chloride) approximately 8 to 9 mils thick. Here the agent must also be dyed, but there is a solvent effect of the agent on the plastic which produces a permanent spot. Figure 2 shows 6" x 6" panels of polyvinyl chloride with spots produced by 200 to 500-micron droplets of dibutyl phthalate dyed with FD&C No. 32.

3. M 6 detector paper, which was developed as a vesicant liquid detector, produces a red spot on contact with certain solvents. Figure 3 shows a 5" x 5" panel of M 6 detector paper with spots produced by 250-micron droplets of undyed BIS.

4. A plastic-dye coated glass microscope slide. Figure 4 shows plastic-dye coated microscope slides with spots produced by 80 to 125-micron droplets of undyed BIS. These slides are prepared by dipping them into a solution of polystyrene and DuPont oil red dye in a mixture of ethylene chloride and acetone. This coat dries very quickly, leaving a red plastic film on the slide. The solvent action of a drop of agent on this film produces a clear spot which is proportional in size to the drop diameter. Figure 5 shows the apparatus which was designed for applying uniform coatings to the microscope slides. We found that it was necessary to devise such an apparatus because there was an annoying variation in the thickness of the coatings on hand dipped slides. This variation in the coatings seriously affected the spread factors.

All of these methods have been used for sampling fall-out from airplane sprays or other dissemination systems, where the size of the drops reaching the ground is of chief interest. The M 6 detector paper and coated slides are of great value where it is not desirable or practical to dye the agent

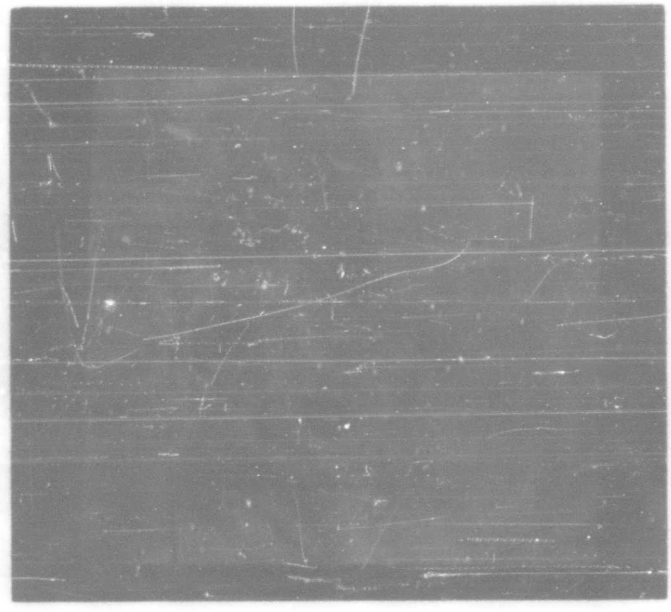

FIGURE 1

Jump Card (6"x6") with spots produced by 225 micron droplets of BIS dyed with 2% FD&C No. 2

FIGURE 2

Polyvinyl chloride panels (6" x 6") with spots produced by 200 to 500 micron droplets of dibutyl phthalate dyed with 2% FD&C No. 32

FIGURE 3

M6 Detector paper (5" x 5") with spots produced by 250 micron droplets of undyed BIS

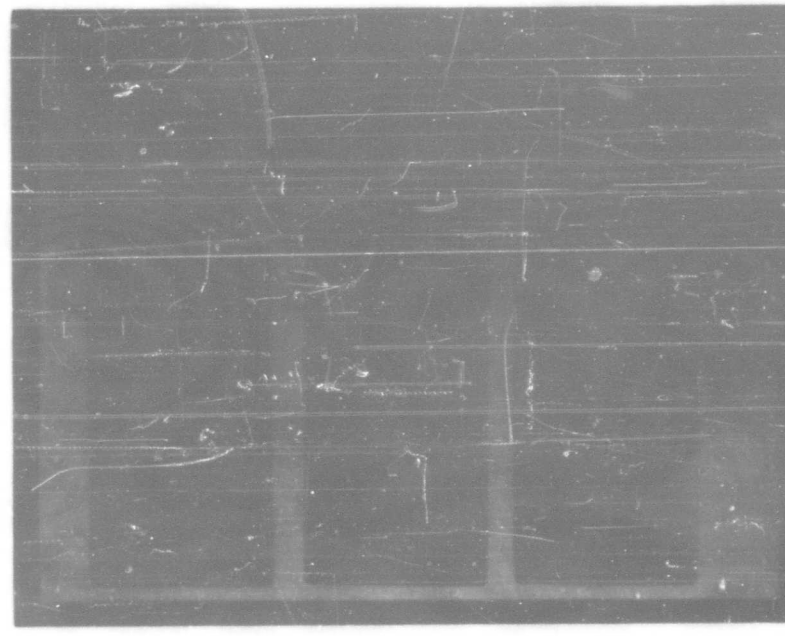

FIGURE 4

Plastic dye coated microscope slides with spots produced by 80 to 125 micron droplets of undyed BIS.

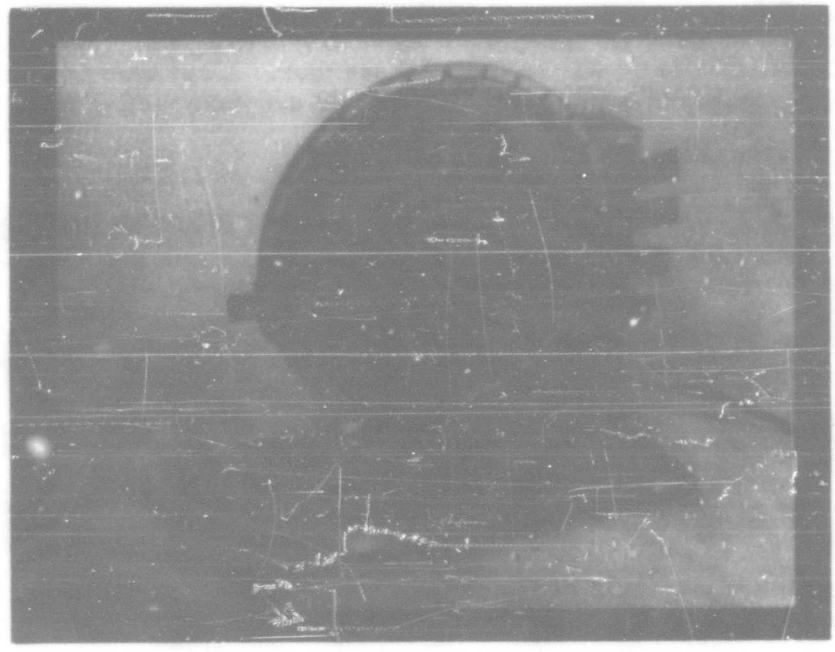

FIGURE 5

Apparatus used for applying plastic dye coatings to microscope slides.

being disseminated since the spot produced is not dependent upon a tracer being present. I might mention here that these surfaces have been used for sampling agents V, G, and H and simulants BIS, dibutyl phthalate and ethyl acetoacetate among others. However, these four surfaces are not being presented as universal samplers. The jump card comes closest to being universal, but here the liquid must be dyed. At present we are attempting to develop a surface for sampling droplets of ethylene glycol, which does not produce satisfactory spots on any of these four. Also there is a need for a flexible surface to accomplish sampling of drops impacting on cylinders.

Having a surface for collecting samples of a droplet cloud, the next step is the determination of the drop sizes represented by the spots. To do this we must have what we call a spread factor. This is the ratio of the spot diameter to the drop diameter. This determination can be divided into four (4) separate steps as follows:

1. The production of uniform size drops.

2. The determination of the diameter of the drops produced.

3. The measurement of the spots on the sampling surface.

4. The evaluation of the data.

Two techniques for producing uniform size drops are being employed here. The first makes use of a device we call the "spinning tip" which was developed here in these laboratories. This device (Figure 6) consists of a small glass reservoir mounted in the chuck of a variable speed motor. An arm projecting from this reservoir contains a small capillary tube with a tip which has been ground to a tapered point. The other end of this capillary extends down into the liquid in the reservoir. When this device is rotated at high speed the liquid travels up the capillary and is thrown from the tip in the form of a small droplet. The size of the droplet can be varied within a certain range by varying the r.p.m. of the motor. The range of drop sizes is dependent on the internal diameter of the capillary tube. For any given capillary being rotated at a constant r.p.m., the drops produced are very uniform and they all impact on the horizontal plane in a narrow circular band around the apparatus. Figures 7 and 8 show the spinning tip in operation and the drops as they are thrown from the capillary.

The other technique used for the production of uniform drops in our laboratories makes use of a vibrating wire (Figure 9). This wire is

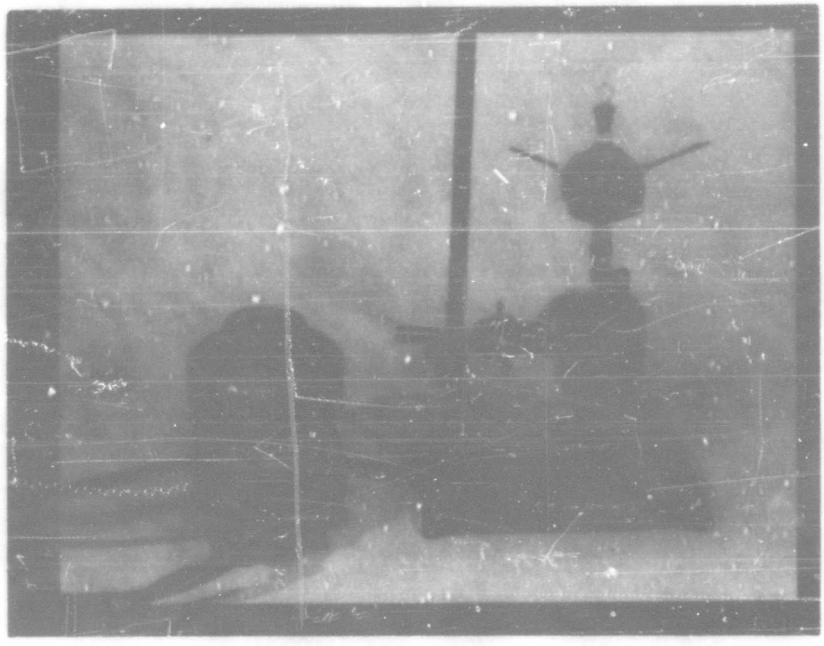

FIGURE 6

Spinning Tip apparatus used for producing uniform size droplets.

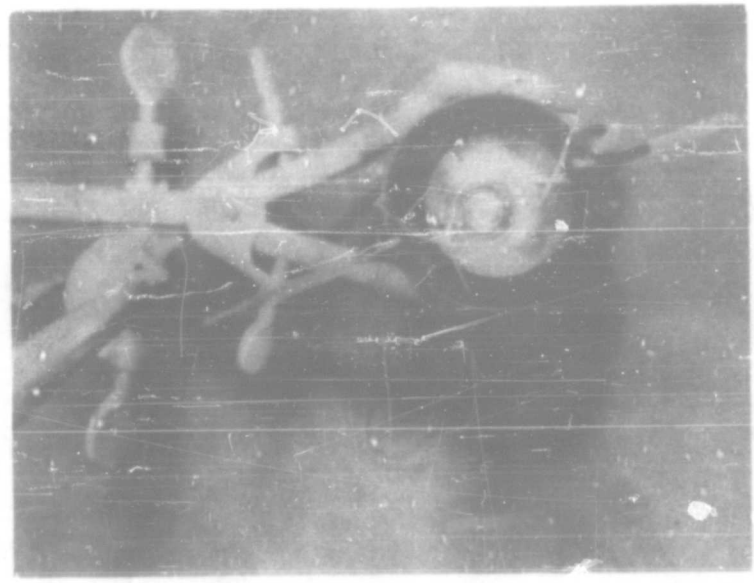

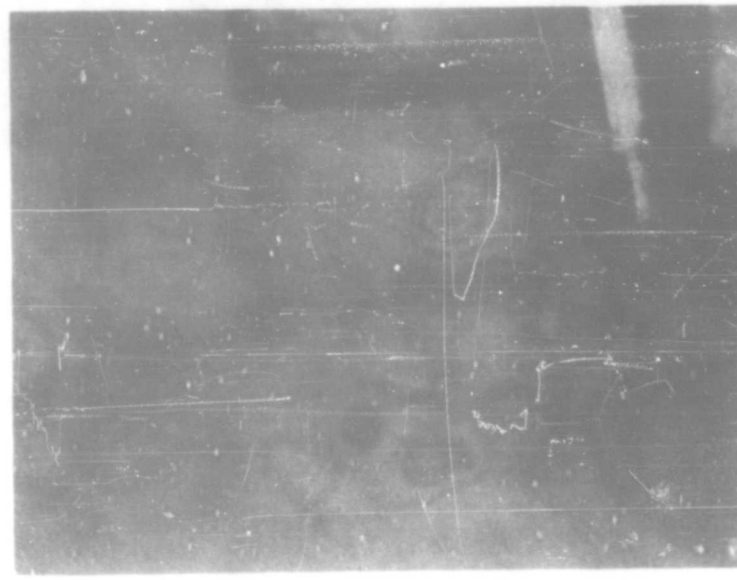

FIGURES 7 & 8

The Spinning Tip in ope ation showing the droplets leaving the tip.

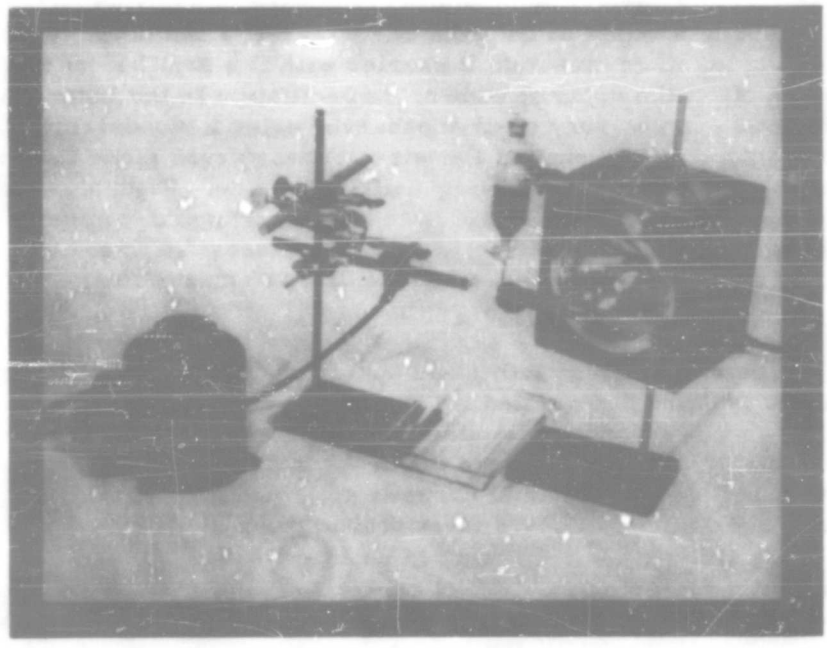

FIGURE 9

Vibrating wire apparatus used for producing uniform size droplets.

attached to the end of a strip of spring steel which is made to vibrate by passing alternating current through a DC coil which is held in close proximity to the steel strip. An intermittent magnetic field is thus created and the vibration is transmitted to the wire. The tip of the wire oscillates in and out of a gap in a fritted glass disc. This gap is kept full of liquid from a reservoir above. By careful manipulation, the wire is adjusted so that the tip enters this pool of liquid at the peak of its travel to one side. As it leaves the gap going in the other direction it carries with it a small amount of liquid. This is thrown off at the opposite side of its oscillation in the form of a small drop. This action can be very clearly observed using a stroboscopic light synchronized with the frequency of the wire. These drops leave the end of the wire in a constant stream and are very uniform in size. Figure 10 shows the stream of drops as they leave the end of the wire. The size can be varied by varying the voltage applied to the coil, which increases the intensity of the vibrations, or by varying the depth to which the wire enters the gap or the pool of liquid.

With one of these methods in operation, the size of the drops being produced must be determined. This is done by collecting a number of drops on a clear glass microscope slide. Using the spinning tip, the slide is placed horizontally in the area where the drops are falling and is allowed to remain until a sufficient number of drops is collected (Figure 11). With the vibrating wire, the slide is passed through the falling stream of drops. This is done as many times as is necessary to collect a sufficient number of drops to give a weight detectable by chemical analysis. These drops on the slide are counted and washed off into a known volume of solvent. This is done as quickly as possible to minimize the losses due to evaporation. A subsequent chemical analysis of this solution will give the total weight of agent present. Dividing this weight by the number of drops gives the weight per drop. Knowing the specific gravity of the agent under investigation the drop diameter is determined by simple mathematics.

Simultaneously with the collection of these drops for weight determination, the surface being calibrated is placed in position for sampling these drops. Figure 12 shows the technique for collecting drops produced by the vibrating wire. The spots produced are allowed to spread to their maximum size and are measured accurately by a prescribed method. The dyed slides and the plastic films are transparent and therefore can be projected using a Wilder Micro projector, Figure 13, and measured on the projection screen. Figure 14 shows how these spots appear on the projector screen. The spot under the scale was produced by a 75-micron drop of BIS on a plastic-dye coated slide. They may also be placed in a photographic enlarger and printed on enlarging paper. The spots on jump cards or M 6

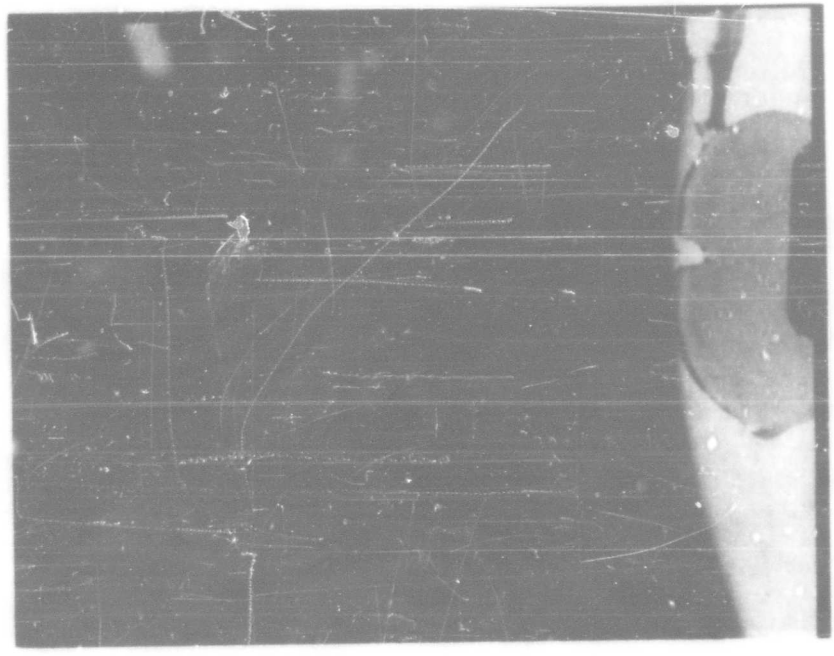

FIGURE 10

Close-up of the vibrating wire in operation showing the droplets leaving the wire.

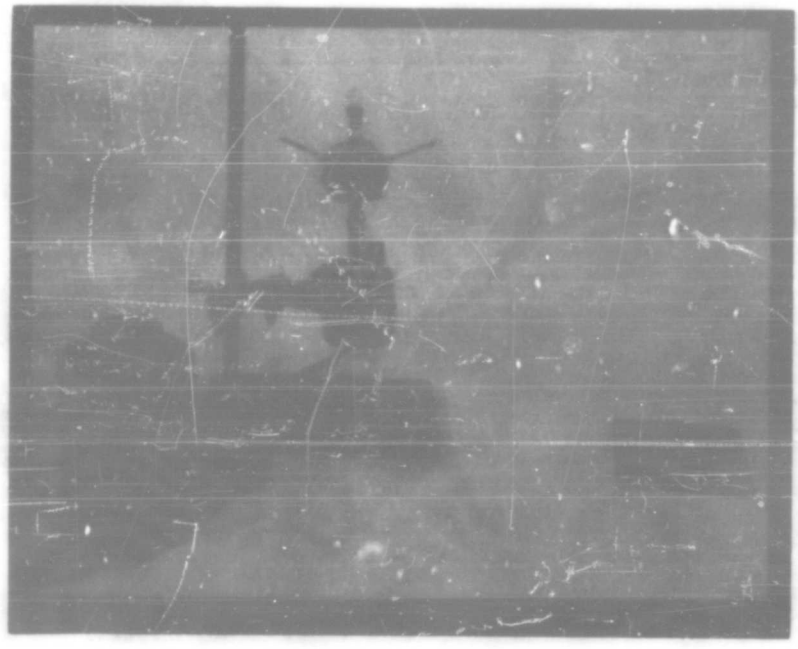

FIGURE 11

Spinning Tip apparatus with samplers in position for collecting droplets for calibration purposes.

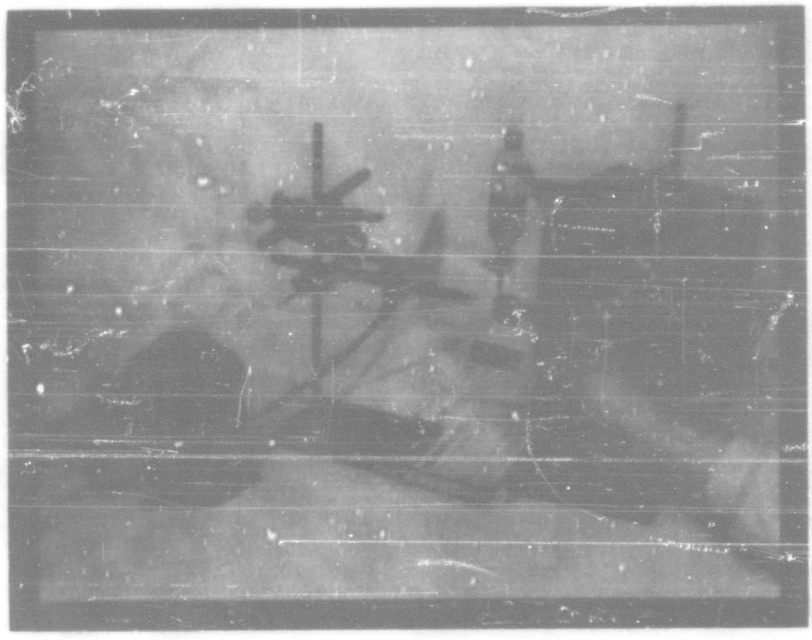

FIGURE 12

Technique used for collecting droplets produced by the vibrating wire.

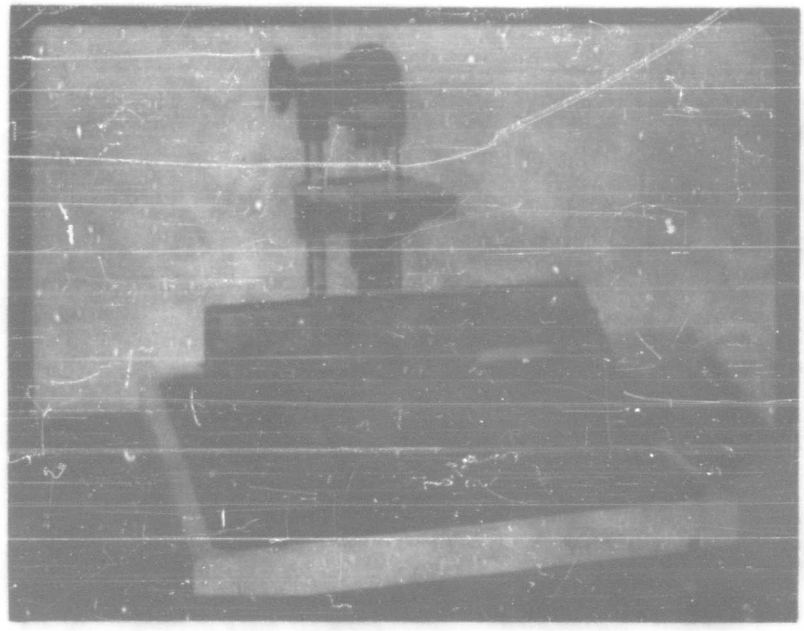

FIGURE 13

Wilder Micro-Projector used for measuring and counting spots on transparent surfaces.

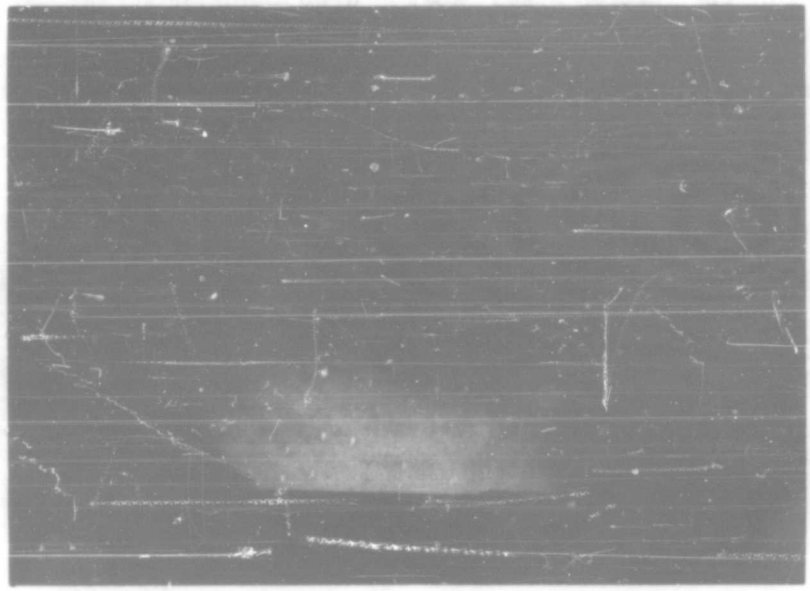

FIGURE 14

Spots on a plastic dye coated microscope slide as they appear on the projection screen of the Wilder Micro-Projector.

detector paper are measured through a binocular magnifier with a calibrated reticule in one eyepiece.

These operations are repeated for drops of several sizes and a plot is made on rectangular graph paper of drop diameter versus spot diameters. Figure 15 is a plot of V-agent spread on M 6 paper, polyvinyl chloride film and on plastic-dye coated slides. Spot sizes in millimeters are plotted along the horizontal axis against drop diameters in microns on the vertical axis. A straight line is produced passing through the origin from which a simple ratio of spot diameters to drop diameter can be obtained. This is the spread factor.

Having a surface for collecting droplets and a spread factor for the liquid on the sur'ace, samples of an aerosol cloud or a spray can be taken and evaluated for an accurate estimation of the drop size distribution. This involves the collection of a large number of samples over a wide area downwind from the source of the spray and the subsequent measuring and counting of vast numbers of spots. This is a very laborious and tedious process but it is necessary for an accurate statistical evaluation of the drop size distribution produced by a spray system.

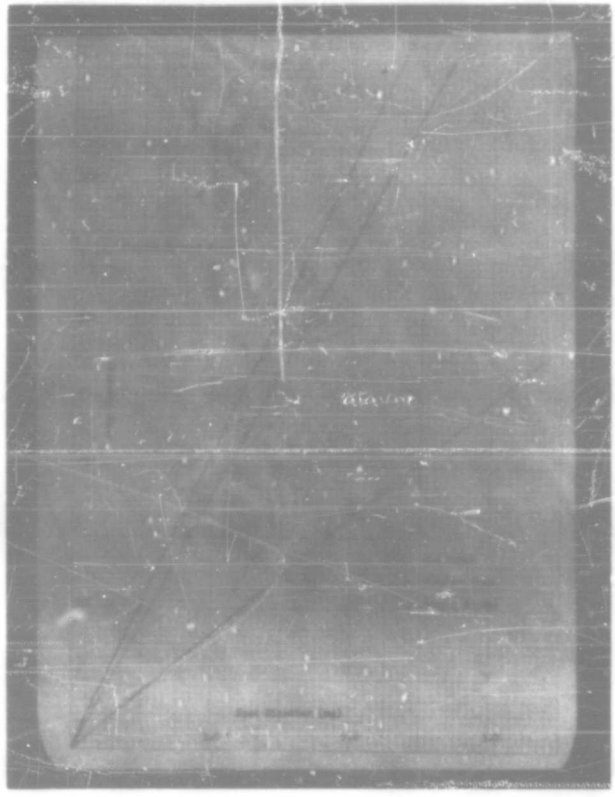

FIGURE 15

Graph of V-agent spread on M6 paper, polyvinyl chloride and plastic cye coated slides. (The units on the vertical axis are microns)

DEVELOPMENT OF A CAMERA TO PHOTOGRAPH HIGH SPEED PARTICLES

John A. Hinckley, and Associates
10316 South Throop Street
Chicago 43, Illinois

A number of severe problems have limited the success of attempts to photograph aerosol particles.

An f2 objective with ordinary light has a resolving power of about 1 micron. An f16 objective has a resolving power of 9 microns. Therefore, if one is interested in studying aerosol particles down to a size of 5 microns, a lens aperture not smaller than about f2 is indicated. At f2 the circle of confusion at the limits of a field of 4 microns depth, is 1 micron. As here used, the term 'circle of confusion' refers to the apparent size of a point of light lying at either boundary of the defined field. In photomicrography we have found that depth of field is independent of the focal length of the lens, practically independent of the magnification and is directly proportional to both the aperture of the lens and the circle of confusion.

A 5 micron particle would require a magnification of about 200 diameters, if its size were to be measured within 20%. At 200 diameters magnification, the total volume photographed would be about 0.01 cubic millimeter. If an aerosol had 5 particles per cubic millimeter, the probability of obtaining an image of one particle in a photograph would be about one in twenty. The Stanford Research Institute developed an ingenious camera which, by repetitive flash, obtained images of many particles on each plate.

Another important problem is that movement of the aerosol particles must ordinarily be avoided. Thus, a 5 micron particle should not move more than about 1 micron. If the flash duration is of the order of 1 microsecond, the maximum tolerable velocity of the particle is one meter per second. Unfortunately one has to go to extraordinary lengths to obtain such low velocities of these small particles.

Another important problem is the difficulty of obtaining adequate illumination. Microsecond flash output is relatively low. If it were attempted to obtain 200 diameters magnification directly, the exposure requirements

would be greater, by a factor of 40,000, than normal photographic requirements. Even if the initial magnification were 20 diameters, the exposure factor is 400 times. These requirements have made necessary the use of some unusually powerful light sources.

The study of the mechanics of aerosol formation would be greatly aided if photographs of the various stages of formation and life of the particles could be made. It did not appear to us that we could hope to accomplish this objective within photographic methods that have been developed, because of the particle velocities which may amount to several hundred feet per second. A 5 micron particle traveling at 200 ft. per second moves 12 times its own diameter in 1 microsecond; at the best, a streaked image would result.

An old photographic trick for photographing rapidly moving objects, if one has free choice of viewpoint, is to photograph the object coming directly toward the camera or going directly away from the camera. Since aerosol particles traveling toward the camera would inevitably impinge on the lens, we attempted to direct a fast moving stream of particles away from the lens. We failed to get any photographs because we could not straighten the flow lines out before the focal plane was reached. We then directed the stream of particles toward the lens and prevented impingement by a high velocity ribbon shaped jet of air traveling at right angles to the axis between the lens and the focal plane. Thus, the particles traveled through the focal plane and were then deflected away from the lens. We did not obtain any photographs by this method.

Our flash duration had been of the order of 4 or 5 microseconds. We reasoned that if we could provide a curtain of light, the thickness of which was of the order of the depth of field, the light could be of long duration since the camera would see the particles only as they passed through the curtain of light. Therefore, if the flash duration was 1 millisecond, the depth of field would be effectively increased from 4 microns to 1000 microns, and the number of particles passing through the curtain would be increased by a factor of 250 times. We used a variety of spherical and astigmatic lenses to effect light concentration in the focal plane, but were unable to obtain photographs. We then used a U shaped 200 watt second flash tube, placed so that the focal plane lay at the center of curvature of the tube. Inasmuch as the level of illumination from a source varies as the square of distance, we increased the illumination level several hundred fold by this means. We immediately obtained photographs of dozens of particles in each exposure. We interposed a diaphragm between the flash tube and the air jet, so that illumination from the tube would not fall directly upon the camera lens. This diaphragm improved matters further by the Bernoulli effect of reducing the pressure upstream in the aerosol jet so that good streamline flow occurred through the focal plane.

We next undertook attempts to confine the illumination to a thin curtain. We made dozens of xenon discharge tubes in which the illumination was collimated by slits, apertures, and various forms of thin sections of glass and plastic. Efforts to obtain photographs by these means were successful. We seem to have achieved the not uncommon result that the crude apparatus was much better than the refined version. It finally occurred to us that we were simply reducing the illumination below a useful level by our various collimating devices.

One of the important reasons that we wanted a thin curtain of light was that we felt a very serious flaw in the method would result from a wide band of illumination, namely, an inaccurate image size would be obtained. We believed that particle traveling through the focal plane in a broad area of illumination would give an inaccurately large image because of the large circles of confusion. We found on calculation that these out-of-focus effects should not be serious, because the contribution of a point of light very far outside the focal plane is small because of the diffuseness of the reflected beam, and that the contribution of the particle, as it passes through the focal plane, is so high from the periphery that no serious error should result. This theoretical conclusion was completely contrary to the usual concepts of food photographic practice. It indicated that if one has a collection of objects in space to photograph, lying inside and outside the focal plane, more accurate results are obtained if these are photographed while moving axially, than if they were photographed while stationary.

In an attempt to check this conclusion, we performed a model experiment in which a glass sphere of about 3/4" diameter was photographed, using for illumination a circular fluorescent tube surrounding the sphere. The sphere was moved uniformly through the focal plane toward the camera. A photograph was obtained which had a bright circle, with inner and outside flare. The size of this circle, while somewhat diffuse, was the true diameter of the sphere within ±2%. The sphere, when photographed in a stationary position, somewhat outside and inside the focal plane, gave images which were inaccurate.

At the present time, our efforts are directed to the use of larger apertures to obtain increased resolving power, to the use of lower levels of illumination and to increasing the duration of the flash. These latter objectives are quite easily attained by the use of low voltage and high capacitance with the necessary modification of the discharge tubes. We believe

that we will achieve a quite small and simple unit, which can obtain relatively accurate photographs of particles down to 1 or 2 micron size with hundreds of particles appearing in each exposure. The lower limit of resolution can probably be usefully increased so that particles of less than 1 micron size can be studied by the use of ultraviolet flash illumination with quartz optics.

DISPERSION VS. DIFFUSION PROCESSES

William G. Tank

Cloud Physics Division
Test Design and Analysis
U. S. Army Chemical Corps Proving Ground
Dugway, Utah

INTRODUCTION

Qualitatively, the problem of atmospheric diffusion is not a particularly difficult one. The spreading of a smoke plume, for example, proceeds in a manner that is not surprising, agreeing as it does with an intuitive idea of what ought to take place; e.g., higher concentrations of smoke are found at the center of the plume, diminishing in intensity with increasing radial distance. Furthermore, it is readily noticed that the windiness and degree of thermal stability in the lower layers of the atmosphere markedly affect this process, again proceeding in a manner that is qualitatively very reasonable; i.e., high winds and unstable thermal stratification favoring rapid diffusion. The real problem remaining then is to express these facts quantitatively in a theory so that predictions can be made.

The search for a precise, quantitative theory of diffusion has received much attention in the past, and many notable contributions have been made by various authors. Historically, the earliest meteorological theory of diffusion was presented independently by Taylor[1] and Schmidt[2], who based their derivations on a statement of Fick's law of molecular diffusion, viz., "diffusion of material is in the direction of decreasing concentration and is proportional to the concentration gradient." Since that time, there have been many restatements of the problem, evidencing a multiplicity of approaches, which lead to various ramifications of the original theory. Roberts presented perhaps the first concise mathematical

---

[1] G. I. Taylor, Diffusion by Continuous Movements, Proc. London Math. Society, 20: 196 (1920).

[2] W. Schmidt, Der Massen austausch in freien Luft, etc., Hamburg, 1925.

model of diffusion based directly on Taylor and Schmidt's original work[3]. Noting then that this original Fickian or "K-theory" of diffusion is not able to cope directly with the increasing scale of turbulent agitations which comes into effect as diffusion proceeds, Sutton[4], and more recently Frenkiel[5], developed their so-called "statistical theories of diffusion," following Taylor's statistical theory of turbulence[6]. Calder[7] presented a modification of the original K-theory designed to take into account the effect of varying surface roughness on diffusion processes by reccurse to the mixing length hypothesis.

It might be argued that a scientific theory has acquired a certain amount of acceptability, or at least of noteriety, when the number of papers on applications becomes much larger than the number of fundamental contributions of which the theory consists. Certainly the above holds true for the previously mentioned theories and ramifications of those theories. However, it must be emphasized that in spite of the many contributions that have been made to the problem, an exact theory of atmospheric diffusion does not exist. All theories of atmospheric diffusion contain certain parameters and coefficients which have to be evaluated by recourse to some hypothesis or else by direct or indirect measurement, usually the latter. To this extent then, all existing theories are partially empirical, at least in actual practice. It is true that Calder's extension of the K-theory via the mixing length

---

[3] O. F. T. Roberts, The Theoretical Scattering of Smoke in a Turbulent Atmosphere, Proc. Roy. Soc. (London), 104A: 640 (1923).

[4] O. G. Sutton, The Problem of Diffusion in the Lower Atmosphere, Quart, Jour. Roy. Meteorol. Soc., 73: 257 (1947).

[5] F. N. Frenkiel, Application of the Statistical Theory of Turbulent Diffusion to Micrometeorology, Jour. Meteorol., 9 (4): 252-259 (1952).

[6] G. I. Taylor, Statistical Theory of Turbulence, Proc. Roy. Soc. (London), 151: 421 (1935); 156: 307 (1936).

[7] K. L. Calder, Eddy Diffusion and Evaporation in Flow over Aerodynamically Smooth and Rough Surfaces, etc., Quart. Jour. Mech. Appl. Math., 2: 153 (1949).

hypothesis can be evaluated independently of direct physical measurements. Nevertheless, in practice, some empiricism will nearly always be employed in determining the appropriate parameters.

In light of what has been said previously then, there can be no a priori statement made concerning which theory presents the best mathematical model of diffusion for practical use. All theories have their own particular advantages and shortcomings. The ultimate choice then of which model to choose rests upon the consideration of a multiplicity of factors such as the degree of accuracy desired, the scale of the phenomena under investigation, the availability of meteorological instrumentation, etc. A detailed discussion of this problem is, to some extent at least, beyond the scope of the present paper. However, it should now be stated that regardless of which mathematical model of diffusion is selected as being an appropriate working equation, the chosen equation will still be applicable strictly to describing the subsequent behavior of gaseous material which is released to the atmosphere. When one deals with airborne aerosols or particulate matter, some factors must be considered that are not common to uninfluenced diffusion. For example, fall-out, wash-out, and rain-out represent three such factors, all three of which would result in the depositing of the aerosols, for example, on any horizontal surface.

Such deposition of material from an aerosol cloud can be divided into dry weather and precipitating weather elements; i.e., fall-out is used to designate deposition during non-precipitating weather, and includes the effects of both gravitational settling and impaction. Wash-out is used to designate removal of material from the air due to capture of the particles by precipitation elements, while rain-out may be defined as removal due to association of the particulate (or for that matter, gaseous) material with the precipitation element prior to its descent. The problem then, in dealing with aerosol clouds, is to find methods whereby existing diffusion equations can be modified to consider the aforementioned effects. The scope of the present paper will include only the fall-out effect, and its purpose will be to find and discuss appropriate modifications to a given diffusion equation such that this fall-out effect may be considered in estimating both air and surface concentrations of particulate agent.

THEORY

In attempting to modify a given diffusion equation such that the effect of fall-out may be accounted for, one must tacitly make a distinction between "diffusion" and "dispersion" processes. Although these two terms

are commonly used interchangeably, a distinction should be made between the two; i.e., diffusion processes, applicable to gaseous matter, depend solely upon the nature of turbulent atmospheric air motions, whereas dispersion processes, applicable to particulate matter, depend not only on such air motions, but also on the dynamic properties of the particles themselves. Of course, when the particle size decreases below a certain threshold value, which depends on such variables as eddy size and kinematic viscosity, the particulates will truly drift with the air motion, and the process may then be considered as being truly diffusive. However, in general, whenever particulate matter must be considered, a diffusion model will at best yield only a first approximation to actuality.

To proceed then, a diffusion model expresses the concentration of gaseous material as a function of space. It is reasonable to suppose that the theory of eddy diffusion represented by a given diffusion equation is applicable to the dispersion of falling particles, since the correlation between the velocity of particles at successive small intervals of time is likely to be of the same functional form as that used for the diffusion of gas molecules, once the particles have attained their terminal velocities. Therefore, in order to apply a given diffusion equation to the case of aerosol clouds, it will be assumed that the particles are small enough such that, for all practical purposes, they take up their terminal velocities immediately upon release. Moreover, it will further be assumed that not only do the particles reach their terminal velocities immediately, but also that they immediately take up the lateral eddy velocity. This assumption, in effect, ignores the inertia effect of the particles. These two above mentioned assumptions then, represent the theoretical basis of the derivations now to be presented.

Having assumed then, that the "classical" diffusion equations yield suitable backgrounds upon which modifications may be made to consider dispersion processes, it remains then to select one particular diffusion model as the basis for what is to follow. As stated previously, such a choice may be governed by many factors. However, suffice it to say here, that in the interests of simplicity and applicability, Roberts' diffusion equation will be used as the basis of the subsequent derivation. The reasoning behind this choice will be somewhat elaborated upon later, but it should be recognized that the Roberts equation can be expressed in terms of other theories of diffusion by recognizing the relationship between the various diffusion parameters expressed by the various diffusion theories. In other words, the derivations to follow are independent of the mathematical model of diffusion upon which they are based.

The Roberts equation for a continuous point source under conditions of isotropic turbulence may be written as follows[8]:

$$\chi(x, y, z) = \frac{2Q}{4\pi Kx} \; e^{\left[-\frac{\bar{u}}{4x}\frac{(y^2+z^2)}{K}\right]} \tag{1}$$

where $\chi(x, y, z)$ = concentration of gaseous material measured in units of mL^{-3},

Q = amount of material emitted measured in units of mt^{-1},
$\bar{u}$ = mean wind speed, measured in units of Lt^{-1},
K = coefficient of eddy diffusivity measured in units of L^2t^{-1}.

Although equation (1) expresses the concentration as a function of space resulting from a continuous point source, it also represents the total dosage equation for an instantaneous point source, since the technique used in deriving both is the same; i.e., the concentration equation for an instantaneous source is integrated from time $t = 0$ to $t = \infty$. The only difference between the total dosage equation for an instantaneous source and the concentration equation for a continuous source lies in the specification of Q. For an instantaneous source, Q is measured in units of m, while for a continuous source Q must be measured in units of mt^{-1}. Thus, according to equation (1), when Q is measured in units of m, the equation yields the usual dosage units, mtL^{-3}, while a Q expressed in units of mt^{-1} applied to equation (1) yields the usual units of concentration, mL^{-3}.

As stated previously then, equation (1) represents the total dosage equation applicable to an instantaneous point source. It can be shown[9] that the analogous solution for an instantaneous volume source may be written to read

---

[8] O. G. Sutton, "Micrometeorology," McGraw-Hill Book Company, Inc. New York, 1953.

[9] W. G. Tank, Multiple Source Prediction Equations, Dugway Proving Ground, to be published.

$$D = \frac{2Q}{\pi\left[4Kx + \bar{u}b^{-1}\right]} e^{-\frac{\bar{u}(y^2+z^2)}{4Kx+\bar{u}b^{-1}}} \qquad (2)$$

where b^{-1}, measured in units of L^2, has the characteristics of the variance of a normal distribution, and is presented by Gifford[10] as a function of the radius of the initial cloud.

The factor 2 appearing in the numerator on the right side of equation (2) appears when one considers that the surface of the earth acts as an impervious boundary for gaseous material. In this sense then, the ground acts as a perfect reflector, and the net effect is that the concentration at any point is twice that found in a cloud formed in an infinite medium.

If the source is elevated, the effect of the boundary is more complicated. Following Sutton, the reasoning employed in analyzing such a case is as follows[11]: if the height h of the source above ground is sufficiently great, the cloud near the source will behave as if the boundary were absent, but as distance downwind, x, increases, the influence of the boundary becomes increasingly evident as the gas diffuses downward. The solution, therefore, must behave like that for an infinite medium for small x/h but for large x/h must resemble the solution for a source placed at ground level.

This problem can be solved by the method of images. The semi-infinite medium $z > 0$ is replaced by the infinite medium $-\infty \leq z \leq \infty$, and the boundary $z = 0$ is abolished. The effect of the impervious surface is introduced by considering not only the real source at $x = y = 0$, $z = h$ but also its image in $z = 0$; i.e., a source of equal strength at $x = y = 0$, $z = -h$. The required concentration at any point in the space $z > 0$ is then equal to the sum of the concentrations from the two sources, since the condition of no net flux across the plane $z = 0$ is automatically satisfied because of symmetry. The required solution then, analogous to equation (2), is thus written

---

10 F. Gifford, Atmospheric Diffusion from Volume Sources, J. Meteorol., 3, 245-251 (1955).

11 Sutton, Op. cit. pp. 139-140.

$$D = \frac{Q\,e^{-\frac{\bar{u}\,y^2}{4kx+\bar{u}b^{-1}}}}{\pi\left[4kx+\bar{u}b^{-1}\right]}\left[e^{-\frac{\bar{u}\,(z-h)^2}{4kx+\bar{u}b^{-1}}}+e^{-\frac{\bar{u}\,(z+h)^2}{4kx+\bar{u}b^{-1}}}\right], \quad (3)$$

where, as before stated, h represents the height above the ground surface of release.

Equation (3) thus represents the total dosage equation applicable to determining the downwind total dosage distribution resulting from the release of gaseous material, in the form of an instantaneous volume source at a height h above the ground. If this equation is to be applied to aerosol clouds then, under the previously mentioned assumptions, the only effect that must be considered is how the finite settling velocities of particles may be included in the diffusion model.

The vertical distance of fall due to the finite settling velocities of the particles may be superimposed on the vertical spreading of the cloud. This may be accomplished mathematically by a translation of axis at each point downwind so that

$$z' = z + \frac{v_s}{\bar{u}}\,x \quad . \quad (4)$$

The second term on the right side of equation (4) thus takes into account the change in the height of the cloud at successive points downwind due to the settling of the cloud particles.

One further modification, however, becomes necessary. When dealing with gaseous material, the ground surface was treated as being a perfect reflector of the gas. Hence, the total amount of the gaseous cloud remains airborne at all times, which permits the writing of equation (3). However, when dealing with aerosol clouds consisting of particles having finite settling velocities, some of the particles of the initial cloud will continue to be deposited at successive downwind distances. Hence, the "image" of the initial source will in effect be continually decreasing in strength as the initial cloud continues its downwind travel. To allow for the deposition of the particles at the plane z = 0 then, the strength of the image must be multiplied by a factor k which is a function of the fraction of the cloud deposited at any point downwind from the source.

As a result of equation (4) and the change in image strength then, equation (3) may be modified as follows to account for the dispersion of particulate matter, the particles of which have finite settling velocities.

$$D = \frac{Q e^{-\frac{\bar{u} y^2}{4kx + \bar{u} b^{-1}}}}{\pi \left[4kx + \bar{u} b^{-1}\right]} \left[e^{-\frac{(z + \frac{v_s}{\bar{u}} x - h)^2}{4kx + \bar{u} b^{-1}}} + k e^{-\frac{(z + \frac{v_s}{\bar{u}} x + h)^2}{4kx + \bar{u} b^{-1}}} \right] \quad (5)$$

For a gas cloud, $k = 1$ and $v_s = 0$. Under these conditions equation (5) reduces to equation (3).

Equation (5) thus represents a dispersion equation stating the total dosage as a function of space. In order to apply the equation, however, it remains to determine the strength of the image, k, as a function of downwind distance x. As a first approximation, however, it may be assumed that the total dosage at the surface is the same as that which would be given by equation (3) when $z = 0$ and $k = 1$; i.e.,

$$D_e \simeq \frac{2Q e^{-\frac{\bar{u} y^2}{4kx + \bar{u} b^{-1}}} e^{-\frac{u h^2}{4kx + \bar{u} b^{-1}}}}{\pi \left[4kx + \bar{u} b^{-1}\right]} \quad (6)$$

Now then, near the surface of the earth, there is an effective stagnant film in which the effect of turbulent diffusion is negligible and through which the particles pass by virtue of free settling only. Consequently, the total amount deposited on the surface is given by the product of the total dosage established by the aerosol cloud adjacent to the stagnant film and the free settling velocity through this film; i.e.,

$$\Delta \simeq \frac{2Q v_s e^{-\frac{\bar{u} y^2}{4kx + \bar{u} b^{-1}}} e^{-\frac{\bar{u} h^2}{4kx + \bar{u} b^{-1}}}}{\pi \left[4kx + \bar{u} b^{-1}\right]} \quad (7)$$

where Δ = amount of agent deposited per unit area.

The amount of agent deposited per unit downwind distance would thus be, according to equation (7).

$$F \simeq \int_{-\infty}^{+\infty} \Delta \, dy = \frac{2Q v_s}{\pi[4kx + \bar{u} b^{-1}]} \, e^{-\frac{\bar{u} h^2}{4kx + \bar{u} b^{-1}}} \int_{-\infty}^{+\infty} e^{-\frac{\bar{u} y^2}{4kx + \bar{u} b^{-1}}} \, dy; \qquad (8)$$

or, performing the integration,

$$F \simeq \frac{2Q v_s}{\{\pi \bar{u}[4kx + \bar{u} b^{-1}]\}^{1/2}} \, e^{-\frac{\bar{u} h^2}{4kx + \bar{u} b^{-1}}} \qquad (9)$$

Finally, the total dosage as a function of space would be, according to equation (5) when k = 1

$$D \simeq \frac{Q \, e^{-\frac{\bar{u} y^2}{4kx + \bar{u} b^{-1}}}}{\pi[4kx + \bar{u} b^{-1}]} \left[e^{-\frac{(s + \frac{v_s}{\bar{u}} x - h)^2}{4kx + \bar{u} b^{-1}}} + e^{-\frac{(s + \frac{v_s}{\bar{u}} x + h)^2}{4kx + \bar{u} b^{-1}}} \right]. \qquad (10)$$

Thus, equation (7) permits the determination of the amount of agent deposited on the surface, and equation (10) permits the determination of the total dosage established at any point in space due to the passage of the aerosol cloud.

As stated previously, equations (6 through 10) represent approximations, based on assuming a strength of the image equal to unity. Such an approximation will, of course, yield more credible results for the smaller sized particles, implying a smaller rate of deposition. However, a second approximation may be obtained by recourse to a material balance in order to obtain a more precise estimate of the image strength, k. Such a material balance states that the undeposited fraction of the aerosol cloud remains airborne; thus, in mathematical terms,

$$\frac{1}{Q} \int_0^x \int_{-\infty}^{+\infty} D_o \, v_s \, dx \, dy = 1 - \frac{1}{Q} \int_0^{\infty} \int_{-\infty}^{+\infty} D \bar{u} \, ds \, dy \qquad (11)$$

where D_o represents the total dosage at ground level (i. e., z = 0). Equation (11) thus states that the cumulative fraction of the cloud that is deposited must equal the fraction of the integrated volume total dosage per unit length. Thus, substitution of equation (5) appropriately into equation (11) yields

$$\int_0^x \frac{v_g}{\left\{\pi \bar{u}\left[4kx + \bar{u}b^{-1}\right]\right\}^{1/2}}\left[e^{-\frac{(v_g x - h)^2}{\bar{u}} \Big/ 4kx + \bar{u}b^{-1}} + ke^{-\frac{(v_g x + h)^2}{\bar{u}} \Big/ 4kx + \bar{u}b^{-1}}\right] dx$$

$$= 1 - \frac{\sqrt{\bar{u}}}{\left\{\pi\left[4kx + \bar{u}b^{-1}\right]\right\}^{1/2}} \int_0^\infty \left[e^{-\frac{(s + v_g x - h)^2}{\bar{u}} \Big/ 4kx + \bar{u}b^{-1}} + ke^{-\frac{(s + v_g x + h)^2}{\bar{u}} \Big/ 4kx + \bar{u}b^{-1}}\right] ds \qquad (12)$$

Since k is a function only of x, it may be removed from the right side of equation (12). However, on the left side of equation (12), since the exact functional form of k is not known, an average value of k between 0 and x must be used. If equation (12) is divided through by k_{av}, and the assumption made that $k/k_{av} = 1$, an approximate value of k_{av} may be obtained. This k_{av} can then be used in the left side of equation (12) to determine the cumulative fraction of the cloud deposited as a function of x. The slope of this curve then yields the fraction deposited per unit distance, which in turn can be used to determine k. Such a procedure will of course represent a better approximation to actuality. However, the method is quite cumbersome, and therefore, in the interests of simplicity, the assumption will be made that $k \simeq 1$ in order to permit at least a qualitative analysis of the implications of the dispersion model.

THEORETICAL IMPLICATIONS

Having arrived at a dispersion model, it now remains to examine the implications of the model in order to show the effect of particle size, release height, and the turbulence regime on the deposition of aerosols. Consider first the expression yielding the cumulative relative amount of the cloud deposited per unit downwind distance; i. e.,

$$\frac{F_d}{Q} = \int_0^x \frac{2v_s}{\left\{\pi\bar{u}\left[4kx + \bar{u}b^{-1}\right]\right\}^{1/2}} e^{-\frac{\bar{u}h^2}{4kx + \bar{u}b^{-1}}} dx. \qquad (13)$$

If a change of variable is introduced such that

$$\tau = 4kx + \bar{u}b^{-1} , \tag{14}$$

then it follows that

$$\int_0^x \frac{2v_s}{\{\pi\bar{u}[4kx + \bar{u}b^{-1}]\}^{1/2}} e^{-\frac{\bar{u}h^2}{4kx + \bar{u}b^{-1}}} dx = \frac{v_s}{2k(\pi\bar{u})^{1/2}} \int_{\bar{u}b^{-1}}^{\tau} \frac{1}{\sqrt{\tau}} e^{-\frac{\bar{u}h^2}{\tau}} d\tau . \tag{15}$$

Now let

$$P = \frac{1}{\sqrt{\tau}} . \tag{16}$$

From the second change of variable as stated by equation (16), it can be seen that

$$\frac{v_s}{2k(\pi\bar{u})^{1/2}} \int_{\bar{u}b^{-1}}^{\tau} \frac{1}{\sqrt{\tau}} e^{-\frac{\bar{u}h^2}{\tau}} d\tau = -\frac{v_s}{k(\pi\bar{u})^{1/2}} \int_{(\bar{u}b^{-1})^{-1/2}}^{p} \frac{1}{p^2} e^{-\bar{u}h^2 p^2} dp \tag{17}$$

Integration by parts finally yields

$$\frac{F_d}{Q} = \frac{v_s}{k(\pi\bar{u})^{1/2}} \left[(4kx + \bar{u}b^{-1})^{1/2} e^{-\frac{\bar{u}h^2}{4kx + \bar{u}b^{-1}}} - (\bar{u}b^{-1})^{1/2} e^{-\frac{h^2}{b^{-1}}} \right] + \frac{v_s h}{k} \left[\operatorname{erf} \frac{\bar{u}h^2}{4kx + \bar{u}b^{-1}} - \operatorname{erf} \frac{h^2}{b^{-1}} \right] . \tag{18}$$

Figure 1 below represents the plot of the cumulative relative amount of the cloud deposited against downwind distance as determined by the application of equation (18), when the following arbitrary parameter values were assumed.

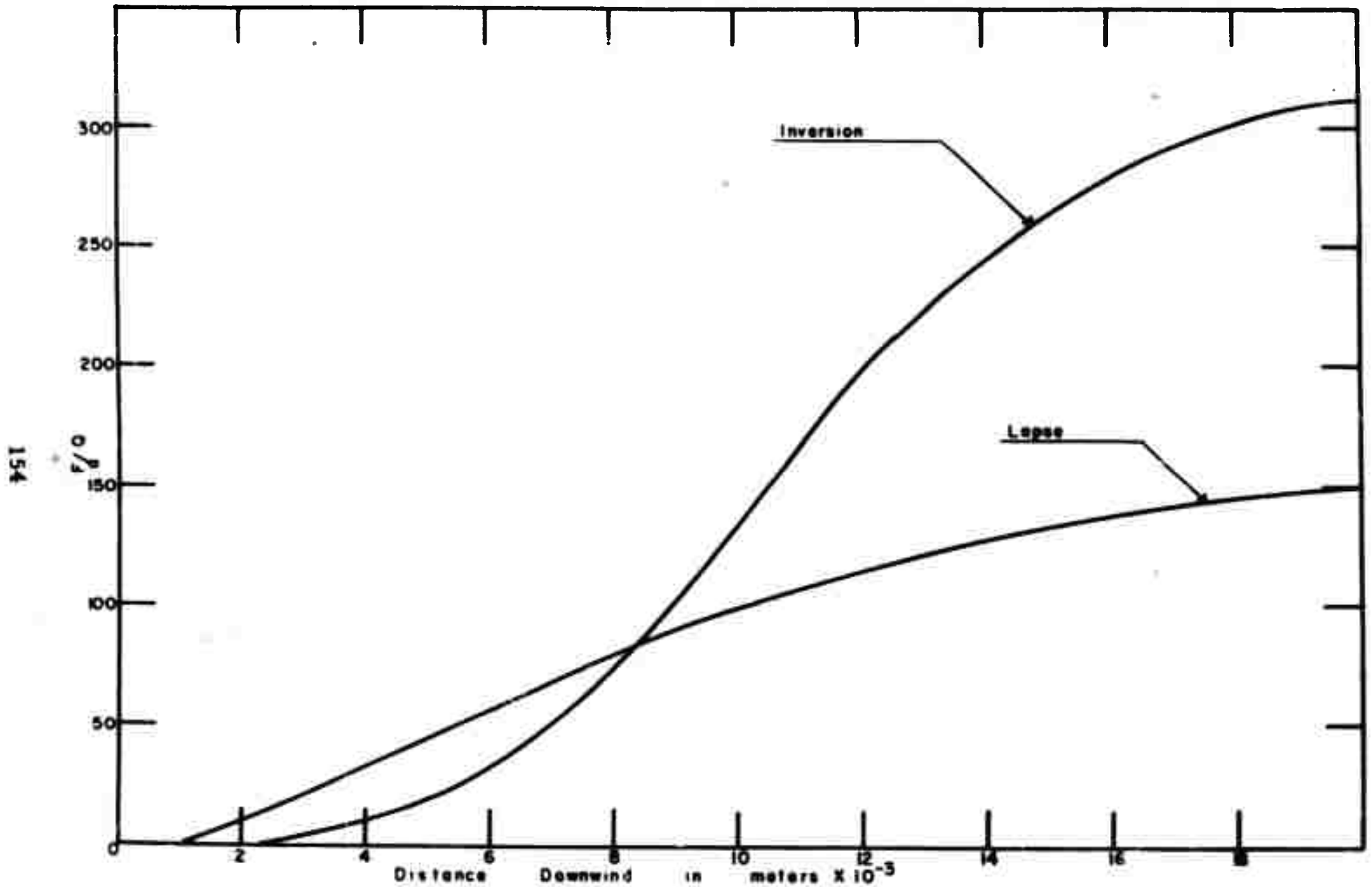

FIG. 1 CLOUD DEPOSITION

$$v_s = 1.14 \text{ m sec}^{-1}$$

$$\bar{u} = 5 \text{ m sec}^{-1}$$

$$h = 100 \text{ m}$$

$$b^{-1} = 125 \text{ m}^2$$

$K = 6 \text{m}^2 \text{ sec}^{-1}$ (lapse) and $K = 1 \text{m}^2 \text{sec}^{-1}$ (inversion).

The two curves shown in the figure indicate that the atmospheric turbulence has a considerable effect on the deposition of the aerosols. First of all, it is to be noted that more deposition occurs closer to the release point under highly turbulent conditions than for inversion conditions. The cumulative amount deposited is greater under inversion conditions than under lapse conditions at greater downwind distances. With regard to the first point of interest, deposition occurs closer to the release point under lapse conditions because of the greater vertical flux of mass being brought about due to the more turbulent nature of the atmosphere. However, the greater the turbulence, the more rapidly will the dilution of the aerosol occur; thus, at greater downwind distances more deposition occurs under inversion conditions than occurs under lapse conditions.

To proceed then, according to equation (9), the relative amount of material deposited per unit downwind distance is given by

$$\frac{F}{Q} = \frac{2 v_s}{\left\{\pi \bar{u} \left[4kx + \bar{u} b^{-1}\right]\right\}^{1/2}} e^{-\frac{\bar{u} h^2}{4kx + \bar{u} b^{-1}}} \tag{19}$$

The rate of change of the relative amount deposited with respect to downwind distance will be given by

$$\frac{dF}{dx} = \frac{4k \bar{u} v_s}{(\pi \bar{u})^{1/2} (4kx + \bar{u} b^{-1})^{3/2}} e^{-\frac{\bar{u} h^2}{4kx + \bar{u} b^{-1}}} \left[\frac{2h^2}{(4kx + \bar{u} b^{-1}} - \frac{1}{\bar{u}} \right]. \tag{20}$$

Equating to zero and solving for x, it is seen that the downwind distance of maximum deposition is given by

$$x_{max} = \frac{\bar{u} (2h^2 - b^{-1})}{4k} \tag{21}$$

Equation (21) indicates that the point of maximum deposition is inversely proportional to the degree of turbulence and directly proportional to the height of release; i. e., the greater the turbulence and/or the smaller the release height, the closer to the source will the maximum deposition occur. Again, the inverse relationship between the degree of turbulence and the point of maximum deposition is due to the greater net vertical flux of mass in evidence under more highly turbulent conditions.

Figure 2 shows the total dosage at the center line of the dosage distribution calculated from equation (10).

In the case of an aerosol cloud, the dosage at ground level at any distance, on the one hand, tends to decrease due to deposition. On the other hand, the effect of free settling in the air tends to increase the dosage at the ground. The relative importance of these two effects determines whether the value of the maximum total dosage of an aerosol cloud at ground level is greater or less than that for a gas cloud under similar conditions.

SUMMARY

The modification of Roberts' diffusion equation in the manner prescribed above gives a reasonable and intuitively correct description of the behavior of an aerosol cloud released to the atmosphere. Briefly, the results presented above may be qualitatively stated as follows: whereas the value of the maximum total dosage of a gas cloud is largely independent of atmospheric turbulence since there is no deposition or free settling effects to be considered, a decrease in turbulence greatly increases the maximum deposition and the maximum total dosage of an aerosol cloud at ground level. A decrease in turbulence shifts the point of maximum deposition and total dosage downwind from the source. Furthermore, an increase in release height decreases the deposition and ground total dosage, especially at the maximum values, and shifts the points of maximum deposition and total dosage downwind.

Thus, on the basis of intuition alone, the predicted implications of the chosen dispersion model appear reasonably correct. The logical question at this point would then be, "why worry about such prediction at all?" The basic consideration here is that <u>any</u> weapons system is no better than the predictability of its results. There is no real "prediction" problem connected with the more conventional munitions, since their effectiveness is usually restricted to the immediate time and area of impact.

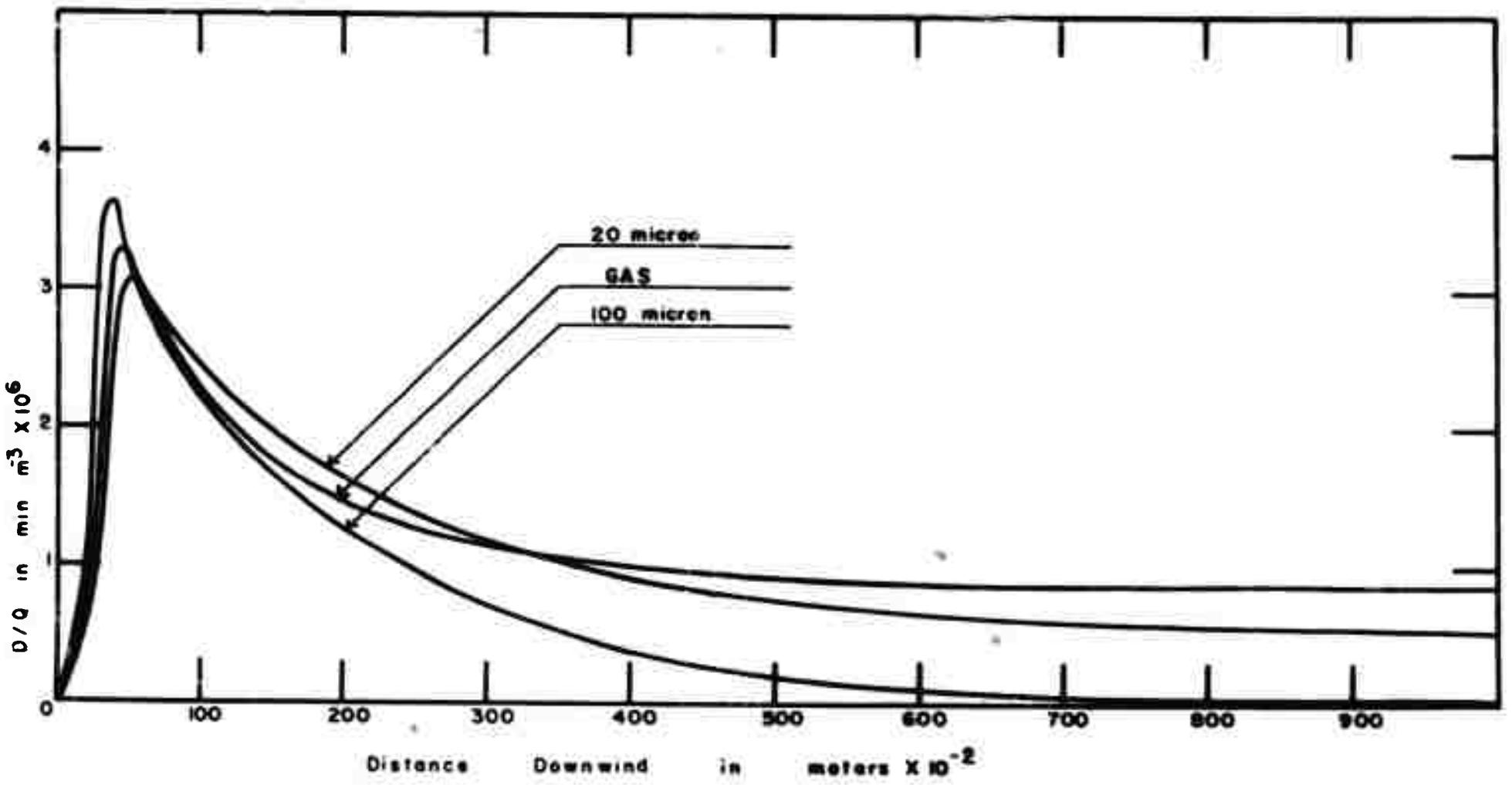

FIG 2 CENTERLINE DOSAGES

Therefore, the human element has a good deal of control over such munitions and can thus, to a large extent, predetermine the results of their use. Chemical or biological munitions on the other hand, are unique in that they are designed to be most effective after impact; i. e., after the time the human element can effect its control over the weapon. A gaseous or aerosol cloud is released to the atmosphere via explosive or other means; henceforth, atmospheric processes are the sole means whereby the agent may be disseminated further to accomplish the desired results. In other words, the atmosphere itself must be considered as being one of the most fundamental components of any chemical or biological weapons system. Therefore, it must be emphasized that in line with recent improvements in the fabricating of new devices for releasing CBR agents, plus the development of improved agents themselves, more attention must be given to understanding the atmospheric processes that determine the subsequent behavior of gaseous and/or aerosol clouds after their release if a truly effective CBR weapons system is to be developed. For, after all, if, after an agent cloud has been released to the atmosphere, one has no idea of where that cloud is going to go, then there really is not too much point in releasing it in the first place.

WILLIAM G. TANK
Cloud Physics Branch
Dugway Proving Ground

DISTRIBUTION LIST

Copies made: 99

1	Mail & Records Project File (Record Copy)
2 - 6	CWL Library, CW Laboratories
7 - 25	Publications Branch, Technical Information Division
26 - 28	Chief, Technical Information Division (For Clearance)
29	Office of Assistant Secretary for Defense (R&E) Room 3E-1071, The Pentagon, Washington 25, D. C.
30 - 35	British Joint Services Mission, 1800 K. St., N. W., Washington 25, D. C., Attn: Mr. W. N. Hewson
36 - 40	Canadian Army Technical Representative, Bldg. 330, Army Chemical Center, Md.
41	Director, Naval Research Laboratory, Department of the Navy, Washington 25, D. C.
42	Commanding Officer, U. S. Army CmlC Research and Development Command, Washington 25, D. C.
43	Headquarters, ARDC (RDTWMB) Andrews Air Force Base, Washington 25, D. C.
44 - 47	Commanding Officer, U. S. Army Biological Warfare Laboratories, Fort Detrick, Md.
48	Headquarters, USAF, The Pentagon, Washington 25, D. C., Attn: D/Requirements
49	Headquarters, USAF, The Pentagon, Washington 25, D. C., Attn: D/Plans
50	Headquarters, USAF, The Pentagon, Washington 25, D. C., Attn: D/Research & Development (DCS/D)
51	President of Board No. 3, Headquarters CONARC, Fort Benning, Ga.
52	Chief, Bureau of Yards and Docks, Department of the Navy, Washington 25, D. C.
53	Director, Central Intelligence Agency, 2430 E. St., N. W., Washington 25, D. C.
54	Commanding Officer, National Security Agency, Fort George G. Meade, Md.
55	Director, Operations Research Group, Bldg. 483, Army Chemical Center, Md.
56	Director, Operations Research Office, 6935 Arlington Road, Bethesda 14, Md.
57	Commanding Officer, U. S. Army CmlC Intelligence Agency, Arlington Hall Station, Arlington 12, Va.
58	Commanding Officer, U. S. Army CmlC Proving Ground, Dugway Proving Ground, Dugway, Utah
59	Director, Project CARAMU, 3rd Floor Logan Hall, University of Pa., Philadelphia 4, Pa.
60	Commanding Officer, U. S. Naval Unit, Bldg. 51, Army Chemical Center, Md.
61	Navy Department, CNO-Op 922 G2, The Pentagon, Washington 25, D. C.

DISTRIBUTION LIST (Contd.)

62 Commandant, U. S. Army CmlC School, Fort McClellan, Ala.
63 Commanding Officer, U. S. Naval Unit, Fort Detrick, Md.
64 CONARC Liaison Officer, Bldg. 330, Army Chemical Center, Md.
65 Headquarters, USAF, The Pentagon, Washington 25, D. C., Attn: ACS/I, AFCIN-3
66 Director, George Washington University Research Laboratory, Area B, Fort Detrick, Md., Attn: Mr. Holland
67 Deputy Chief Chemical Officer for Scientific Activities, Office of the Chief Chemical Officer, Dept. of the Army, Bldg. T-7, Gravelly Point, Washington 25, D. C.
68 Commanding General, The Infantry School, Fort Benning, Ga.
69 Commanding General, U. S. Army Chemical Center & Chemical Corps Materiel Command, Bldg. 1, Army Chemical Center, Md.
70 Commanding Officer, U. S. Army CmlC Engineering Command, Army Chemical Center, Md.
71 - 80 Armed Services Technical Information Agency, Arlington Hall Station, Arlington 12, Va., Attn: TIPDR
81 CmlC Advisory Council, Bldg. 330, Army Chemical Center, Md.
82 President, CmlC Board, Bldg. 483, Army Chemical Center, Md.
83 Director of Development, U. S. Army Chemical Warfare Laboratories, Army Chemical Center, Md.
84 Director of Medical Research, Bldg. 355, U. S. Army Chemical Warfare Laboratories, Army Chemical Center, Md.
85 Director of Technical Services, U. S. Army Chemical Warfare Laboratories, Army Chemical Center, Md.
86 Director of Research, U. S. Army Chemical Warfare Laboratories, Army Chemical Center, Md.
87 Commanding General, Research & Development Division, Dept. of the Army, Washington 25, D. C., Attn: Col. H. E. Sheppard
88 Chief, Bureau of Aeronautics, Department of the Navy, Washington 25, D. C.
89 Headquarters, Combat Development Section, U. S. CONARC, Fort Monroe, Va.
90 Naval Aviation Ordnance Test Station, Bureau of Ordnance, Chincoteague, Va.
91 Bombs and Warheads Branch, Headquarters APGC, Eglin Air Force Base, Florida
92 Georgia Institute of Technology, Atlanta, Georgia, Attn: Dr. Thomas W. Keithley
93 Edo Corporation, 13-10 111th St., College Point 56, New York,
Attn: Mr. C. L. Fenn
Mr. E. L. Cicero
Mr. R. O. Romaine
Mr. Daniel H. Shapiro
Mr. Laurence M. Swanson
94 Franklin Institute Laboratories, Philadelphia, Pa., Attn: Mr. Frederick H. Gaskins

DISTRIBUTION LIST (Contd.)

95 Battelle Memorial Institute, 505 King Avenue, Columbus 1, Ohio, Attn: Mr. Ralph I. Mitchell

96 Olin Mathieson Chemical Corporation, 1000 Connecticut Avenue, Washington 6, D. C., Attn: Dr. John W. Churchill, Director of Military Chemicals Research

97 Armour Research Foundation, 10 W. 35th St., Chicago 18, Illinois

98 Dow Chemical Company, Midland, Michigan, Attn: Dr. John J. Grebe, Director of Nuclear and Basic Research

99 University of Illinois, 108 E. Chemistry Bldg., Urbana, Illinois, Attn: Dr. H. Frazer Johnstone

NOTIFICATION OF MISSING PAGES

INSTRUCTIONS: THIS FORM IS INSERTED INTO ASTIA CATALOGED DOCUMENTS TO DENOTE MISSING PAGES.

DOCUMENT	CLASSIFICATION (CHECK ONE)		
	UNCLASSIFIED	CONFIDENTIAL	SECRET
AD			
ATI			

THE PAGES, FIGURES, CHARTS, PHOTOGRAPHS, ETC., MISSING FROM THIS DOCUMENT ARE:

Missing Pg. Blank

DO NOT REMOVE

ASTIA FORM AUG 52 32